Faculty of Science and Engineering
Department of Petroleum Engineering

A Network Model for Capture of Suspended Particles and Droplets in Porous Media

Changhong Gao

This thesis is presented for the Degree of
Doctor of Philosophy
of
Curtin University of Technology

May 2008

Declaration

To the best of my knowledge and belief this thesis contains no material previously published by any other person except where due acknowledgment has been made.

This thesis contains no material which has been accepted for the award of any other degree or diploma in any university.

Signature: …….

Date: …….

Acknowledgement

I wish to thank my supervisors Dr. Mayela Rivero and Dr. Edson Nakagawa for their encouragement, guidance and support during my pursuit of PhD.

I am very grateful for the financial support from Curtin University of technology, WAERA (Western Australia Energy Research Alliance), CSIRO (Commonwealth Scientific and Industrial Research Organisation) and APPEA (Australian Petroleum Production and Exploration Association). I could not have carried out this research without the generous support from the above organisations.

During my pursuit of PhD, I also had the opportunity to teach some lectures to undergraduate students and serve as the teaching assistant for postgraduate students. I wish to thank the department of petroleum engineering at Curtin University for allowing me to gain such valuable experiences. The administrative support from the department is also appreciated.

I dedicate this thesis to my father Gao Rongchang and my mother Bao Xiuhua.

Awards Received during PhD Study

March 2005 to March 2008	*Curtin International Research Tuition Scholarship*
March 2005 to March 2008	*CSIRO-WAERA PhD Studentship*
April 2006	*APPEA Tony Noon Memorial Scholarship*
March 2008	*Chinese Government Award for Outstanding Self-financed PhD Students Abroad*

Publications during PhD Study

1. C. Gao, M. Rivero, E. Nakagawa, and G. Sanchez, 2007. Downhole separation technology – past, present and future. *APPEA Journal*, 47 (1): 281-290.

2. C. Gao, M. Rivero, E. Nakagawa, and T. Rajeswaran, 2007. Pore network modeling of formation damage due to suspended particles. *APPEA Journal*, 47 (1): 187-196.

3. C. Gao, T. Rajeswaran, and E. Nakagawa, 2007. A literature review on smart well technology. SPE 106011 presented in the *SPE Production and Operations Symposium*.

4. C. Gao, 2007. Factors affecting particle retention in porous media. *Emirates Journal of Engineering Research*, 12 (3): 1-7.

5. C. Gao, 2008. Simulation of reservoir permeability decline due to invasion of large particles. Accepted for publication in *APPEA Journal.*

6. C. Gao, 2008. A network model for capture of emulsion droplets in porous media. Accepted for publication in *APPEA Journal.*

7. C. Gao, 2008. Understanding capture of suspended particles and resultant permeability damage with pore network model. Accepted for publication in *Asia-Pacific Journal of Chemical Engineering*.

Abstract

Produced water presents economical and environmental challenges to oil producers. Downhole separation technology is able to separate oil or gas from produced fluid in downhole environment and injects waste water into deeper formations, thus saving energy and reducing waste emission. More than 120 downhole separation systems have been installed worldwide, but only about 60% of the installations achieved success. Most of the failures were due to the injectivity decline under the invasion of impurities in the injected water, such as suspended particles and oil droplets. A reliable model is needed to predict the reaction of reservoir permeability under the invasion of such impurities and serves as a tool to screen appropriate formations for downhole separator installations.

Previous experimental studies on particle-induced permeability damage reveal that high particle concentration, low fluid velocity, large particle size lead to more severe damage. The damage mechanisms are attributed to surface interception, bridging and size exclusion of particles in porous media. While for droplets, the resultant permeability decline is mostly due to surface interception. Empirical correlations with key parameters determined by core flooding data are widely applied to the simulation of permeability decline under invasion of particles and droplets. These correlations are developed based on characteristics of certain rocks and fluids, thus their applications are very restricted.

A more scientific method is to model the flow and capture of particulates at pore level. Reservoir rocks are porous media composed of pores of various sizes. Pore network models employ certain assumptions to imitate real porous media, and have been proved realistic in simulating fluid flow in porous media. In this study, a 2-dimensional square network model is used to simulate capture of particles and droplets in porous media. Pore bodies are represented by globes and pore throats are imitated with capillary tubes. The flow rates in the network are obtained by simultaneously solving mass balance equations at each pore body. The network model is tuned to match the porosity and permeability of a certain rock and serves as the infrastructure where the capture process takes place.

Particles are categorized as Brownian and non-Brownian particles according to size. For Brownian particles, diffusion is dominant and Fick’s law is applied to each pore inside the network to obtain deposition rate. For non-Brownian particles, their trajectories are mainly

governed by gravity and drag force acting on them. Besides, the size of each particle is compared with the size of the pore where it is captured to determine the damage mechanism. For particles much smaller than the pore size, surface deposition is dominant and the permeability decline is gradual. For particles with sizes comparable to pore size, bridging and clogging are dominant and the permeability decline is much more severe.

Unlike particles, droplets can not be captured on top of each other. Accordingly, a capture-equilibrium theory is proposed. Once the pore surface is covered by droplets, equilibrium is reached and droplets flow freely through porous media without being captured. The simulation on capture of oil droplets reveals that the surface wettability has significant influence on the resultant permeability damage. Most natural reservoirs are neutrally or oil wet. It is thus recommended to apply these surface conditions to future simulations.

The proposed model is validated with test data and reasonably good agreements are obtained. This new mechanistic model provides more insights into the capture process and greatly reduces the dependence on core flooding data.

Table of Contents

List of Figures

List of Tables

Nomenclature

A	area of the rock subject to flow
c	solid or particle concentration
Cd	hydraulic conductance of a bond
c_o	inlet particle concentration
D	diffusion coefficient
Dc	drag coefficient
F_d	drag force
F_g	gravity
h	height of the injection zone
H	thickness of oil layer
I	Current (damaged) injectivity
I_o	Original (undamaged) injectivity
J	volume particle deposition rate
K	current permeability after deposition
K_B	Boltzmann constant
K_o	original permeability
L	length of the rock
L_b	length of the bond
L_n	length of the unit network
n	number of particles captured by a certain bond
N_{PV}	number of pore volumes of injection required to reduce permeability to a certain value
P_r	reservoir pressure
PV_s	total pore volume within the invasion depth
P_{wf}	well flowing pressure
ΔP	pressure loss across the rock
ΔP_b	pressure loss in a bond
q	volume flow rate through the rock
$Q_{i,j}$	volume flow rate in bond (i,j)
R	tube radius
r_b	radius of a bond
r_d	damage radius or invasion depth

r_e	reservoir radius
r_P	particle radius or droplet radius
r_s	radius of a site
r_w	wellbore radius
R_b	equivalent bond radius after damge
S	skin factor
t	time
T	absolute temperature
u	fluid superficial velocity
Vb	volume of a bond
Vbt	combined volume of nodes in a network
v_L	velocity of the suspension
Vnw	total volume of a network
v_p	velocity of the particle
V_p	volume of the particle
Vs	volume of a site
Vst	combined volume of sites in a network
vt	particle terminal velocity
x	coordinate
y	coordinate

σ	unit particle retention volume
λ	filtration coefficient
Δ	diffusion parameter
Φ	porosity
ρ_p	density of the particle
ρ_L	density of the liquid
μ_L	viscosity of the suspension
θ	contact angle

CHAPTER 1

INTRODUCTION TO PRODUCED WATER

1.1 Background

Mature oil and gas fields produce large amount of water from the natural aquifer, water flooding, or generally a combination of both. Water cuts in mature oil and gas fields can exceed 90% (Veil et al., 1994). Management of produced water presents challenges and costs to operators. The cost of managing produced water can be more than several dollars per barrel of oil produced. Moreover, more and more stringent environmental regulations have been established to restrict produced water discharge. If the amount of water to be lifted and treated can be reduced, costs and risks can be reduced. With this idea in mind, various technologies were developed to control water from flowing into the well or to separate oil and gas downhole.

1.2 Produced Water Characteristics

The physical and chemical properties of produced water vary considerably, depending on the compositions of the reservoir formation where the produced water has been resided, and the type of hydrocarbon product being produced. If water flooding operations are conducted, these properties and volumes may vary even more dramatically as additional water is injected into the formation. Oil and grease are the constituents of produced water that receive the most attention in both onshore and offshore operations. In addition, produced water contains many other organic and inorganic compositions.

1.2.1 Produced Water from Oil Production

Table 1-1 shows typical concentrations of pollutants in treated offshore produced water samples from the Gulf of Mexico (EPA, 1993). These data were compiled by EPA during the development of its offshore discharge regulations and are a composite of data from many different platforms. The first column of data represents the

performance for a very basic level of treatment (best practicable technology, or BPT) while the second column of data represents a more comprehensive level of treatment (best available technology, or BAT). The data show that many constituents are present in produced water, with the majority being oil and grease.

.

Table 1-1: Produced water characteristics following treatment

Constituent	Concentration after BPT-Level Treatment (mg/L)[a]	Concentration after BAT-Level Treatment (mg/L) – Gas Flotation Treatment[b]
Oil and grease	25	23.5
2-Butanone	1.03	0.41
2,4-Dimethylphenol	0.32	0.25
Anthracene	0.018	0.007
Benzene	2.98	1.22
Benzo(a)pyrene	0.012	0.005
Chlorobenzene	0.019	0.008
Di-n-butylphthalate	0.016	0.006
Ethylbenzene	0.32	0.062
n-Alkanes	1.64	0.66
Naphthalene	0.24	0.092
p-Chloro-m-cresol	0.25	0.010
Phenol	1.54	0.54
Steranes	0.077	0.033
Toluene	1.901	0.83
Triterpanes	0.078	0.031
Total xylenes	0.70	0.38
Aluminum	0.078	0.050
Arsenic	0.11	0.073
Barium	55.6	35.6
Boron	25.7	16.5
Cadmium	0.023	0.014
Copper	0.45	0.28
Iron	4.9	3.1
Lead	0.19	0.12
Manganese	0.12	0.074
Nickel	1.7	1.1
Titanium	0.007	0.004
Zinc	1.2	0.13
Radium 226 (in pCi/L)	0.00023	0.00020
Radium 228 (in pCi/L)	0.00028	0.00025

[a] BPT = best practicable technology.
[b] BAT = best available technology.
Source: EPA (1993).

In addition to its natural components, produced water from oil production may also contain groundwater or seawater injected to maintain reservoir pressure, as well as miscellaneous solids and bacteria. Most produced waters are more saline than seawater (Cline, 1998). They may also include chemical additives used in drilling and producing operations and in the oil/water separation process. Treatment chemicals are typically complex mixtures of various molecular compounds. These mixtures can include corrosion inhibitors, scale inhibitors, biocides, emulsion breakers, and paraffin inhibitors etc.

1.2.2 Produced Water from Gas Production

Produced water is separated from gas during the production process. In addition to formation water, produced water from gas operations also includes condensed water. Produced waters from gas production have higher contents of low molecular-weight aromatic hydrocarbons such as benzene, toluene, ethyl-benzene, and xylene (BTEX) than those from oil operations; hence they are relatively more toxic than produced water from oil production. Studies indicate that the produced water discharged from gas/condensate platforms are about 10 times more toxic than the produced waters discharged from oil platforms (Jacobs et al., 1992). However, for produced water discharged offshore, the volumes from gas production are much lower, so the total impact may be less.

The chemicals used for gas processing typically include dehydration chemicals, hydrogen sulfide-removal chemicals, and chemicals to inhibit hydrates. Significant differences between offshore oilfield produced water and offshore gas produced water exist for other parameters as well. For example, the sea water in the North Sea has pH of 8.1 and chlorides content of are about 19 g/L (Jacobs et al, 1992). Produced water discharges from oil platforms in that area have pH levels of 6-7.7, while those from gas platforms are more acidic (about 3.5-5.5). Chloride concentrations range from about 12 to 100 g/L in produced water associated with crude oil production and from less than 1 to 189 g/L in produced waters associated with natural gas production.

1.3 Produced Water Discharges and Regulations

According to the American Petroleum Institute (API), about 18 billion barrels of produced water was generated by U.S. onshore operations in 1995 (API, 2000). Additional 1.75 billion barrels of produced water are generated at U.S. offshore fields. It is estimated that in 1999, an average of 210 million bbl of water was produced each day worldwide (Khatib and Verbeek, 2003). This volume represents about 77 billion bbl of produced water for the entire year. Natural gas wells typically produce much lower volumes of water than oil wells.

The chemicals in produced water, when present in high concentrations, can present a threat to aquatic life when they are discharged offshore. Produced water can have different potential impacts depending on where it is discharged. For example, discharges to small streams are likely to have a larger environmental impact than discharges made to the open ocean. The most common practice is to dilute the produced water to an acceptable concentration of oil and discharge into the ocean.

Numerous studies have been conducted on the fate and effects of produced water discharges in the coastal environments of the Gulf of Mexico (Rabalais et al., 1992). These have shown that produced waters can contaminate sediments and that the zone of such contamination correlates positively with produced water discharge volume and hydrocarbon concentration.

Recognising the potential for shallow-water impacts, EPA banned discharges of produced water in coastal waters with a phase-out period starting in 1997, except for the Cook Inlet in Alaska where offshore discharge limits apply. For offshore discharge, EPA regulates the daily maximum concentration of oil and grease can not exceed 42 mg/L and the monthly average can not exceed 29 mg/L. In Australia waters, similar regulations apply: the concentration of dispersed petroleum is not to exceed 50 mg/L at any time and average lass than 30 mg/L during each period of 24 hours (Cobby, 2004). In North Sea, the limit is 40 mg/L by Oslo-Paris Commission (PARCOM).

The oil companies have taken responsibilities to protect the ocean. The oil content in the produced water discharged in 1991 from all North Sea production platforms was 34 mg/L, less than the Paris Commission (PARCOM) target monthly average of 40 mg/L. However, the absolute amount of discharge is still huge. In that year the total discharge volume was 160 million cubic meters, with 95% of it from oil wells and 5% from gas production. These discharges were estimated to contain about 52,600 tons of organic compounds and about 1,000 tons of heavy metals. Latest treatment technologies helped to reduce this number even further. In 1998, the oil concentration was reduced to 22 mg/L in North Sea.

1.4 Water Control and Management Methods

Historically, produced water was managed in ways that were the most convenient or least expensive. Today, many companies recognise that water can be either a cost or a value to their operations. For example, Shell has established a formal Water-to-Value program through which the company attempts to minimise the production of water, reduce the costs of water treatment methods, and look for ways in which existing facilities can handle larger volumes of water (Khatib and Verbeek, 2003). Greater attention to water management allows production of hydrocarbons to remain viable.

Within a reservoir, water and petroleum hydrocarbons are not fully mixed, but exist as separate adjacent fluid layers, with the hydrocarbon layer lying above the water layer by virtue of its lower specific gravity. Operators try to design wells to produce from the hydrocarbon layer. As hydrocarbons are removed from the formation, the pressure gradient changes so that the water layer often rises up in the vicinity of the well, creating a coning effect. As production continues, an increasing portion of the produced fluids will be water.

It is challenging to minimise the amount of water produced into the well, but there are some strategies that can be used to restrict water from entering the wellbore. These involve mechanical blocking devices or chemicals that “shut off” water-bearing channels or fractures within the formation and prevent water from making its way to the well. On the other hand, lifting water to the surface represents a substantial expense for operators. A variety of technologies have been developed that attempt to manage water either in the well bore itself or at a remote location like the sea floor.

1.4.1 Mechanical Blocking Devices

Operators have used various mechanical and well construction techniques to block water from entering the well. Examples of these techniques include straddle packers, bridge plugs, tubing patches, cementing, well bore sand plugs, well abandonment, infill drilling, pattern flow control, and horizontal wells.

These techniques have been used for many years, but do not work well in all applications. Operators often do not put forth the time or expense to diagnose the cause of their overabundant water. Consequently, incorrect solutions are not uncommon. For example, Seright et al. (2001) identified 13 types of events that lead to excess water; these are divided into four categories of most viable remedies. They recommend that mechanical approaches can be used to block casing leaks or flow behind pipe without flow restrictions and unfractured wells with barriers to cross flow. Those approaches may not be effective in solving other types of water production problems.

1.4.2 Water Shut-Off Chemicals

Another approach to shutting off water production while allowing continued oil production relies on chemicals that are injected into the formation. Most of these products are polymer gels or their pre-gel forms - gelants. Gel solutions selectively enter the pathways that the water flows and displace the water. When the gels set up in the cracks, they block most of the water movement to the well while allowing oil to flow to the well.

In the United States, most of the polymer gel treatments are made in wells producing from fractured carbonate or dolomite formations that operate under a natural water drive (Reynolds et al., 2002). The results of many successful gel treatment jobs have been reported in the literature. Seright et al. (2001) reported on 274 gel treatments conducted in naturally fractured carbonate formations. The median water-to-oil ratio (WOR) was 82 before the treatment, 7 shortly after the treatment, and 20 a year or two after treatment. The oil production increased following treatment and remained above pretreatment levels for 1 to 2 years.

1.4.3 Dual Completion Wells

Oil production can decline in a well because water forms a cone around the production perforations, limiting the volume of oil that can be produced. This situation can be reversed and controlled by completing the well with two separate tubing strings and pumps. The primary completion is made at a depth corresponding to strong oil

production, and a secondary completion is made lower in the interval, at a depth with strong water production. The two completions are separated by a packer. The oil collected above the packer is produced to the surface, and the water collected below the packer is injected into a lower formation. This technology has also been called a downhole water sink. In another version of the process, the water can be separately produced to the surface for management there.

Swisher (2000) reports on the performance of a dual-completion well compared to three wells with conventional completions in a north Louisiana field. Although the dual completion well cost about twice as much to install, it took the same or fewer number of months to reach payout as the other wells. At payout, it was producing 55 bpd of oil compared to about 16 bpd from the other three wells. The net monthly earnings at payout for the dual completion well were nearly $26,000 compared to $5,000 to $8,000 for the other wells.

1.4.4 Downhole Separation Technology

Downhole separation technology employs certain downhole tools to separate water from oil and gas. The oil-rich or gas-rich stream is produced to the surface, while the water-rich stream is injected to an underground formation without ever being lifted to the surface. These devices are known as downhole oil/water separators (DOWS) and downhole gas/water separators (DGWS). DOWS and DGWS technologies received a great deal of attention in the late 1990s (Ogunsina and Wiggins, 2005).

DOWS system has two primary components – an oil/water separation component and one or more pumps. Two basic methods of separation have been developed. One type uses hydrocyclones to mechanically separate oil and water, and the other relies on gravity separation that takes place in the well bore.

Based on the pumping methods, DGWS technology can be classified into four main categories: bypass tools, modified plunger rod pumps, ESPs, and progressive cavity pumps. There are tradeoffs among the various types, depending on the depth involved and the specific application. Produced water rates and well depth determine which type of DGWS tool is appropriate.

1.4.5 Subsea Separation

This technology involves remote oil/water separation at the sea floor rather than downhole. A Norwegian company developed a subsea separation and injection system (SUBSIS) that separates the produced fluids from an offshore well at a treatment module located on the sea floor.

Initial field results indicated that 23,000 bpd of produced fluids were separated into 16,000 bpd of oil and gas and 7,000 bpd of water. The water was injected into a dedicated injection well directly from the SUBSIS unit (Wolff, 2000). During the trial, the SUBSIS handled a maximum flow of 60,000 bpd and a typical flow of 20,000 bpd. The oil concentration in the separated water stream dropped from an initial level of about 600 ppm to a much lower 15 ppm. Because the water injected from the SUBSIS did not need to come to the surface, Troll platform was able to produce an additional 2.5 million bbl of oil during the year-long trial.

1.4.6 Produced Water Re-injection (PWRI)

The most commonly used approach for managing onshore produced water is re-injection into an underground formation. Although some produced water is injected solely for disposal, most produced water (71%) is injected to maintain reservoir pressure and to hydraulically drive oil toward a producing well. This practice is referred to as water flooding, or if the water is heated to make steam, as steam flooding. For example, California has nearly 25,000 produced water injection wells. The annual injected volume is approximately 1.8 billion bbl, distributed as follows: disposal wells - 360 million bbl; water flood - 900 million bbl; and steam flood - 560 million bbl (Tibbetts et al., 1992).

1.5 Objectives

The common practice in offshore Australia is to discharge produced water into the ocean. During this process, produced water needs to be treated, diluted then discharged into the sea. This method is costly and environmentally risky. Australia has

gigantic gas reserves in Northwest shelf, where the marine environment is very sensitive. To develop the natural gas fields and also reduce waste water emission as much as possible, an effective technology is essential to manage and control the produced water from the gas fields.

Among the available water control methods, downhole separation technology has several distinguishable advantages. This technology separates oil and water inside wellbore and disposes waste water downhole. If applied successfully, the amount of produced water can be drastically reduced, thus saving energy from lifting produced water. Moreover, for offshore deepwater fields, reduction in produced water also reduces the risk of hydrate formation. It can be seen that downhole separation technology may have great potential in Australian gas field development.

The objectives of this thesis are:
(1) Survey previous installations of downhole separation systems, and identify the causes of failure for previous installations
(2) Research possible methods to understand and improve certain aspects of downhole separation technology

The literature survey finds that one of the major challenges facing downhole separation technology is the injectivity decline induced by particle and droplet plugging. Severe injectivity decline was also reported in several produced water re-injection (PWRI) projects. A reliable method of modeling these effects is needed as a tool to screen and optimise the choice of formation for down-hole separator installations.

1.6 Thesis Outline and Methodology

This thesis includes two parts. Chapters 1 to 8 are thesis texts. Most content in this thesis has been published in journals. The appendix contains my publications related to this thesis during the course of PhD. The texts provide more details and insights, while the publications are more condensed.

Chapter 2 surveys the field installations of DOWS and DGWS systems. It is discovered that among more than 120 installations, only about 60% achieved success.

The major challenge facing downhole separation technology is that the particles and droplets in injected water caused the injection zone to lose injectivity. In order to screen the potential wells for downhole separation technology or to determine workover frequency, it is necessary to understand the factors affecting capture of particles and droplets in reservoir rocks. Based on such understanding, a reliable model can be built to predict the reservoir performance under the influences of particulate fluids.

Chapter 3 reviews and analyses the published experimental data in flow and capture of particles in porous media. Large amount of test data have been published in this topic. The previous test data show that high particle concentration, low fluid velocity, and large particle size lead to more severe damage.

Chapter 4 discusses available models of porous media and models of particle-induced formation damage. Most established formation-damage models rely on core flooding tests to determine the key parameters. As such, their applications are restricted to certain reservoirs and fluids. Pore network models provide more realistic characteristics of porous media and have been successfully applied to the simulation of static and dynamic properties of porous media. However, limited research has been conducted to study capture of particles and droplets in porous media with network model. The author decides to employ a 2-dimentional square network model to study this phenomenon.

Chapter 5 simulates the capture of Brownian particles in porous media and resultant permeability decline. For Brownian particles, diffusion is dominant. Fick's diffusion law is used to obtain the deposition rate inside porous media. The model is validated with test data and reasonably good match is achieved.

Chapter 6 simulates capture of non-Brownian particles in porous media and resultant permeability decline. For large particles, their movements are governed by the forces acting on them. A force analysis is carried out to gain the particle invasion depth. And a 1/3 rule is employed to determine the damage mechanisms. The model is validated with test data and reasonably good results are achieved.

Chapter 7 simulates capture of oil droplets in porous media and resultant permeability decline. Droplets can be captured by sand surface or at narrow pore throats. A capture-equilibrium theory is proposed for surface capture of oil droplets inside porous media. The model is validated with test data and reasonably good match is achieved.

Chapter 8 provides some final discussions and conclusions.

1.7 Contributions

This thesis attempts to simulate the complex process of capture of particles and droplets in porous media, and quantify the resultant permeability damage. The contribution of this thesis is that the author investigates the issue from a mechanistic point of view.

Each porous medium has very complex and unique structures. The traditional empirical models rely on core flooding / filtration data to determine the key parameters. This work looks into the capture of particles and droplets at pore level. Every porous medium is a combination of pores with different sizes. Pore network model provides a realistic description of porous media; hence it is employed to gain better descriptions of the reservoir rocks and better understanding of particulate movement inside porous media.

Moreover, the captures of Brownian particles, non-Brownian particles and oil droplets are governed by different laws. Traditional models failed to incorporate the respective damage mechanisms. This thesis models the capture process according to the respective damage mechanisms. Moreover, available models rely on empirical parameters to gain good match with test data. The model in this thesis avoids empirical parameters.

In brief, this work provides more scientific insights into the capture of particles and droplets in porous media.

CHAPTER 2

APPLICTIONS AND CHALLENGES

OF DOWNHOLE SEPARATION TECHNOLOGY*

2.1 Introduction

In mature oil and gas field developments, large amount of produced water is brought to the surface along with oil or gas. The water cuts in mature oil field often exceed 90%. In offshore environment, the produced water is generally separated, treated and discharged into the ocean. Managing produced water can cost more than several dollars per barrel. Moreover, improper handling of produced water can cause severe pollution.

A relatively new technology, downhole separation technology has been developed to reduce the cost of handling produced water. This technology separates oil and gas from produced water at the bottom of the well and injects some of the produced water into another formation, while the oil and gas flow to the surface.

2.2 Downhole Oil-Water Separation (DOWS)

Although a full DOWS system includes many components, the two primary components are an oil-water separator and at least one downhole injection pump. Two types of separators, hydrocyclone and gravity separators, and three types of pumps: electric submersible pumps (ESP), progressing cavity pumps, and beam pumps have been employed. The individual components of DOWS technology have proven to work in the field. The challenge is to make separators and pumps work together in the confined space of a 7-inch or smaller casing in a bottomhole environment.

2.2.1 DOWS with Hydrocyclone Separator

Hydrocyclones have been used for surface treatment of produced water for the past 25 years. Hydrocyclones have no moving parts and separate substances of different density by centrifugal force. Hydrocyclones can separate liquids from

** Published in APPEA Journal, Vol. 47, Part 1, 281-289.*

solids or liquids from other liquids. The liquid/liquid type of hydrocyclone is used in DOWS. Figure 2-1 shows a schematic drawing of a hydrocyclone. Produced fluid is pumped tangentially into the conical portion of a hydrocyclone. Water, the heavier fluid, spins to the outside of the hydrocyclone and moves toward the lower outlet. The lighter fluids, oil and gas, remain in the center of the hydrocyclone and are carried toward the upper outlet and produced to the surface (Gomez et al., 2001).

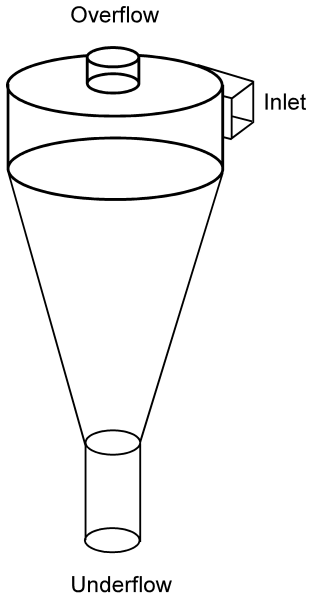

Figure 2-1: Schematic of a hydrocyclone separator

The separation of fluids in a hydrocyclone is not 100% complete: some oil is carried along with the water fraction, and a significant portion of water (typically 10% to 15%) is brought to the surface with oil and gas production. Nevertheless, hydrocyclones can rapidly and effectively separate most of the oil from the water fraction. For example, typically wells with a water-to-oil ratio in the range of 5 to 100 can achieve water-to-oil ratios between 1.0 and 2.0 with the help of a hydrocyclone-type DOWS (Petty and Parks, 2004).

Hydrocyclones used in DOWS tend to be narrow and tall. Hydrocyclones could be smaller than 50 mm in diameter and 1 to 2 meters in length. If a single hydrocyclone does not provide enough capacity to handle the total fluid volume, several hydrocyclones can be installed in parallel. The capacity limits for hydrocyclone type DOWS with three different types of pumps are listed in Table 2-1 (Matthews et al., 1996).

Table 2-1: Capacity limits for hydrocyclone-type DOWS

Pump type	Casing size (inch)	Total volume (bbl/day)	Maximum volume to surface (bbl/day)
Electric submersible pump	5.5	3,800	440
	7.0	10,000	940
Progressive cavity pump	5.5	2,200	450
	7.0	3,800	1,360
Rod pump	5.5 (85% watercut)	1,700	530
	5.5 (97% water cut)	1,200	70
	7.0 (85% watercut)	2,500	790
	7.0 (97% water cut)	1,900	190

DOWS systems can take different configurations. The system illustrated in Figure 2-2 is referred to as a 'push-through' system. In this design, the injection pump discharge is connected directly to the inlet of the separator. The injection pump provides the pressure required to operate the separator and inject the separated water. In some cases, where the pressure required to inject the water is equal to or higher than the pressure required to lift the oil stream to surface, the injection pump can serve both purposes and only one pump is required. Where injection pressure is low, it is normal practice to use a second pump to lift the oil stream. If two pumps are used, a common motor normally drives both.

Reduced power requirement is the primary justification for using two pumps in a push-through system. Significant power savings can result if the injection pressure is low and the water cut is high. In this situation, the total production volume is pumped only to the pressure required for injection, while the production pump boosts only a fraction of the produced fluid to the pressure required to reach the surface. This reduction in power requirement has been used to either install lower horsepower motors, reducing energy requirement and extending motor life, or to increase total drawdown and oil production without an increase in the motor size or energy consumed, as compared to a conventional lift system.

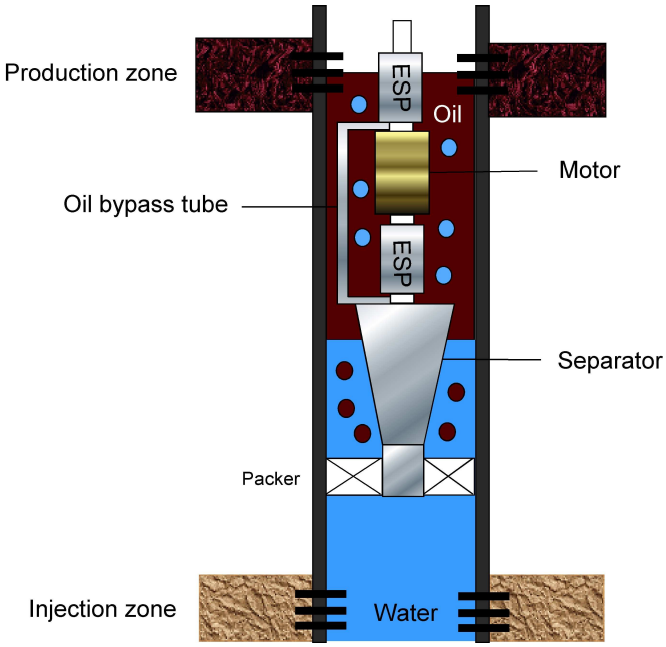

Figure 2-2: Push-through type DOWS

Figure 2-3 shows a 'pull-through' system. In this configuration, the suction of the injection pump is connected to the water outlet of the separator. The pump draws separated water from the separator and boosts pressure to a level suitable for injection. Unless the well is free flowing (i.e., does not require an artificial lift system to produce to the surface), a second pump is required to lift the oil stream to the surface (Bower et al., 2000).

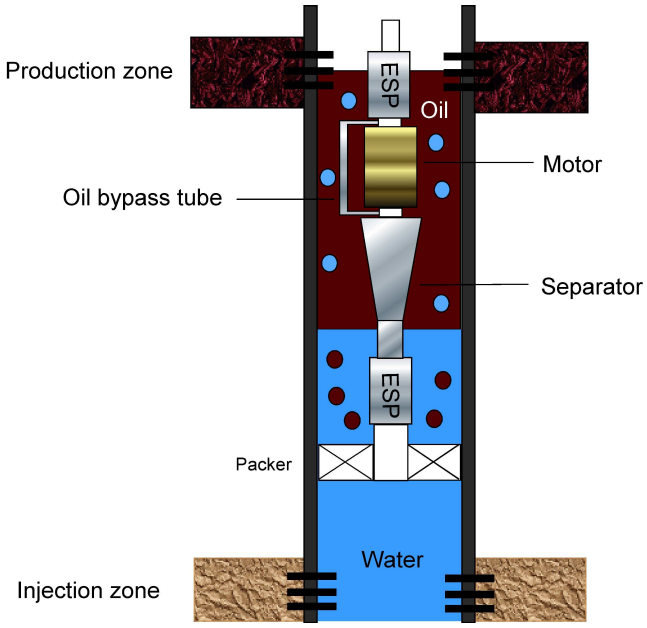

Figure 2-3: Pull-through type DOWS

2.2.2 DOWS with Gravity Separator

Oil and water exist as separate fractions downhole. Emulsions are typically formed when oil and water are mixed by pumping. The gravity separator type of DOWS takes advantage of the gravity separation of oil and water that occurs in the casing/tubing annulus. The dual action pumping system (DAPS), which is the most commonly used type of gravity separator, is constructed by modifying a rod pump to contain two separate pump chambers and inlets, and adding an injection valve and packer.

Figure 2-4 is a schematic drawing of the DAPS developed by Texaco in 1994 (Peachey and Mathews, 1994; Ogunsina and Wiggins, 2005). The upper inlet is located at an elevation near the oil/water interface, so that a mixture of oil and water enters the upper pump and is brought to the surface on the upstroke. The lower inlet is located below the oil/water interface, so that primarily water enters the lower pump and is subsequently injected during the down-stroke. Proper sizing of the two pump chambers is critical in preventing oil from being disposed of to the injection zone. If the working fluid level drops below the upper inlet, no fluids will be pumped to the surface, and both water and oil will be injected to the injection formation.

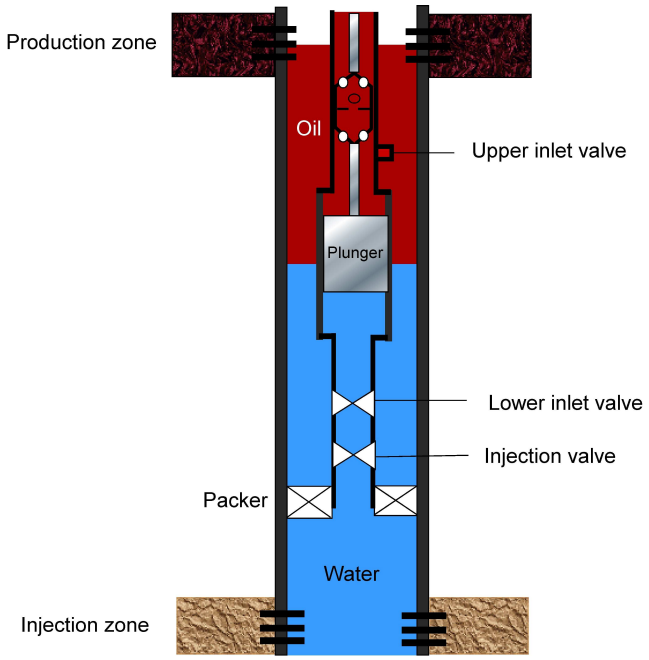

Figure 2-4: DAPS schematic

The sucker rod strings of conventional rod pumps are designed to tolerate a tension strain but not a compression strain. The force required to inject water into a formation can place an undue compression strain on sucker rods, so sinker bar weights are often added above the top pump on a DAPS to overcome the injection pressure.

DAPS have been installed in more than a dozen wells. DAPS are most commonly used on wells with 4.5-inch casing. Because of size constraints, the largest DAPS that will work in that size casing can pump about 1,000 bbl/day. Another limitation is that DAPS can not effectively handle gas and solids. Moreover, DAPS requires enough vertical space between the injection and production zones for sufficient gravity separation.

2.2.3 Previous DOWS Installations

Till 2005, totally 59 worldwide DOWS trials were identified from literature (Veil et al, 1999; Veil and Quinn, 2005). Some of the general trends are discussed in this section.

(1) Costs: Two-thirds of the installations used hydrocyclone-type DOWS. A hydrocyclone DOWS system can cost between $90,000 and $250,000 (USD), excluding the cost of a workover to install the equipment, which can add another $100,000 or more. Hydrocyclone DOWS systems are from two to three times the cost of a comparable conventional ESP. Gravity separation DOWS systems are considerably less expensive, and range between $15,000 and $25,000, plus the cost of an installation workover. The total cost of a DOWS application ranges from $120,000 to $300,000 USD.

The cost/benefit analysis of an offshore DOWS system can be quite different from that of an onshore system. Many onshore fields have very high water handling and disposal costs. In these cases, the cost of a DOWS system can be justified purely by lifting and handling less water, particularly if the installed cost of the system is low. For offshore cases, operating costs associated with water handling are not likely to be so high. Given the required investment for offshore DOWS installation, incremental oil production is almost mandatory for justification.

(2) Geographical location: Among the total 59 applications worldwide, most of the DOWS installations were in North America (34 in Canada and 14 in the United States); 6 were in Latin America, 2 were in Europe, 2 were in Asia, and 1 was in the Middle East. All trials were at onshore facilities, except for 1 trial in China.

(3) Casing size: Among 40 hydrocyclone-type DOWS, 15 installations were in 5.5-inch casing, 1 was in 6.625-inch casing, 17 were in 7-inch casing, 1 was in 8.625-inch casing, 4 were in 9.625-inch casing, and 2 were unspecified. Among the 19 gravity separator type DOWS, 10 were in 5.5-inch casing, 3 were in 7-inch casing, and 6 were unspecified.

(4) Volume of oil produced: The volume of oil production increased in 31 of the trials, decreased in 17 of the trials, stayed the same in 8 trials, and was unspecified in 3 trials. For the 40 hydrocyclone type DOWS, 19 trials showed an increase in oil production, 11 trials showed a decrease, and 8 trials showed unchanged production, and 2 did not specify oil production; For the 19 gravity separator-type DOWS, 12 trials showed an increase in oil production, 6 trials showed a decrease, and 1 did not specify oil production; The top three performing wells with hydrocyclone showed oil production increases ranging from 457% to 1,162%, while one well lost all oil production. The top three gravity separator-type wells showed oil production increases ranging from 106% to 233%, while one well lost all oil production. Based on the change in oil production, the successful rate is only about 53%.

Incremental oil production can be achieved in a number of ways, most of which are made possible by the reduction in loading on existing water handling and injection systems with the help of DOWS systems. For example, if a well is not operating at maximum recommended drawdown because the water handling facilities are fully loaded, installation of DOWS systems will allow increased drawdown and incremental production. On the other hand, if a well is already being produced at maximum rates, the reduction in water to the surface can allow shut-in wells to be returned to production. Either way, incremental oil is generated.

(5) Lithology: It was believed that the produced sand from sandstone can clog the water disposal zone, which causes the DOWS fail to reduce water production. Therefore it is necessary to investigate if the failures of DOWS are related to the geology environment where they are installed. DOWS were installed in 24 wells

producing from carbonate formations, and in 30 wells producing from sandstone formations. Information on production zone geology was not available for 5 other installations. On the injection side, 19 DOWS injected to carbonate formations and 32 injected to sandstone formations. No information was available for 8 of the installations. Based on the statistics in Table 2-2, the success rates for Carbonate/Carbonate and Sandstone/Sandstone combinations are very close: 58% versus 57%. There is no clear relationship between a successful DOWS application and formation geological combinations (Veil and Quinn, 2005).

Table 2-2: DOWS performance and geology environment

Geology of producing formation/injection formation	Trials rated good	Trials rated poor	Total number of trials	Trials rated good (%)	Trials rated poor (%)
Carbonate/Carbonate	11	8	19	58	42
Carbonate/Sandstone	2	2	4	50	50
Carbonate/Unknown	1	0	1	100	0
Sandstone/Sandstone	16	12	28	57	43
At least one is Sandstone	1	1	2	50	50
Unknown	4	1	5	80	20
Total	35	24	59	59	41

2.2.4 Experiences with Problems

The problems encountered during DOWS applications are either due to the hardware or the formation conditions (Ogunsina and Wiggins, 2005):

(1) Injectivity decline: For DOWS technology to function properly, the injection zone must have sufficient permeability and porosity to accept brine at a pressure within the capability of the pump. Several installations by Texaco, Pinnacle and Alliance suffered from low injectivity of the receiving zone. Inappropriate fluids contacted sensitive sands and damaged part of the permeability. Particles in the produced water clogged the injection zone.

(2) Solids plugging: Excessive sands not only damage the injection zone, they also result in premature mechanical failure of the separator, pumps, or bypass tubing. In at least two cases, solids production was so excessive that the entire

pump/separator assembly was packed with solids when inspected at the surface. In one case the solids were formation solids, and in the second case the solids were iron sulfide scale.

(3) Isolation problems: To protect the producing reservoir, the injection zone must be adequately isolated by an integral confining zone and sound cement behind production casing. If isolation is not sufficient, the separated water can migrate into the producing zone and then short-circuit into the producing perforations. The result will be recycling of the produced water, with oil production rates dropping to nearly zero. Crestar and Chevron reported these problems during their applications.

(4) Mechanical / corrosion problems: It is a big challenge to fit the separator inside a well. In particular, channels to bypass oil flow around the pump and motor assembly must be fitted into a very small cross section, and are exposed to very high flow rates. This creates risks of erosion/corrosion. Additionally, because these flow bypass channels are normally formed from thin walled tubing and often attached to the outside of the pump assembly, there is a high potential of damage to these tubes in the course of installation, especially when the well is deviated. Talisman and Texaco both reported that trials were cancelled because of corrosion problems with their DAPS tools.

2.2.5 How to Select a Good Candidate Well for DOWS

It is attractive to reduce produced water handling and disposal costs, and possibly produce more oil through installation of a DOWS. However, not all wells are good candidates for a cost-effective DOWS installation. Several authors have indicated the criteria they have used in selecting candidate wells for installations of hydrocyclone-type DOWS systems.

Matthews et al. (1996) described the selection criteria used to site three hydrocyclone-type DOWS systems in the Alliance field in east-central Alberta, Canada. From a production standpoint, wells had to have a water-to-oil ratio of 8 or higher and productivity of greater than 1,260 bbl/day. The reservoir had to contain sufficient incremental reserves and provide a suitable disposal zone. The casing had to be at least 5.5 inches in diameter, and the well bore had to have good mechanical integrity and a minimum separation of about 80 ft between the

production zone and disposal zone. The well bore had to be already open below the production zone so that additional drilling would not be necessary.

Peats and Schrenkel (1997) described the selection criteria used to site a hydrocyclone-type DOWS in the Swan Hills Unit One field in Alberta, Canada. Only wells having a water cut of 94% (a water-to-oil ratio of about 16) were considered. Since a DOWS sized to fit in a 5.5-inch casing would be very long and costly, a well with 7-inch casing was preferable to maximise the rate of production and allow for better clearance. Wells with a history of asphaltene and scale problems or wells with high gas-to-oil ratios were avoided.

Stuebinger et al. (1997) identified several screening criteria for DAPS. The most important is the availability of a suitable injection zone that is isolated from and at least 10 ft deeper than the production zone. The pressure required to inject water cannot be excessive. The injection pressure gradient must be less than 0.45 psi per foot of depth. The chemistry of the produced water must be compatible with the injection zone; it is usually inadvisable to mix water from carbonate and sandstone formations. As with all other types of DOWS, the casing must be in sufficiently good condition to withstand setting of a packer and the pressures needed for injection. In order to promote proper gravity separation of oil and water, the wellbore should be as vertical as possible between the upper and lower intakes. Wells producing cold, heavy crude oil with API gravity of 10° or less may not be good candidates for gravity separation. 15°API gravity may be a more appropriate cut off for gravity separation-type DOWS.

To sum up, a good candidate well for DOWS application should meet the following requirement:

(1) A compactable injection zone: The injection zone needs to have sustainable permeability for long-term water disposal, which is the most import requirement for DOWS applications. The injection zone should also be compactable with the injected water, which means the chemical properties of the injected water will not cause severe permeability damage. Due to the uncertain separation efficiencies for various DOWS systems, and the different solids specifications from various production zones, there is no clear criteria for cut-off permeability. However, formations that produce no or little sand are favorable.

(2) Production requirement: The oil should have a gravity of 15°API or higher. The total production should be less than 1,200 bbl/day for a gravity-type DOWS, or higher flow rates for a hydrocyclone-type DOWS with water cut of at least 90%.

(3) Well requirement: The well has to be straight or slightly deviated. The casing had to be at least 5.5 inches in diameter, and the well bore had to have good mechanical integrity and a minimum separation of about 80 ft between the production zone and disposal zone. There is no connection between production zone and injection zone.

2.3 Downhole Gas-Water Separation (DGWS)

DGWS technologies can be classified into two main categories: gravity separation and hydrocyclone separation. The majority of downhole gas-water separation was achieved by allowing gas and water naturally separate in the tubing-casing annulus. The separated gas flows to surface, and the separated water is injected with bypass tools, modified plunger rod pumps, ESPs, and progressive cavity pumps. Few hydrocyclone type separators were also developed, but no field installations have been reported.

2.3.1 DGWS Systems

The simplest DGWS device is a bypass tool in which the bottom end of an insert sucker rod pump is seated (Nichol and Marsh, 1997). The pumping action acts to load the tubing with water from the casing tubing annulus. When the hydrostatic head in the tubing is great enough, the water drains into the disposal zone below the producing perforations and packer. Gas flows up the tubing-casing annulus. The pump provides no pressure for water injection; water flows solely by gravity. Bypass tools are appropriate for water volumes from 25 to 250 bbl/day and a maximum depth in the 6,000 to 8,000 ft range.

A second type of rod-pump operated DOWS uses a modified plunger pump, as seen in Figure 2-5. This system consists of a short section of pipe with one to five ball-and-seat intake valves and an optional back-pressure valve, run below a tubing pump in which the traveling valve has been removed from the plunger. On the upstroke the solid plunger creates a lower pressure area in the barrel, allowing the ball-and-seat valves to open and water to enter. On the down-stroke, the plunger

moves the fluid down and out of the barrel and into a disposal zone below the packer. This type of DGWS can generate higher pressure than the bypass tool, which is useful for injecting into a wider range of injection zones. Modified plunger rod pump systems are better suited for moderate to high water volumes (250 to 800 bbl/day) and depths from 2,000 to 8,000 ft (Veil and Quinn, 2004).

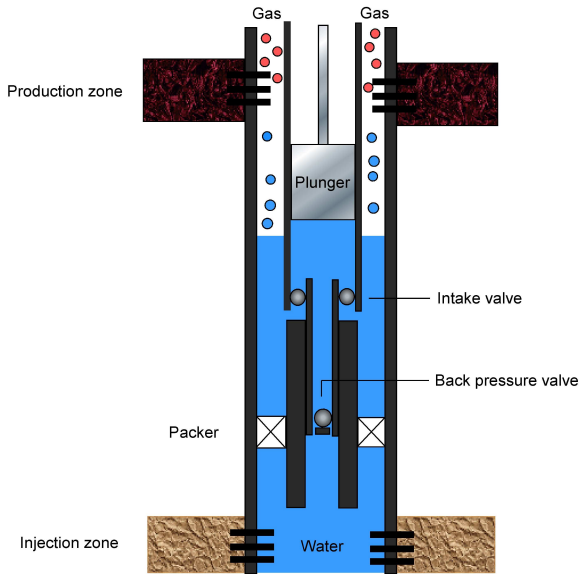

Figure 2-5: DGWS with modified plunger pump

ESPs are commonly used in the petroleum industry to lift fluids to the surface. In a DGWS application, they can be configured to discharge downward to a lower injection zone. A packer is used to isolate the producing and injection zones. ESPs can handle much higher flow rates (above 800 bbl/day) and can operate at great depths (more than 6000 ft). They do require a substantial supply of electricity that is not always available in the field. ESPs are available from many suppliers. Centrilift and REDA (now part of Schlumberger) both offered DGWS systems using ESPs in 1990s.

The fourth type of DGWS uses progressive cavity pumps. For DGWS applications, the pump is configured to discharge downward to an injection zone, or the pump rotor can be designed to turn in a reversed direction. In an alternate configuration, the progressive cavity pump can be used with a bypass tool. Then the pump would push water into the tubing, and the water would flow by gravity to the injection formation. Progressive cavity pumps can handle solids (sand grains or scale) more readily than rod pumps or ESPs. Weatherford offered a DGWS system using progressive cavity pumps.

C-FER Technologies developed two types of hydrocyclone gas-water separators. One type uses a one-stage hydrocyclone to separate water and gas, and a centrifugal pump to inject the separated water. The other type uses two stages of hydrocyclone: the first hydrocyclone separates gas and liquid, and the second stage separates oil from liquid.

2.3.2 Previous DGWS Installations

Compared with DOWS data, DGWS data are relatively incomplete. Among the 62 of the DGWS installations worldwide, 39 of the installations were in the United States, with Oklahoma (20) and Kansas (12) heading the list; 22 installations were in Alberta, Canada. 57% of the installations (35) used modified plunger rod pump systems. Bypass tools were used in 19 installations, and ESPs were used in 7 installations (Veil and Quinn, 2005).

Table 2-3 again attempts to relate success or failures of applications to geology conditions. It can be seen the Sandstone/Sandstone combination gains higher success rate (94%) than that for Carbonate/Carbonate combination (70%). However, the authors are not confident enough to draw the conclusion. Data in Table 2-3 also shows that the overall success rate for DGWS applications is only 61%, similar to that for DOWS applications (59%).

Table 2-3: DGWS performance and geology environment

Geology of producing formation/injection formation	Trials rated success	Trials rated failure	Total number of trials	Trials rated success (%)	Trials rated failure (%)
Carbonate/Carbonate	7	3	10	70	30
Carbonate/Sandstone	1	0	1	100	0
Coal/Sandstone	3	2	5	60	40
Sandstone/Sandstone	15	1	16	94	6
Sandstone/Unknown	0	3	3	0	100
Unknown/Unknown	12	15	25	48	52
Total	38	24	62	61	39

For water production rates less than 50 bbl/day, conventional surface disposal is most cost effective. Bypass tool systems are more cost effective in the 25-250 bbl/day range, up to a maximum depth of about 8,000 ft. A modified plunger system was shown to be most cost effective for 250-800 bbl/day over about the same depth range. For high water rates (above 800 bbl/day) and depths below 6,000 ft, ESP systems are typically more cost-effective.

A DGWS system stands the best chance of success when it is installed in a well with: well cemented casing, minimal sand production, soft water (minimal scaling), water production of at least 25-50 bbl/day, disposal costs above $25-$50/day, and a low pressure, high injectivity disposal zone below the production zone. These criteria are similar to those for DOWS.

2.4 Recent Activities in Downhole Separation Technology

DOWS developments and new installations have been mostly stagnant for the past few years. The lack of DOWS sales has changed the DOWS market. In 1998, three companies were actively marketing DOWS tools in the United States: Centrilift, REDA Pumps, and Dresser/Axelson. During 2002, only Centrilift continued to market this technology. By 2004, none of these companies were promoting DOWS.

Because of low DOWS sales, Centrilift currently does not actively market its DOWS tools any more. REDA was subsequently taken over by Schlumberger, which reports that REDA's DOWS tool Aqwanot is no longer being marketed because it was not sufficiently reliable.

Texaco was a leader in developing the gravity-type DOWS sold by Dresser/Axelson. However, since 1999, Texaco's DOWS team has been disbanding. One Texaco well with an installed DOWS was sold, and the DOWS was removed from the well.

Kudu Industries provides a downhole water injection tool that relies on a progressing cavity pump and a Chriscor downhole injection tool. Chriscor Downhole Tools is now a division of Kudu Industries. The Chriscor tool is installed with a beam pump or a progressive cavity pump and has a bypass area that allows the water in the tubing string to move downward.

In Canada, Quinn Pumps marketed several DOWS tools in the late 1990s but has not made many installations during recent years. Quinn is still marketing downhole separation systems but has focused more on gas wells rather than oil wells. Quinn Pumps has two DGWS technologies available. One is the Q-Sep Gas T, which pumps water off a gas well and directly injects the water into a disposal zone in the same wellbore. The Q-Sep Gas R, which is coupled with a Chriscor injection tool, pumps the water upward, where it flows by gravity to the injection zone.

Centrilift developed and installed an ESP-DGWS tool called GasPro in 2002, which has the ability to control the water disposal rate. Centrilift also has a progressing cavity pump DGWS system. But these tools are no longer being sold.

C-FER Technologies is a developer rather than a vendor. C-FER played an active role in developing the original hydrocyclone-type DOWS systems and continues to develop new DOWS technologies, such as the gas-lift DOWS. C-FER is also engaged in developing hydrocyclone type DGWS to handle high gas flow rates.

What resulted in so few installations recently? Downhole separation technology is theoretically feasible, but technically immature. Even though some applications gained benefits, the overall success rate is only 60%. High cost and low reliability have slowed down the acceptance of this relatively new technology.

It is common sense that deploying more downhole tools leads to more risks and failures. Downhole separation systems generally combine two pumps, one motor and one separator. Multiple components inevitably brought more problems. Moreover, downhole separation is a very complicated process. The downhole environment can be very different from well to well. Production rate, water cut, pressure, temperature, and the related fluid properties all affect the efficiencies of the separators and pumps. However, the in-depth knowledge of these effects has not been fully understood. As a result, the system optimisation is indeed a trial-and-error process. It is unlikely that a system with so many unknowns can function properly. It is also unlikely that one design can suit many wells.

Above that, most of the DOWS and DGWS systems were installed in wells with poor integrity. The installations were mostly trials in nature, thus the wells with minor importance but with loads of problems were selected. The common problems for aged wells include bad cement, sand production, and low liquid supply. All of the

above problems can fail downhole separation and injection processes. In other words, these wells were not producing properly even under mature production technologies, it is unlikely that they can be saved by downhole separation technology.

2.5 Potential of Downhole Separation Technology

Like other fields in the world, Australia's offshore gas fields are producing large amount of water. The production data of Barrow Island in 2005 are listed in Table 2-4. The water production from Barrow Island in 2005 averaged about 50,000 bbl/day. Chevron's Thevenard Island asset is producing similar amount of water (DoIR, 2006).

Table 2-4: Production data of Barrow Island in 2005

Date	Oil production (bbl)	Water production (bbl)	Gas production (km^3)
Jan. 2005	233,415	1,544,428	3,949
Feb. 2005	214,885	1,443,964	3,513
Mar. 2005	235,309	1,593,138	3,881
Apr. 2005	215,583	1,512,236	3,684
May. 2005	218,219	1,519,784	3,724
Jun. 2005	221,521	1,560,341	3,836
Jul. 2005	233,063	1,609,510	4,169
Aug. 2005	224,641	1,571,406	4,025
Sep. 2005	213,281	1,658,554	3,691
Oct. 2005	222,647	1,526,533	4,013
Nov. 2005	210,696	1,448,040	4,055
Dec. 2005	215,690	1,566,292	4,196
Annual total	2,658,950	18,385,636	46,737

Unlike other fields in the world, offshore Australia is more environmentally sensitive. Produced water from Woodside's Enfield and Chevron's Thevenard Island has to be injected back to the reservoir rather than dumped overboard. If downhole separation technology is employed, not only the energy to lift the produced water is saved, the environmental issue is also solved.

It is an appealing idea to apply DGWS technology to the gas fields in Australia's Northwest shelf. However, the available downhole separation technology is neither mature nor applicable to Australia's gas fields. The developed DGWS system separates gas and water in the tubing-casing annulus, which indicates the gas flow rate is very low. The gas fields in Australia can produce several million SCF of gas per day. Gas at this flow rate can not be separated in the annulus by gravity.

Researchers at Commonwealth Scientific Industrial Research Organisation (CSIRO) and Curtin University of Technology are developing a novel systematic solution for the gas wells in Northwest shelf. This project is divided into three aspects to tackle the problems encountered in previous installations. First, a prototype separator was designed and is being tested in CSIRO's fluid mechanics laboratory to optimise the separation process. To improve the separation efficiency, CFD (computational fluid dynamics) simulation package is used to study the separator's behaviors under various conditions. With the test data from the prototype separator and the simulation results from CFD, separator designs can be customised for wells with unique characteristics. Third, the choice of candidate wells is crucial for a successful application. As discovered earlier, it is crucial to study the damage caused by the impurities in the produced water, hence being able to predict the reactions from the injection zone. Based on the results, candidate wells can be selected more scientifically to reduce the risk. This thesis tackles the third issue.

Nevertheless, reducing water production is not the only benefit of downhole separation technology. One of the main functions of an offshore platform is to separate oil and gas from water. If a downhole separator is successfully deployed, the produced gas will contain minor amount of water. This will not only greatly reduce the risk of hydrate formation, bust also reduce the load of the platform, so that more gas can be produced.

In the future, if a subsea dehydration unit is installed to remove nearly all of the water content in the produced gas, then the dry gas can flow directly to shore through tiebacks. If the blueprint in Figure 2-6 comes true, a platform is no longer necessary. Because this subsea system could save the high costs in platform construction and operation, many small and remote deepwater reservoirs that can not be developed economically with a platform may become economical. Downhole separation technology may hold the key to a new era of offshore development.

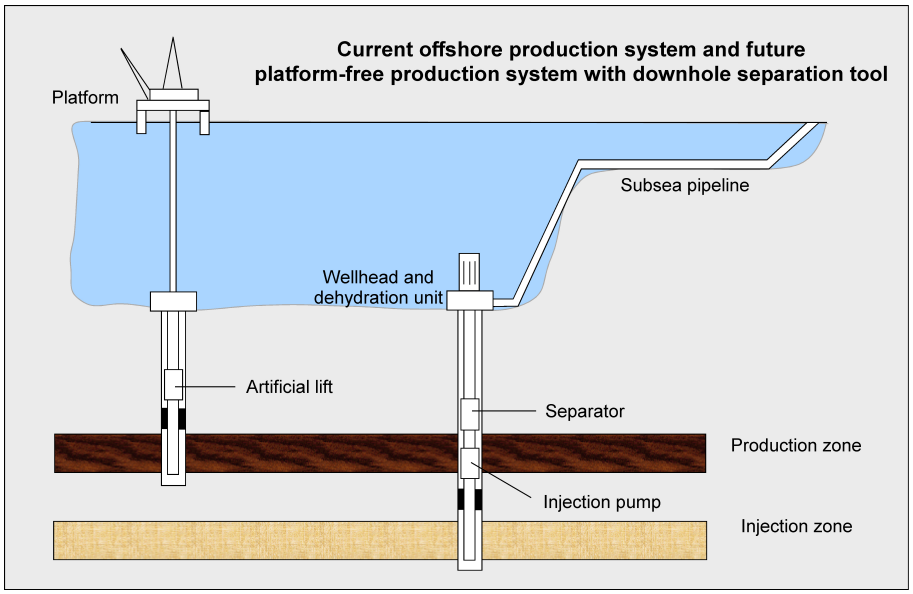

Figure 2-6: Future platform-free field with downhole separation technology

2.6 Concluding Remarks

- Downhole separation technology has great potential in gas well dewatering and deepwater reservoir development.

- Downhole separation technology is theoretically feasible, but technically immature. Based on the review, only about 60% of the worldwide applications were successful. This low reliability slowed down its adoption. As a result, most service companies have abandoned downhole separation tools.

- The most recognised problem from the previous applications is the injectivity decline during injection of separated water. The impurities in the injected water clogged the formation and caused the whole process to fail.

- Previous experimental work should be reviewed and analysed to gain better understanding of the factors affecting reservoir permeability decline under produced water re-injection.

CHAPTER 3

MAJOR FACTORS AFFECTING

PARTICLE RETENTION IN POROUS MEDIA*

3.1 Introduction

As explained in the previous chapter, reservoir rocks that bear oil and gas are porous media and can be severely affected by particle invasion. In petroleum industry, impairment of rock permeability by particles is referred to as an aspect of formation damage and it can happen in many operations.

Drilling, completion, and workover fluids generally contain large amounts of particles in order to balance reservoir pressure. Once these fluids come in contact with the reservoir, these particles may invade and clog the pores, reducing the permeability of the rock and causing severe loss of productivity.

In water flooding, produced water re-injection (PWRI), or water disposal projects, suspended particles in the injected water can cause the injection wells to become impaired. Even though the solid concentration in injected water is much lower than that in drilling fluid, the quantity of injected water is usually very large and these solids may still lead to serious damage on rock permeability.

Moreover, once formation damage has occurred, it is unlikely to be completely removed by subsequent treatment. As a result, the composition of any fluid that comes in contact with the reservoir formation has to be carefully selected to minimize the potential for causing formation damage.

In water treatment process, deep-bed filters have been in common use for more than 100 years. Deep bed filtration removes impurities in waste water by flowing it through a packed bed of solids. Its greatest application is in drinking water filtration and final filtration of waste water before discharge into natural environment (Rushton, 1996). Researchers have been studying the filtration process to improve efficiency of deep bed filters.

* *Published in Emirates Journal of Engineering Research, Vol. 12, Issue 3, 1-7.*

Although the research on particle retention in porous media has been conducted for many years, its understanding is still limited. Formation damage takes place in the near wellbore region. The reservoir simulators in the market cannot quantify the severity of formation damage and the user simply applies an overall skin factor to the near wellbore region to account for the damage.

Many experiments have been conducted to investigate the factors that affect the complex process of particle retention in porous media. It is meaningful to summarise the findings from previous experiments to gain better understandings.

3.2 Field Experiences

Several authors reported injectivity declines for PWRI projects. Mature fields produce large amounts of water. Produced water can be from natural water drive, injected water, or usually a combination of both. As oil and gas production declines, water production increases and water cuts can exceed 90% in many mature fields.

Produced water contains various impurities and pollutants, including organic and inorganic particles, hydrocarbon droplets, and treatment chemicals. As such, to avoid or reduce environmental impact, produced water needs to be carefully treated before being released into the environment. It thus presents significant costs and potential risks for oil and gas producers. Alternatively, produced water is injected back into the reservoir to maintain reservoir pressure. This is especially the case in onshore fields. More and more offshore fields are also adopting PWRI to minimise waste water discharge.

Filtration is usually used to reduce the concentration of suspended solids in water prior to injection, but the high costs of water treatment should be justified against other alternatives, such as periodic well stimulation. In many mature fields, untreated water is injected to reduce the costs. Also due to the high costs, water can only be filtered to a certain level, generally between 10 and 50 microns (μm). Smaller impurities are carried by the water and injected into the formation. These impurities can still cause severe injectivity decline.

For example, many injection wells in the Lost Soldier Unit located in central Wyoming demonstrated severe injectivity decline, even though the mean size of the particles in the injected water was as low as 3 microns (Rickford and Finney, 1991).

On average, injection rates dropped by 35 to 40% per year, and the wells were frequently worked over to maintain injection rates.

The wells in the Forties field in North Sea also demonstrated continuous injectivity decline during produced water re-injection (Paige and Murray, 1994). The injection rate deceased from 38,000 bbl/day to 13,000 bbl/day in 500 days.

Another field case is the offshore Siri field in the southern Persian Gulf (Moghadasi et al, 2004). To maintain reservoir pressure and to increase oil recovery, water injection was started in 1984 at a rate of 9,100 bbl/day. However, the injectivity declined until the injection was stopped in 1990, when the water injection rate had dropped to 2,200 bbl/day.

Another 5 wells in the Gulf of Mexico demonstrated even faster decline (Sharma et al, 2000). The water injection rate declined from 7,000 bbl/day to less than 1,000 bbl/day in just 200 days. In this case, the particles in water were filtered to 10 microns, yet the decline was very severe.

In the above cases, suspended particles in the injected water were identified as the cause of injectivity decline. As we can see, the severity of injectivity decline varies from case to case, depending on the particle sizes, solid concentrations, and different reservoir properties. A reservoir with high porosity and high permeability tends to sustain its injectivity longer.

3.3 Mechanisms of Particle-Induced Formation Damage

Particle movement in porous media is a very complex process due to the complexity of porous media and forces governing solids movement in porous media. The paths of the solids are determined by numerous factors, such as the shape of the particles and their surface properties, the morphology of the medium, the chemistry of the carrying fluid, the flow field in the pore space, and various interaction forces between the particle and the medium. These factors acting together significantly affect the particle transportation, adsorption or deposition and the resulting reduction in the permeability of the porous medium.

Once entrained by the fluids flowing through porous media, the various particles can be captured by three primary mechanisms (Civan, 2000): (1) adsorption of the

particles because of the Brownian motion, and the electrostatic interaction between the migrating particles and the solid surface of the pores; (2) size exclusion when the effective size of the pores are smaller to those of the migrating particles; (3) sedimentation or gravity settling when the densities of the moving particles and the carrying fluid are very different. These mechanisms are illustrated in Figure 3-1.

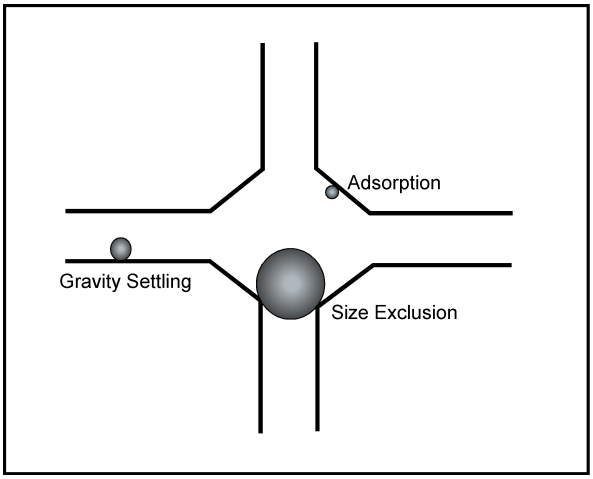

Figure 3-1: Mechanism for particle capture

For sub-micron particles, adsorption due to Brownian motion is dominant. For the particles with sizes comparable to or bigger than pore neck, pore-throat bridging and size exclusion are likely to be dominant. The particles with sizes in between are likely to settle down due to gravity.

When multiple particles invade the porous media at the same time, the damage mechanism becomes more complicated. Deposited particles reduce the flowing path inside the porous media, thus increasing the possibility of bridging. Large particles may form a filter cake on the face of the rock, namely external cake formation. Small particles may invade the formation, bridge, and form an internal filter cake, namely particle invasion, internal cake formation or deep bed filtration. Since the solids are of various sizes, the damage can be attributed to more than one mechanism, as shown in Figure 3-2.

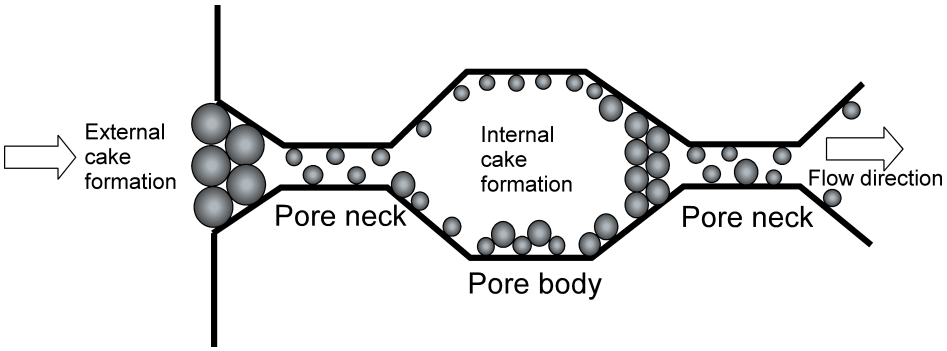

Figure 3-2: Mechanism for formation of filter cake

3.4 Review of Previous Experiments

The research in particle transport in porous media has been active since 1950s. Two types of experimental methods have been developed to test the permeability impairment caused by suspended solids. In the early years, membrane filter tests were used. In the recent years, core flowing tests have become the standard method.

Different researchers used very similar test apparatus, as illustrated in Figure 3-3. A stirrer keeps the particles suspended in the tank. A pump sends the mixture through the core holder. And the differential pressure transducer monitors the pressure loss across the core, which translates into permeability decline. In some cases, pressure taps are installed along the core holder to monitor the damage profile.

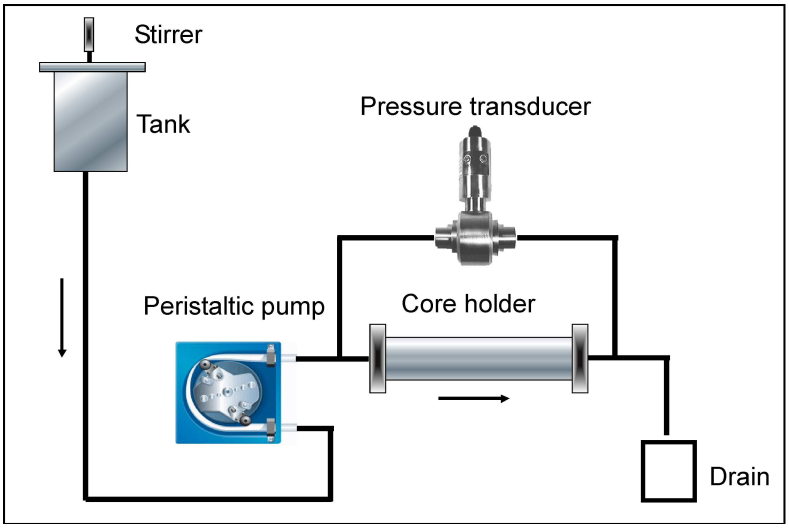

Figure 3-3: A typical test apparatus

Table 3-1: Test parameters used in some previous experimental studies

Author information	Todd et al. (1984)	Vetter et al. (1987)	Baghdlklan et al. (1989)	Todd et al. (1990)	Roque et al. (1995)	Moghadasi et al. (2004)
Tested porous media	Sandstone cores	Berea sandstone cores	Ottawa sand pack	Clashach sandstone core	Sandstone cores	Packed glass beads
Media length (cm)	7.62	3.8 to 5.1	32.2	8	About 10	58
Media diameter (cm)	2.54	2.54	6.3	2.54	5	3.2
Media porosity (%)	15.9 and 19.8	21	37.5	14.5	10.2 to 17.4	38
Media permeability (Darcy)	0.562 to 2.012	0.1 to 0.2	8.0	0.2 to 1	0.224 to 3	161
Test particle	Alumina particles	Chromium Oxide and Cerium Oxide particles	Kaolin and Bentonite clay	Alumina particles	Latex particles	Alumina particles
Particle diameter (μm)	0 to 10	<0.06, 0.05, 1.0 and 7.0	Mostly < 1	0 to 3	0.8 to 7.6	7 and 16
Particle concentration (ppm)	5	90, 250 and 500	200 to 4000	1, 5, 10 and 15	2 to 20	500, 1000 and 2000
Flow rate (ml/s)	1.8	0.033 to 0.167	0.09 to 0.36	0.45 to 1.80	0.012 to 1	0.42 and 0.83

Todd et al. (1984) injected aluminum oxide particles through Clasach and Lochaline cores. The test conditions are listed in Table 3-1. To quantify the damage at different depth, they measured pressures along the 3 inch (7.6 cm) long core. The cores damaged by particles of 0 to 3 microns exhibit damage throughout their entire lengths, and no external filter cake was observed; The particles with sizes of 4 to 6 microns caused more severe damage to the first 12 mm of the core, and no external filter cake was visible; The 8-10 micron particles caused the first 5 mm of the core to lose 90% of its permeability, and filter cake was apparent.

Vetter et al. (1987) conducted particle-filtration tests to study the effects of particle sizes, flow rates, particle concentration and particle charges. The test conditions are listed in Table 3-1. It was concluded that particles of all sizes (from 0.05 to 7 microns) cause formation damage. The larger particles cause a rapid decline in permeability with shallow damage. Smaller particles (in the sub-micron range) enter the core and cause a gradual permeability decline. Fluid flow rate is another important factor. The higher the linear flow rate, the less severe is the damage to the core plug. Third, higher particle concentration causes more severe damage. Fourth, NaCl, anionic and cationic surfactants were added to the suspensions and the resulted damages were much more severe. This shows the ionic strength of the fluid also has effects on particle retention in porous media.

Baghdlklan et al. (1989) injected kaolin and bentonite clay suspensions through packed sand. The sizes of clays in the suspension are mostly in the sub-micron range. The test conditions are shown in Table 3-1. Their reported data were among the most complete, including measurements of particle size and pore size distributions. The authors tested the effects of flow rate, solid concentration, pH and ionic strength. The results showed that clay suspensions at low flow rates, high particle concentrations, high ionic strengths and low pH cause more rapid permeability reduction, which agrees with the findings of Vetter et al. (1987).

In another study by Todd et al. (1990), suspended solids were injected through pressure-tapped Clasach sandstone cores to study the effects of flow rates and particle concentrations similar to North Sea situations. The test conditions are listed in Table 3-1. The injection duration was very large, up to 144 hours or 60000 pore volumes. They first compared the tests results for broken-faced core and cut-faced core. For cut-faced cores, the scanning electron micrographs taken before core flowing tests showed the presence of fine particles at the core face resulted from

cutting the end face with a saw. At the end of the experiments, an external filter cake is clearly seen on the inlet face of the cut-faced core, but is not so obvious on that of the broken faced core. Their experiments for the first time revealed a simple semi-log relationship between permeability decline and flow velocity, also between permeability decline and particle concentration. Their test results show that smaller velocities and larger particle concentrations result in greater permeability decline. The four pressure transducers along the core indicated that the first 5 mm of the core was most severely damaged, while the damage spread to the whole core.

Roque et al. (1995) injected latex particles with various sizes to 15 sandstone cores to study the effect of flow rate. Their test conditions are listed in Table 3-1. In some cases, the average pore size, the invasion depth and effluent concentration were also measured. The test data agree with previous findings: lower flow rates lead to greater damage. Their test data also revealed an interesting trend: particles under same linear flow velocity caused very similar damages, regardless of the particle diameters and particle concentrations.

Moghadasi et al. (2004) injected Aluminum Oxide solids through the porous media formed by packed glass beads. The test conditions are listed in Table 3-1. The glass beads were of a quite large diameter, which resulted in an extremely high permeability. The test section has 6 pressure taps along its length, each of them connected to a separate pressure transducer. They tested the effects of flow rates, particle concentrations and particle sizes on permeability reduction. Their results agree with previous findings.

3.5 Analysis of Previous Findings

Thirty years have passed since Abrams first proposed the “1/3-1/7” rule-of-thumb (Abrams A., 1977). He proposed that particles larger than 1/3 of the pore diameter can bridge at pore throats and form an external filter cake; Particles smaller than 1/3 but larger than 1/7 of the pore diameter invade the formation and form internal cake; Particles smaller than 1/7 of the pore diameter are carried through and cause no damage. Later, a new rule of “1/3-1/14” was proposed by Van Oort et al. (1993) based on new developments.

Unfortunately, both the “1/3-1/7” and “1/3-1/14” rules were proved invalid by many experimental studies. Experimental studies show that particles with sizes much smaller than the mean pore size of the porous media can still cause severe permeability damage. Due to the complex nature of porous media and injected fluids, a simple criterion is unlikely to be sufficient to describe transport and capture of particles in porous media.

The previous test results have shown that flow rate, particle concentration, particle size, fluid pH and fluid ionic environment all have certain effects on the permeability damage. In this section, these factors are analyzed individually.

3.5.1 Effect of Flow Rate and Fluid Velocity

Previous tests reveal that lower flow rate causes greater damage, and higher flow rate leads to greater invasion depth. This indicates that particles under low flow rate settle down very quickly, resulting in severe and shallow damage to the core. Higher flow rate can carry the particles further, thus the damage is averaged along the core. This mechanism is easy to understand but difficult to quantify. Each porous medium has unique pathways. As a result there is a very high uncertainty while determining the location where a particle settles.

Nevertheless, Figure 3-4 plots flow rates versus T75 based on the test data by Todd et al. (1990). T75 is defined as the pore volumes injected when the overall permeability of the core decreased to 75% of its original permeability. It is apparent that lower flow rate leads to smaller T75 (i.e., more damage).

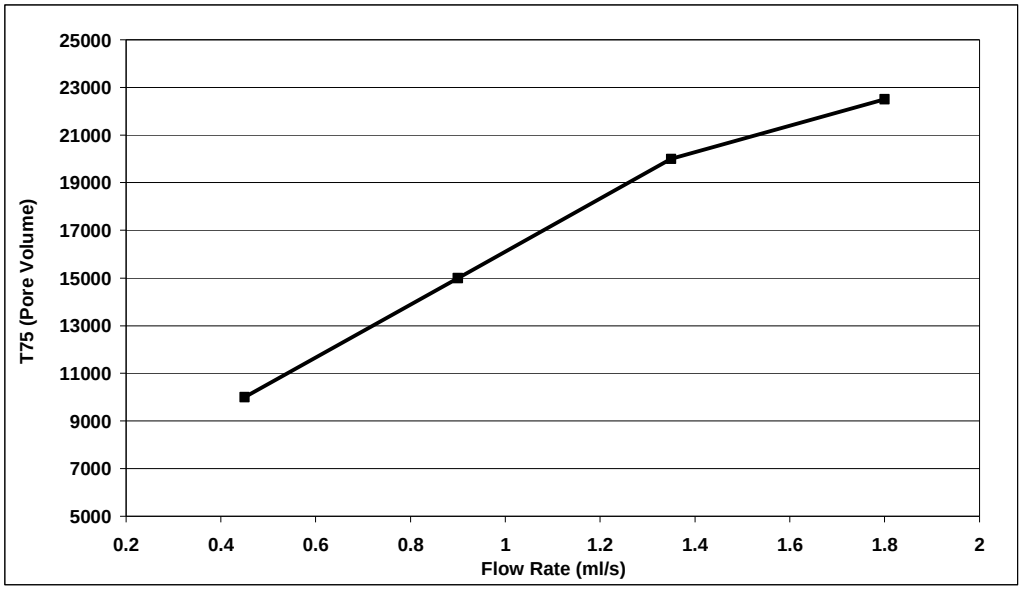

Figure 3-4: Effect of flow rate on permeability reduction

3.5.2 Effect of Particle Concentration

It is obvious that higher particle concentration leads to greater damage. Higher concentration leads to more deposition and also increases the tendency of pore throat bridging. Figure 3-5 shows the effect of particle concentration on T75 based on the test data from Moghadasi et al. (2004).

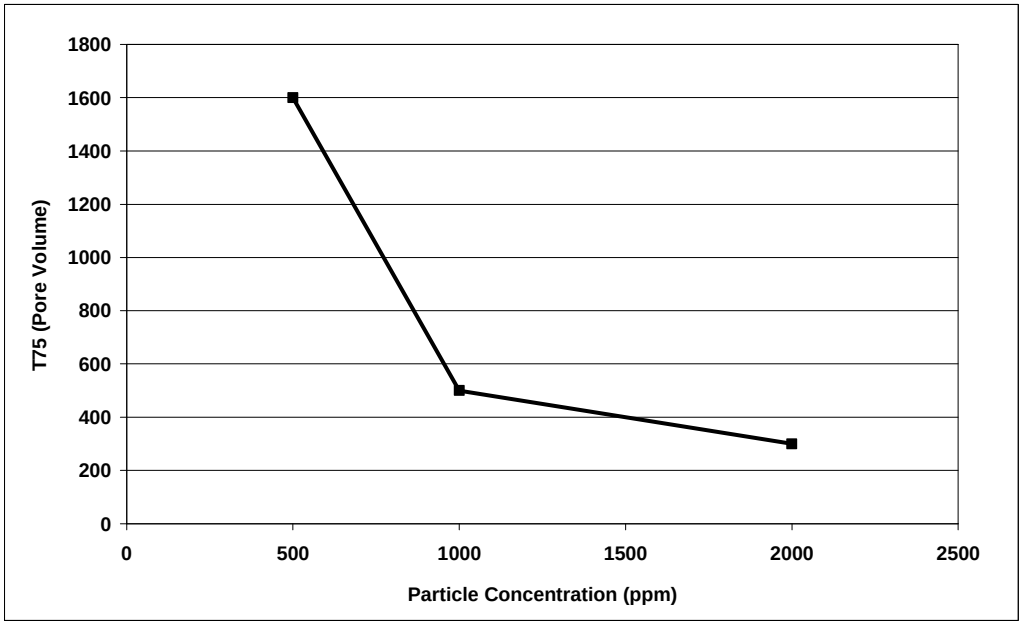

Figure 3-5: Effect of particle concentration for large particles

Another group of test data (Baghdlklan, 1989) with much smaller particles sizes and a sand pack with much lower permeability revealed a close to linear relationship between T75, T50 and particle concentration, as seen in Figure 3-6. T50 is defined as the pore volumes injected when the overall permeability of the core decreased to 50% of its original permeability.

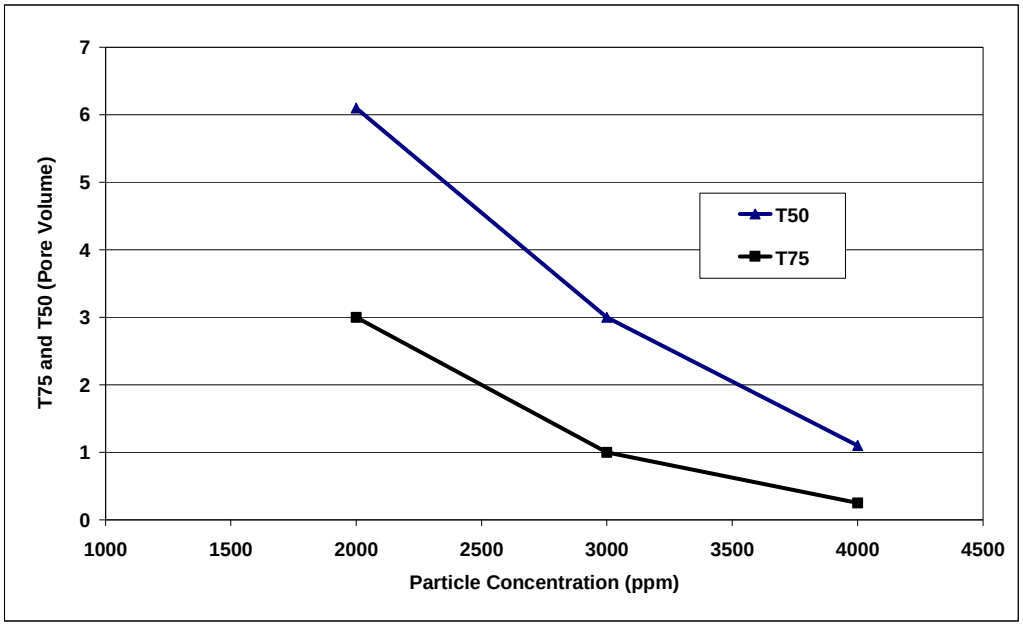

Figure 3-6: Effect of particle concentration for colloidal particles

Figures 3-5 and 3-6 indicate that the impairment mechanisms are different for large particles and small particles. For small particles, the damage is almost proportional to increase of particle concentration. This indicates that surface deposition is the main cause of permeability decline, since the amount of deposit increases linearly with time. For large particles, a much greater damage was observed when the concentration increased from 500 ppm to 1,000 ppm, which may be attributed to pore throat bridging as the main cause of permeability reduction.

3.5.3 Effect of Particle Size

A study by Todd et al. (1984) shows that bigger particles cause more damage, as seen in Figure 3-7. Large particles have higher tendency to settle down and block or bridge at the pore throat, causing more severe damage.

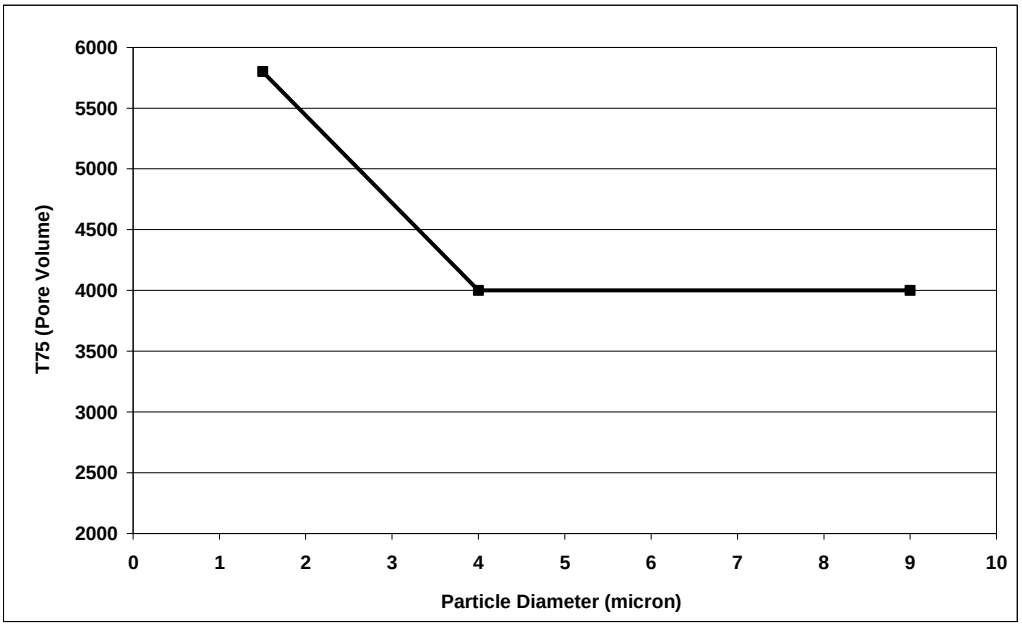

Figure 3-7: Effect of particle size on permeability reduction

Todd et al. (1984) also measured the pressure along the core, which translated into the permeability for different sections of the core. For small particles (0 to 3 microns), the first section lost about 50% of its original permeability, and the last section lost about 20% of its original permeability. While for large particles (8 to 10 microns), the first section lost about 90% of its original permeability, and the last section lost only 5% of its original permeability. In other words, large particles have higher settling tendency and cause severe but shallow damage.

3.5.4 Effect of Ionic Strength

The research on the effect of ionic strength was done by adding salts, commonly NaCl or KCl to the injected fluid.

Chang and Vigneswaran (1990) added NaCl to the injected solution and observed similar phenomena: more particles deposited when NaCl concentration increased from 8.6×10^{-4} mol/L to 0.438 mol/L. Similar phenomena were observed when Comprere et al. (2001) added $CaCl_2$ into clay suspensions. Baghdlklan et al. (1989) tested the effect of KCl concentrations and found that the damage was more severe at high salt concentration. Addition of KCl to Kaolin suspension and Bentonite suspension led to more severe permeability damage.

This phenomenon is attributed to the salts' ability in reducing the ζ-potential of particle surfaces, resulting in more particles colliding with pore surface (Eastman, 2005). However, this phenomenon may have more complex mechanisms behind. Baghdlklan et al. (1989) also measured the particle size distributions of the Kaolin suspension at two KCl concentrations. It was revealed that the distribution shifted towards larger particle sizes at higher KCl concentration.

Santiwong et al. (2008) observed the filter cake under microscope and discovered that the structures of deposits are different at different pH. At low ionic strength, the deposit shows a honeycomb-type structure. While at high ionic strength, the clay particles form denser yet more permeable deposits. This indicates that salts not only accelerate particle aggregation, but also alter deposit structures.

3.5.5 Effect of Solution pH

Baghdlklan et al. (1989) tested permeability decline under fluid pH numbers of 2.5 and 10. The test results revealed the effect of pH was not significant. Stephan and Chase (2003) injected clay suspensions into Berea sandstone cores. The average size of the injected clay was 1.45 microns. The objective was to study permeability decline at various salt concentrations and pH numbers. The test data revealed that permeability decline was much more severe with low salt concentration and low pH.

Santoro and Stotzky (1967) studied the effect of pH on particle size distribution. They discovered that particle size distributions are narrowest at pH 5-8 and become wider at higher or lower pH. This means that particles may aggregate at high or low pH, and the generated larger particles can lead to more deposition inside porous media.

3.5.6 Effect of Presence of Organic Compounds

For PWRI projects and deep bed filtration, oil droplets commonly coexist with suspended particles. Few researches were conducted to inject particles together with oil droplets into porous media. Zhang et al. (1993) conducted experiments with 40 sandstone cores. The cores had permeability lass than 550 mD. The injected oil droplets and solids had mean sizes less than 10 microns. Oil concentration was less than 500 ppm and solids concentration was less than 50 ppm. More severe damages were observed while oil droplets were injected together with particles, and

damage spread further along the core. Their findings are supported by Ali et al. (2007). Another study showed that addition of organic substance such as Fulvic acid greatly enhanced capture of particles (Jegatheesan and Vigneswaran, 1997). However, it is not confident to draw conclusions with the limited studies conducted.

3.5.7 Invasion Depth

Many factors determined how far a particle travels inside a porous medium. Large particles tend to settle down quicker than small particles. Particles with high density tend to settle down quicker than light one. High flow rate (velocity) can carry particles further inside a porous medium. And the capture of particles is also greatly affected by the characteristics and internal structure of the porous media, such as pore size and tortuosity. The surface charges of the particles and pore surface also have effect on how far a particle travels.

Theoretically, the invasion depth is the furthest distance any injected particle can travel in a porous medium. However, the many parameters involved make it impossible to give a definite measurement of invasion depth. Previous tests revealed that the damage generally spread to the whole core. But it was very clear that the rock sections close to the injection entrance are always much more severely damaged than the deeper sections.

As such, there is no definite cut-off point for invasion depth. Invasion depth generally refers to the length of the most severely damaged section. The following invasion depths were reported: 12mm (Todd et al., 1984), 12mm (Van den Broek et al., 1999), 15mm (Zhang et al., 1993), 25mm (Moghadasi et al., 2004), 35mm (Roque et al., 1995), and 40mm (Al-Abduwani et al., 2003). Therefore, it may be safe to say the invasion depth is generally less than 50mm.

3.6 Concluding Remarks

- Particle deposition in porous media is a complex process due to the complex nature of porous media and the properties of injected particles and fluids. This process is controlled by many factors.

- Since 1950s, abundant experiments have been conducted to study particle-induced permeability damage. The need to run more experiments is

minimal. These tests focused on the effects of particle concentration, flow rate, particle size, fluid pH and ionic strength.

- Previous test results reveal that fluid flow rate, particle size, particle concentration, and fluid ionic strength all have significant effects on capture of particles. Low fluid velocity and large particle size lead to shallow and severe damage. Higher particle concentration causes more severe permeability damage. The particle invasion depth is generally less than 50 mm into the porous media.

- In next chapter, the models for the capture of particles in porous media are examined.

CHAPTER 4

MODELS OF POROUS MEDIA

AND PARTICULATE-INDUCED FORMATION DAMAGE*

4.1 Introduction

The prediction of transport properties of porous media is a long-standing problem of great theoretical and practical interests, with particular applications to petroleum reservoir engineering. The microscopic properties of porous rock, such as the absolute and relative permeabilities, and the drainage and imbibition capillary pressure curves, are intimately related to the fluid flow in porous rocks. The determination of these properties is vital to the estimation of reserves, reservoir simulation and production forecast, and is the subject of laborious experimentation. Therefore, much effort has been devoted to simulation of porous media and their properties.

4.2 Established Models of Porous Media

The earliest studies consider porous media as a bed packed with spheres (Smith, 1932). However, the complexity of the pore geometry in the packed bed prevented the derivation of any accurate descriptions of fluid flow in porous media.

Later, capillary tube model was proposed to simulate the microscopic structure of porous media (Carman, 1938). The approach assumes the pores as a bundle of capillary tubes with a size distribution measured by mercury injection. With the bundle of tubes model, the flow properties of the porous media can be easily derived. This model has been used with fair success to correlate certain properties of porous media. However, bundle of tubes model oversimplifies the structure of porous media. For example, one of the most distinguished features of porous media is the interconnectivity of pores. But the bundle of tubes model fails to incorporate this feature.

** Accepted for publication in APPEA Journal with some modifications*

Fatt (1956) first pioneered the work in pore network model with pencil and paper calculations. He ingeniously combined the advantages of packed bed model and bundle of tubes model. The premise of network models is that the void space of a porous medium can be represented by a network of interconnected pores in which larger pores (pore bodies) are connected by smaller pores (pore throats). He proposed that networks with various structures can represent a porous medium, as shown in Figure 4-1. Fatt (1956) also derived the capillary pressure curves and relative permeability curves for the proposed structures.

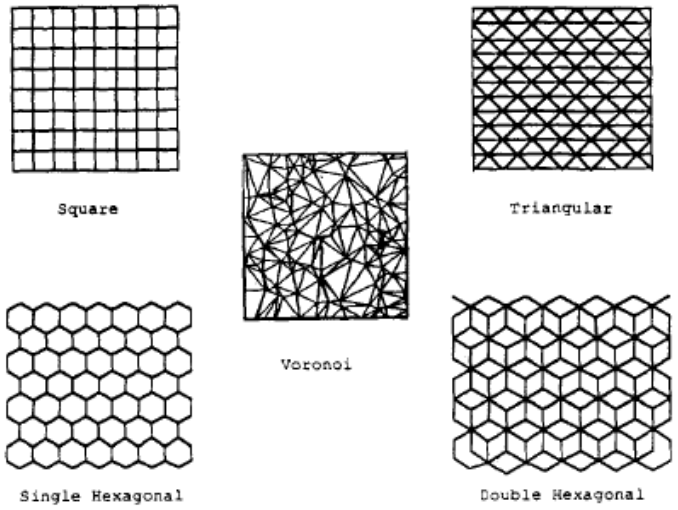

Figure 4-1: Various network structures

Due to the high demand in computation, the development of network models was stagnant for many years. With the availability of modern computers, the applications of network models have become more active since 1990s. Table 4-1 lists some of the distinguished publications in this topic. A more detailed evaluation of network models can be found in a literature review in this topic (Blunt, 2001).

Pore network models assume porous media as certain structures, by which the calculation of microscopic flow fields becomes possible. Despite the assumptions and simplifications, network models have been successful in studying displacement processes in porous media. As seen in Table 4-1, most applications of network models were devoted to the simulation of relative permeability curves.

Table 4-1: Previous applications of network models

Authors	Type of network	Objectives of simulation
Fatt (1956)	2-D network	Relative permeability curves
Rege and Fogler (1988)	2-D network	Deep bed filtration
Imdakm and Sahimi (1991)	3-D network	Capture of particles
Hampton et al. (1993)	2-D network	Filter clogging
Constantinides and Payatakes (1996)	2-D network	Relative permeability curves
Oren et al. (1998)	3-D network	Relative permeability curves
Tsakiroglou and Payatakes (2000)	2-D network	Drainage and imbibition
Maximenko and Kadet (2000)	2-D network	Relative permeability curves and polymer flooding
Patzek (2001)	3-D network	Relative permeability curves
Blunt et al. (2002)	3-D network	Relative permeability curves
Chang et al. (2004)	2-D network	Deep bed filtration
Stevenson et al. (2005)	2-D network	Miscible two-phase flow

The network is composed of a number of pore bodies connected by pore throats. Pore bodies in network models are generally referred to as nodes, and pore throats as bonds. Real pore bodies and throats have complex and variable cross sections. In network models, they have to be represented by structures that can be computed mathematically. Pore bodies are generally simulated as cubes or globes. Pore throats are represented by capillary tubes with triangular, circular or square cross sections. Some advanced model employs an arbitrary combination of sites and bonds with different cross sections (Patzek, 2001). For most network models, bonds take the form of cylindrical tubes for the convenience of computation.

The pore throats in a porous medium have a range of sizes, genially between 1 to tens of microns. The sizes of the throats in the network model follow a certain size distribution to imitate this feature. When a non-wetting liquid such as mercury is injected into the reservoir rock, a capillary pressure curve is obtained. The pressure curve can be interpreted to generate a pore size distribution, assuming the pores as a bundle of tubes (Allen, 1997). The pore size distribution is then assigned

randomly to the pore throats (bonds) in the network and serves as an approximate yet realistic representation of the porous media.

Pore network model is a powerful tool for studying multiphase flow in porous media, but it has not been widely used to simulate the capture of particles and droplets in porous media. However, several other models are available for this purpose, typically empirical correlations.

4.3 Established Models for Capture of Particles in Porous Media

The most widely used models can be categorized into three types. The 1/3-1/7 rule is purely based on experimental observations, and just a rough guideline for designing drilling fluid. Empirical models rely on the microscopic continuum conservation equations, and generally ignore the details of the morphology of the pore space. Network models rely on a more realistic description of the pore space. Therefore, this approach involves large-scale computer simulations.

4.3.1 The 1/3 – 1/7 Rule

In 1977, Abrams first observed the 1/3 - 1/7 rule: (1) Particles larger than 1/3 the pore diameter bridge pore entrances at the formation face to form an external filter cake; (2) Particles smaller than 1/3 but larger than 1/7 the pore diameter invade the formation and are trapped, forming an internal filter cake; (3) Particles smaller than 1/7 the pore diameter cause no formation damage because they are carried through the formation. This rule has served as a guideline for mud design and reservoir formation damage for years. Apparently, this model is only a simple rule-of-thumb which can not predict the important parameters such as invasion depth and permeability decline. And this rule is believed to be valid only at high injection velocities exceeding 10 cm/min. For low injection rate, a 1/3-1/14 was proposed (Van Oort et al., 1993).

4.3.2 Empirical Model

The most widely used formation damage models are empirical correlations in nature. The model (Ison and Ives, 1969) considers the porous medium to be a

closed system within which deposition occurs. A volume balance equation for the suspended particles in the porous media takes the form:

$$\frac{\partial \sigma}{\partial t} + u \cdot \frac{\partial c}{\partial x} = 0 \qquad \text{(Equation 4-1)}$$

where σ is unit particle retention volume (volume of particles / volume of rock); t is time; u is superficial velocity; c is solid concentration; and x is axial distance. In order to solve this equation, a rate law for deposition is required. Several forms of this rate law have been suggested and an example (Iwasaki, 1937) is shown below:

$$\frac{\partial \sigma}{\partial t} = u \cdot \lambda \cdot c \qquad \text{(Equation 4-2)}$$

where λ is the filtration coefficient, whose value is obtained by fitting the effluent concentration history to the experimental data at initial time. The two equations then can be solved to yield the amount of deposition as a function of distance and time. The changes in pressure drop and permeability are then related to amount of deposition by an empirical correlation like the following equation:

$$\frac{K}{K_o} = \frac{1}{(1+\beta \cdot \sigma)^{\alpha}} \qquad \text{(Equation 4-3)}$$

where K is the permeability after deposition, and K_o is the original permeability. α and β are both empirical parameters.

In the past years, some researchers continued to work on improving empirical models. Van Oort et al. (1993) proposed the relationship between injected volume and the resultant injectivity damage. Their model requires values for the damage factor and the volume filter coefficient as input parameters, which must be obtained by core flooding experiments. Another model (Pang and Sharma, 1997) relies on the shapes of the injectivity decline curves to determine the damage mechanisms. They identified four types of damages curves: straight line, curves with increasing

slope, curves with decreasing slope, and S-shaped curves. Based on different mechanisms, the transition time required to achieve external filtration is computed. Moghadasi et al. (2004) proposed a correlation between volume of particle deposit and change of porosity. The change of permeability is then correlated to the change in porosity.

Even though the empirical models take different forms, they all heavily rely on core flowing data to determine the key parameters. Empirical models are easy to use, but they fail to take into account the physical parameters involved in the deposition process, such as pore size and particle size. The key parameters in the models are determined by fitting core experiment data. As a result, one empirical model can only be successfully applied to a certain well. When applied to another well, these parameters need to be adjusted. Otherwise, the prediction will be quite poor.

4.3.3 Trajectory Analysis Model

The trajectory analysis model (Payatakes et al., 1973; Payatakes et al., 1974) assumes the porous media as a bundle of tubes with constricted geometries. The trajectory of each particle within the tube is calculated with streamline functions, combined with the forces (gravitational, inertial, hydrodynamic, and van der Waals forces) acting on the particle. The computation is sophisticated and improved the understanding of deep bed filtration at pore level. But this approach is based on a modified bundle-of-tube model, and ignores the connectivity of the pores. As a result, the model can not accurately predict permeability change.

4.3.4 Network Model

Unlike empirical models, network models take into account the details of pore structures. Generally, network models use cylindrical tubes or prisms (referred to as bonds) to simulate pore neck, and globes or cubes (referred to as nodes or sites) to simulate pore body. In previous research, square and triangular networks have been used, thanks to their relative simplicity in computation.

The network model was first used to simulate formation damage by Todd et al. (1984), who used an unbiased random walk to move the particles through the square network. Two methods of capture were employed in the simulations: random capture and capture by 1/3 – 1/7 geometric rules. Model predictions using

both these techniques did not match the experimental data, which was attributed by the authors to the inadequacies of the capture mechanisms. The random walk was an unbiased process, i.e. the probability of having the particles move in any direction was essentially the same. As such, the random walk represents a pure diffusion process and cannot take into account the effect of a flow field, which has been shown to be important especially for straining dominated particle capture (Rege and Fogler, 1988). The absence of a flow field is probably a reasonable explanation of the discrepancy difference between model prediction and experimental data.

Rege and Fogler (1988) developed a 2-dimensional triangular network model to simulate flow of emulsions and solids in porous media. They first assigned random pore throat diameter distribution to the bonds. The bond lengths were assigned to be constant. The fluid field through the individual bonds was then calculated by simultaneously solving mass balance equations for the fluid at every node. Particle movement abided by two fundamental concepts: flow biased probability and wave front movement. Based on the fluid field and these two concepts, particle entrainment and entrapment can be simulated.

Rege and Fogler (1988) applied an empirical correlation to particle capture probability when the particle is moving in the bond larger than itself. That is, at the entry section of the bond, if the center of the particle is placed at the distance smaller than a certain distance from the bond wall, the particle is captured. This certain distance is based on a correlation that takes into account many effects on the particles, such as gravitational, inertial, hydrodynamic, electric double layer and van der Waals forces. The model was well validated by the experimental results, in both suspended particles and emulsion. However, the key feature of this model is the empirical correlation proposed for capture probability. In other word, even though Rege and Fogler (1988) employed network model as a mechanistic infrastructure for deposition, the core is still an empirical correlation.

4.4 Network Formulation

The advantage of network model lies in that it describes the porous media in a more detailed yet efficient way. The network can be build with regular core measurement data, namely porosity, permeability, and pore size distribution.

4.4.1 Determination of Network Structure

The most common network structures are square, triangular, and honeycomb networks. Previous research reveals that both 2-D and 3-D pore network models are able to produce the transport properties of reservoir rocks. 2-D network models are able to generate good simulation results with less computation. In other words, 2-D network model is a practical and realistic tool to study porous media.

More advanced techniques, such as microtomographic imaging and serial sectioning provide a detailed description of the pore space at micrometer resolution (Tsakiroglou and Payatakes, 2000). In practice, however, information of the microstructure of reservoir rocks is obtained from 2-D thin-section images and pore throat sizes determined from mercury injection. These data are not sufficient to construct 3-D pore network models. Moreover, CT scanning and reconstruction facilities are not readily available. Yet pore size distribution measurement is a standard laboratory procedure nowadays.

In this study, the square network is chosen because of its relative simplicity. Moreover, little research was conducted with square network to simulate capture of particles and droplets. The 2-D square network proposed by Fatt (1956) and Stevenson et al. (2006) is adopted in this study. The pore bodies (sites) are represented by globes, and pore throats (bonds) are represented by cylindrical tubes, as illustrated in Figure 4-2. In each unit cell, a pore body is connected to 4 pore throats, forming rectangular structures.

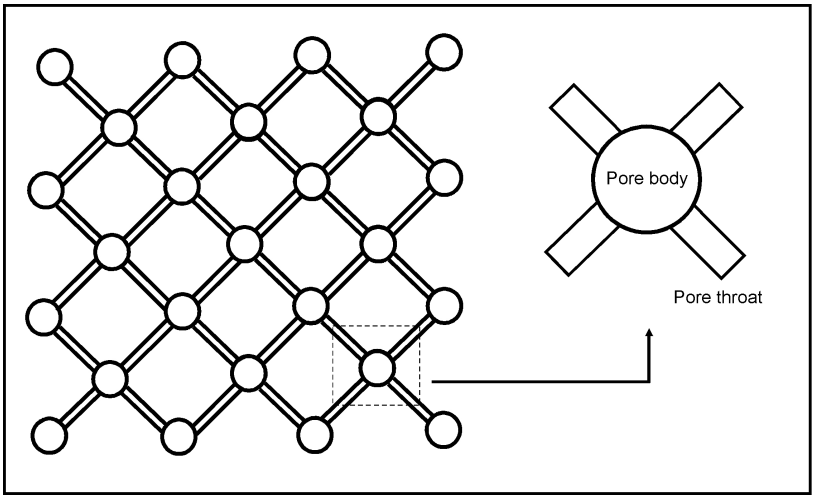

Figure 4-2: The 2-D square network used in simulation

In previous research, networks with various sizes ranging from less than 100 bonds to several hundred bonds have been used. The number of bonds equals the number of the equations to be solved. In this research, a network with 10 bonds in each direction is chosen, which means 100 equations need to be solved to obtain the flow fields in the network.

In the next chapter, network model is applied to the simulation of the capture of particles and droplets in porous media. The laboratory tests on core filtration generally require injection of many pore volumes of suspension. This means the network simulation will also run for a few realisations in order to obtain the permeability decline curve. This relatively small size is chosen to achieve quick simulation realisations. Moreover, a network with the same size was successfully applied to the simulation of rock transport properties (Ioannidis and Chatzis, 1993).

4.4.2 Calculation of Original Porosity

The bond lengths can be set constant, randomly assigned, or related in some manner (directly or inversely proportional) to the diameter. In this study, the bonds are considered to have a constant length. The fraction of the volume occupied by the bonds and sites in the network is the porosity.

The volume of a site is:

$$Vs = \frac{4}{3} \cdot \pi \cdot r_s^{\,3} \qquad \text{(Equation 4-4)}$$

The volume of a bond is:

$$Vb = \pi \cdot r_b^{\,2} \cdot L_b \qquad \text{(Equation 4-5)}$$

In Equations 4-4 and 4-5, Vs and Vb are the volumes of each site and bond respectively; r_s and r_b are the radius of the site and bond respectively; and L_b is the

length of the bond. The combined volumes of the bonds and sites make up the total void space of the network, by which the porosity can be calculated.

A network is composed of a few unit cells like the one in Figure 4-3. The following sample calculation of porosity and permeability is based on this unit cell.

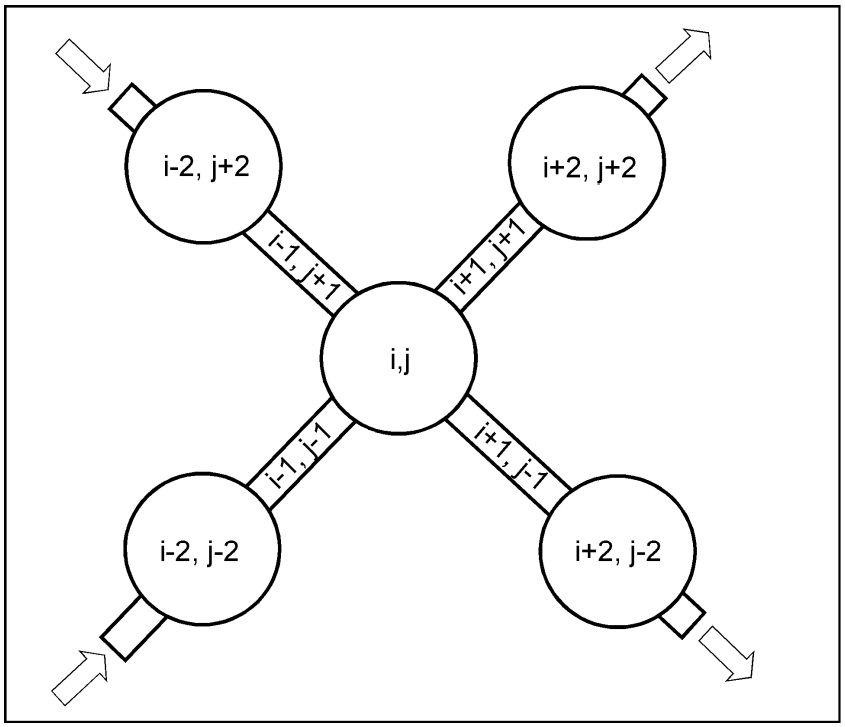

Figure 4-3: A unit cell in the network

For the unit network cell in Figure 4-3, the combined volume of sites (*Vst*) is:

$$Vst = 2 \cdot Vs \qquad \text{(Equation 4-6)}$$

The combined volume of nodes (*Vbt*) is:

$$Vbt = \sum_{i-1}^{i+1} \sum_{j-1}^{j+1} Vb_{i,j} = \sum_{i-1}^{i+1} \sum_{j-1}^{j+1} [\pi \cdot (r_{b(i,j)})^2 \cdot L_b] \qquad \text{(Equation 4-7)}$$

The sum of Vst and Vbt is the volume of the void space in the unit cell. If the total volume of the network is known, porosity can be calculated. The total volume that the network occupies Vnw is:

$$Vnw = 2 \cdot r_s \cdot L_n^{\,2} \qquad \text{(Equation 4-8)}$$

where the length of the unit network L_n is expressed as:

$$L_n = \frac{4 \cdot r_s + 2 \cdot L_b}{\sqrt{2}} \qquad \text{(Equation 4-9)}$$

Put the expression of L_n in Equation 4-9 into Equation 4-8, the total volume that the network occupies (Vnw) is:

$$Vnw = r_s \cdot (4 \cdot r_s + 2 \cdot L_b)^2 \qquad \text{(Equation 4-10)}$$

Therefore, the porosity Φ can be expressed as:

$$\phi = \frac{Vst + Vbt}{Vnw} \qquad \text{(Equation 4-11)}$$

If the calculated porosity does not match that of the real core, the diameter of the sites can be adjusted. Sites generally have much bigger sizes than bonds. It is much more efficient to adjust the sites to obtain desired porosity. Moreover, the bonds abide by the pore size distribution which can not be violated.

4.4.3 Calculation of Original Absolute Permeability

The following conditions must be met in order to satisfy Darcy's law: flow regime in porous media is laminar flow, fluid is Newtonian fluid, and there is no reaction between fluid and porous media. The model calculation shows that the Reynolds number in porous media is generally less than 1 for a typical water flooding project, which indicates the flow regime as laminar. Injected suspension is a dilute mixture of water and particulates. It is reasonable to assume the fluid to be Newtonian and incompressible. As such, Darcy's law is valid for calculation of rock permeability under water injection.

To obtain the permeability of the network model with Darcy's law, three unknowns are to be solved: network geometry, injection flow rate and pressure loss. The network geometry has been discussed in the previous section (Equation 4-9). According to Darcy's law, the flow rate is proportional to resultant pressure loss. Therefore, a pressure boundary can be applied to the inlet and outlet of the network. The flow rate in a bond is then determined by Hagen-Poiseuille Equation (Darby, 1996):

$$Q = \frac{\Delta P_b}{L_b} \cdot \frac{Cd}{\mu_L} \qquad \text{(Equation 4-12)}$$

In Equation 4-12, Q is the flow rate in a certain bond; ΔP_b is the pressure loss in a certain bond; Cd is the hydraulic conductance of a certain bond; and μ_L is the viscosity of the fluid flowing in the bond. The conductance (Cd) of a bond is determined by the size of the bond:

$$Cd = \frac{\pi}{8} \cdot r_b^{\,4} \qquad \text{(Equation 4-13)}$$

A sample calculation is given below for the unit cell in Figure 4-3. The flow rate in each bond can be written with Equation 4-12. Since there are four bonds in the unit cell, the following four equations can be obtained:

$$Q_{i-1,j+1} = \frac{Cd_{i-1,j+1} \cdot (P_{i-2,j+2} - P_{i,j})}{L_b \cdot \mu_L} \quad \text{(Equation 4-14)}$$

$$Q_{i-1,j-1} = \frac{Cd_{i-1,j-1} \cdot (P_{i-2,j-2} - P_{i,j})}{L_b \cdot \mu_L} \quad \text{(Equation 4-15)}$$

$$Q_{i+1,j+1} = \frac{Cd_{i+1,j+1} \cdot (P_{i,j} - P_{i+2,j+2})}{L_b \cdot \mu_L} \quad \text{(Equation 4-16)}$$

$$Q_{i+1,j-1} = \frac{Cd_{i+1,j-1} \cdot (P_{i,j} - P_{i+2,j-2})}{L_b \cdot \mu_L} \quad \text{(Equation 4-17)}$$

The pressure at the node (*i,j*) is unknown. One more equation is required to solve for all the unknowns. There is no accumulation of mass at node (*i,j*). A mass balance at this node (*i,j*) is expressed as:

$$Q_{i-2,j+2} + Q_{i-2,j-2} = Q_{i+2,j+2} + Q_{i+2,j-2} \quad \text{(Equation 4-18)}$$

With Equations 4-14 to 4-18, the flow field in the unit cell can be obtained. The either side of Equation 4-18 can serve as the inlet flow rate.

When applying inlet and outlet pressure boundaries, there is only one inlet pressure boundary and one outlet pressure boundary. For the inlet of the unit cell:

$$P_{i-2,j+2} = P_{i-2,j-2} \quad \text{(Equation 4-19)}$$

Similarly, for the outlet pressure boundary:

$$P_{i+2,j+2} = P_{i+2,j-2} \qquad \text{(Equation 4-20)}$$

After obtaining the flow rates inside the network, the permeability (*K*) of the network is calculated by Darcy's law:

$$q = \frac{K \cdot A}{\mu_L} \cdot \frac{\Delta P}{L} \qquad \text{(Equation 4-21)}$$

where q is the volume flow rate through the rock, A is the area of the rock subject to flow; L is the length of the rock; and ΔP is the pressure loss across the rock. When applying Darcy's law to the network, q is the flow rates entering the network; and ΔP is accumulated along the length of the network.

The computation algorithm can be seen in Figure 4-4. The measured mean pore size and standard deviation are the key inputs for the network model. The above procedure applies a pressure boundary, and computes the flow rates in the network. It is also feasible to apply flow rate boundary conditions to the inlet and outlet of the network, and calculate the pressure losses in the bonds. These two methods should produce the same permeability data, according to Darcy's law.

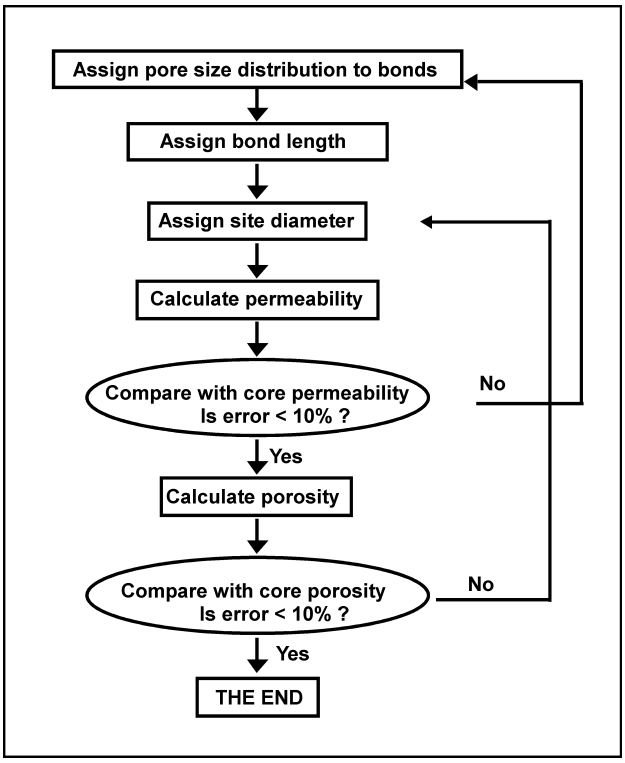

Figure 4-4: Computation algorithm to obtain desired network parameters

4.5 Discussions

Even though network model is a simplified approach, it still involves many parameters, such as pore size distribution, length of bond, and site diameter. Among these parameters, the pore size distribution has the most significant effect on the computed permeability.

4.5.1 Effect of Pore Size Distribution

The measured pore size distribution contains information such as mean pore size and standard deviation. The previous research revealed that both normal distribution and log-normal distribution can represent the real pore size distributions very well (Hampton et al., 1993).

The computed permeability is generally different from the measured value. This may be caused by two factors. A number generator is used to produce a group of

numbers that follow a certain distribution. Then these numbers are randomly assigned to the bonds in the network. However, many combinations of numbers may match the distribution. The values in a certain batch may not produce desired permeability.

On the other hand, the measured pore size distribution is different from the real distribution of the core. The pore size distribution is obtained by converting measured capillary pressure data, assuming the pores as capillary tubes and neglecting pore interconnections (Allen, 1997). In fact, the measured pore size distribution overweighs narrower pores. As a result, a trial-and-error process may be required to find the appropriate combination.

It is obvious that porous media with large pore have high permeabilities. According to the conductance calculated in Equation 4-13, a larger average pore size leads to a much higher permeability. Figure 4-5 illustrates this effect. Assign a pore size distribution that abides by a Normal distribution with a certain mean pore size and a standard deviation of 1 to the bonds in the network. If the average pore radius in the network increases from 10 microns to 50 microns, the calculated permeability increases from less than one Darcy to almost 9 Darcy.

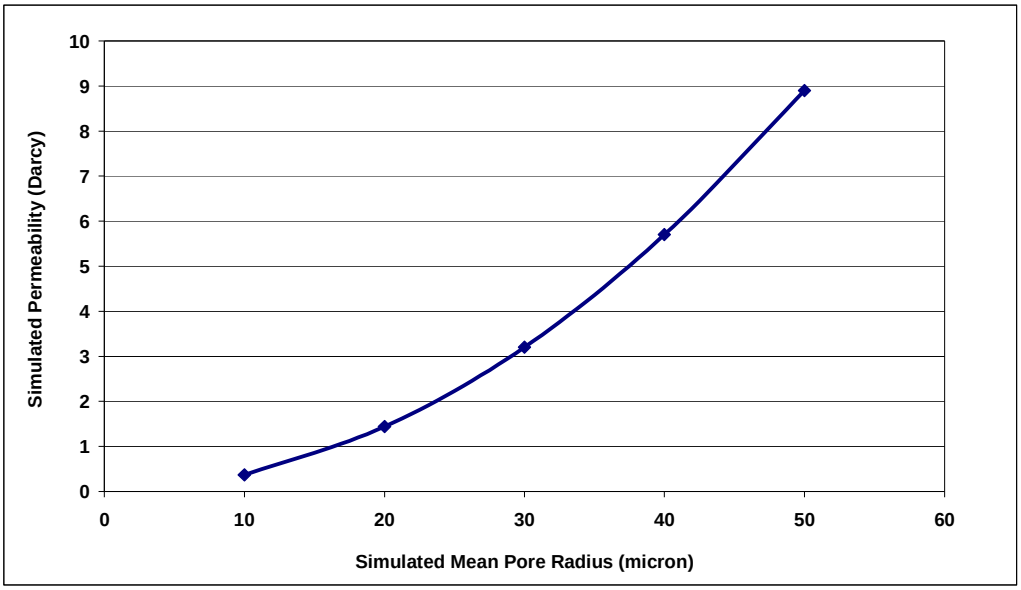

Figure 4-5: Effect of pore size on calculated permeability

4.5.2 Effect of Network Size

Traditionally, the fluid flow in porous media is solved with Darcy's law. The simplicity of Darcy's law allows calculation of large porous media. Network models consider the microscopic structure of porous media, thus requiring much more computations. Due to the high demand in computation, only a very small portion of the rock can be simulated, even with a large network.

In the network model, a pore size distribution is assigned randomly to each column of the bonds. In other words, the sizes of the 100 bonds are within a certain range and center around the mean pore size. If the network is too small (i.e., when the uncertainty is high), the computed permeability is going to be different when the network is extended. The uncertainty diminishes when the network is large enough.

Networks with different sizes obtained similar absolute permeabilities, as seen in Figure 4-6. This on the other hand proves that the 10x10 network is adequately large for obtaining stable output of absolute permeability.

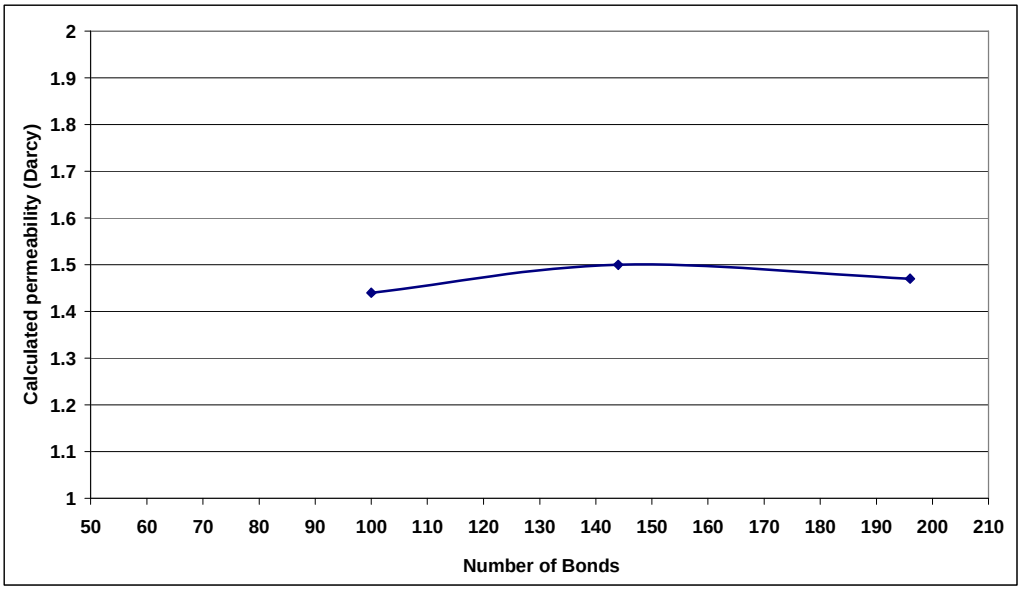

Figure 4-6: Effect of network size on computed permeability

4.6 Concluding Remarks

- Pore network models have been a popular tool for studying the static and dynamic properties of reservoir rocks. But limited research was conducted with network models in the capture of particles and droplets in porous media.

- Most established models for particle-induced permeability decline are empirical correlations in nature. A 2-dimentional square network is proposed to gain better understanding of the particle capture processes in porous media.

- The network size is set to be 10x10. Calculations show that the mean pore size has significant effect on calculated permeability, while the network size has minor effect on simulated permeability.

- The impurities in produced water such as particles and droplets can severely damage the reservoir permeability. In following chapters, these aspects will be investigated individually.

CHAPTER 5

CAPTURE OF BROWNIAN PARTICLES IN POROUS MEDIA AND RESULTANT PERMEABILITY REDUCTION *

5.1 Introduction

Particles can be categorized as Brownian particles and non-Brownian particles. Particles with diameters smaller than 1 micron are generally referred to as Brownian particles. Particles with diameters larger than 1 micron are generally referred to as non-Brownian particles.

Brownian motion (or Brownian movement) can be defined as the random movement of microscopic particles suspended in a fluid. In 1827, Robert Brown noticed that pollen grains suspended in water jiggled about under the lens of the microscope, following a zigzag path. Even more remarkable was the fact that pollen grains that had been stored for a century moved in the same way (Renn, 2005).

5.2 Model Formulation

Porous media have very complex internal geometries. It is not an easy task to define the pathways inside porous media, not to mention to calculate the particles' trajectories inside such complex structures. Previous models developed for fine particle deposition are often based on simple geometries, such as deposition in a channel or between parallel plates.

It is clear that Diffusion dominates sedimentation for small particles, while the earth's gravitational field governs the movement of large particles (Vincent, 2005). In previous research, diffusion equation was solved to obtain the particle concentration in a cylindrical channel (Davies, 1973), in a short channel (Chen, 1977), in a narrow channel (Philip, 1995), in a convergent channel (Chen et al., 1996), and in a long and wide channel (Myers, 2001). Prieve and Ruckenstein (1974) studied the deposition of Brownian particles onto an ideal spherical collector, taking account of London force.

** Published in APPEA Journal, vol.47, part 1,187-196 with some modifications*

Previous models are based on geometries very different from a network stricture. However, the pore throats are represented by cylindrical tubes. The particle volume deposition rate in a tube can be calculated with Fick's law of diffusion (Cussler, 1976; Salles et al., 1993): neglecting the double layer force and London force:

$$J = D \cdot \frac{dc}{dr_b} \qquad \text{(Equation 5-1)}$$

where J is the volume deposition rate; D is the diffusion coefficient; and c is the particle concentration; r_b is the radius of a certain bond where deposition takes place.

Due to their very small sizes, Brownian particles are suspended uniformly in injected fluid. When particles enter the pores, the particle concentration on pore surface is zero, thus exerting a concentration difference between pore wall and the centre of the pore. Pores (bonds) have various sizes. As a result, the deposition rate in each bond is different, according to Equation 5-1.

The diffusion coefficient D in Equation 5-1 can be determined by Stokes-Einstein Equation (Bird et al., 2002):

$$D = \frac{K_B \cdot T}{6 \cdot \pi \cdot r_P \cdot \mu_L} \qquad \text{(Equation 5-2)}$$

In the above equation, K_B is the Boltzmann constant (1.380622x10^{-23} J/K); T is the absolute temperature (K); r_P is the particle radius; and μ_L is the viscosity of the suspension. There are many modifications to the Stokes-Einstein equation. The original form is directly used here because the classic diffusivity has been proved especially valid for Brownian diffusion (Bird et al., 2002).

Equations 5-1 and 5-2 can be solved to obtain the deposition rate in each bond of the network. Then the volume of deposits in each bond over a certain period of time can be calculated. With the volume of deposition, the reduced bond diameters can be obtained. Based on the new network geometries, a realisation is carried out to

obtain the reduced permeability. This procedure is repeated until the necessary duration is met. This process is summarised in Figure 5-1.

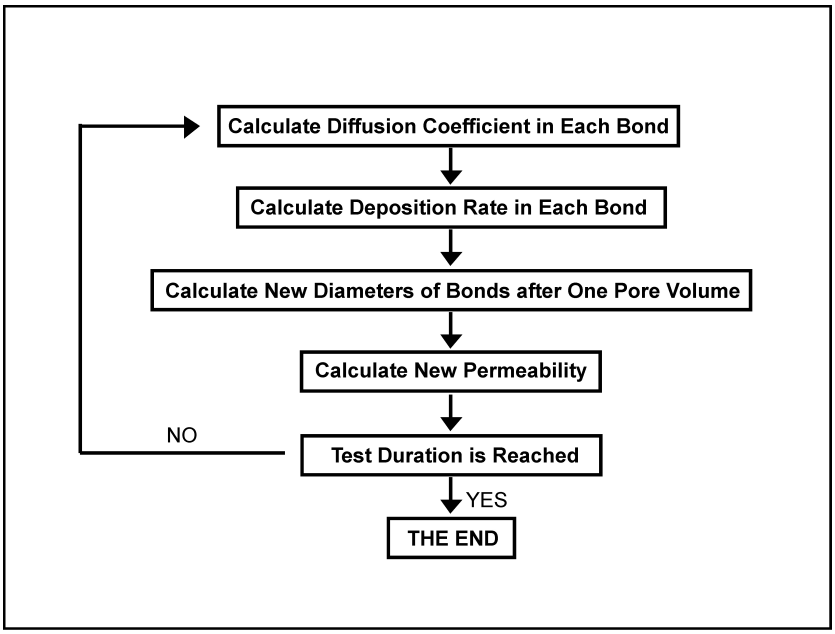

Figure 5-1: Computation algorism for deposition of Brownian particles

5.3 Model Validation

Baghdlklan et al. (1989) documented their tests data particularly well and these data were used to validate the model. In their tests, Bentonite and Kaolin clay suspensions were injected through packed sand to study the permeability damages under different flow rates, solid concentrations, and ionic strengths. The properties of the sand pack used in their tests are shown in Table 5-1.

Table 5-1: Properties of the sand pack (Baghdlklan et al., 1989)

Sand pack parameter	Value
Length (mm)	322
ID (mm)	63
Porosity vs. simulated porosity (%)	37.5 vs. 37.0
Permeability vs. simulated permeability (Darcy)	8 vs. 7.7
Range of Pore Radius (μm)	1 to 65
Average Pore Radius (μm)	18

First, a log-normal pore size distribution with a mean radius of 18 μm and a standard deviation of 0.85 μm was assigned to the bonds in the network. The bond length equals the mean pore throat radius which is 18 μm. The radius of sites is set as a constant of 75 μm.

Figure 5-2 compares the measured and simulated pore size distributions. It can be seen that the simulated distribution is narrower than the real distribution. By following the network computation algorithm described in Chapter 4, the network is found to have a porosity of 37% and a permeability of 7.7 Darcies, which well match those values of the sand pack.

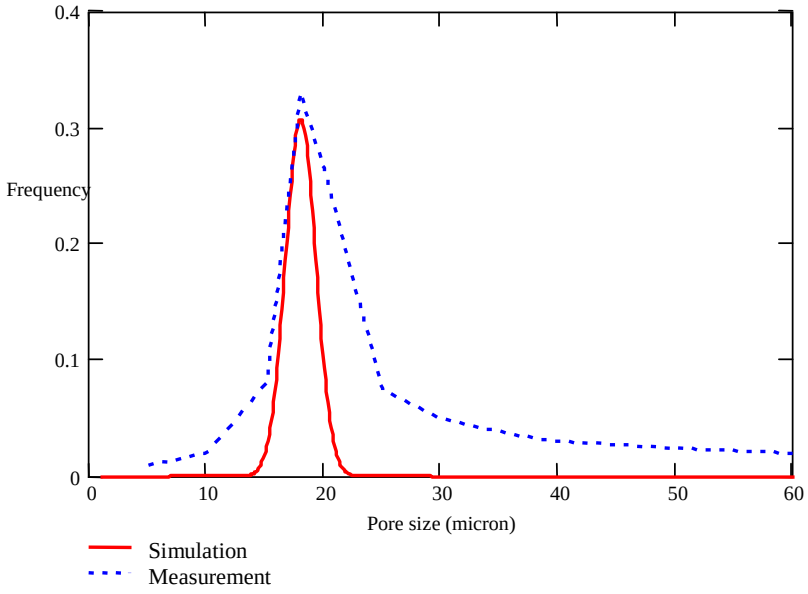

Figure 5-2: Comparison of measured and simulated pore size (radius) distributions

5.3.1 Effect of Flow Rate

Baghdlklan et al. (1989) first studied the impact of flow rates. Bentonite clay suspensions were injected through the packed sand at flow rates of 5.4, 11.4, and 21.4 cm^3/min. The particles in the suspension were mostly in the submicron range. The detailed test conditions are listed in Table 5-2.

Table 5-2: Test conditions with Bentonite clay suspension

Test parameter	Test value
Particle concentration (ppm)	400
Flow rate (cm^3/min)	5.4, 11.4, 21.4
Particle size range (μm)	0.01 to 0.2
Mean particle size (μm)	about 1

Figure 5-3 reproduces the test data on the effect of flow rates. The y axis, K/K_o represents the ratio of damaged permeability (K) over original permeability (K_o). The x axis, pore volume (also referred to as pore volumes injected) represents the amount of liquid injected. One pore volume equals the total volume of the core multiplied by its porosity. It gives a direct sense of the amount of fluid the core has accepted.

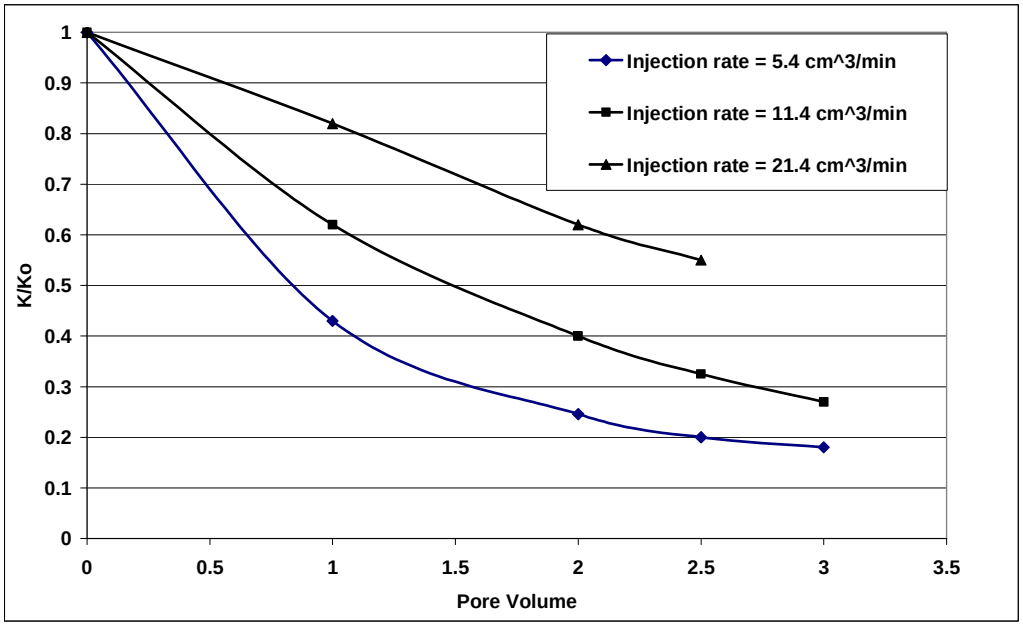

Figure 5-3: Test data with different flow rates

It can be seen that pore volume is indeed a form of dimensionless time. One core can be tested for different flow rates, and each test core can have different porosities. Using pore volumes instead of real time makes the comparisons between tests much easier. For this reason, it is an international standard to use pore volume instead of time while plotting core flooding data.

According to Figure 5-3, it seems that the damage is much more severe at low injection rate. However, because the injection rate or velocity is not involved in the calculation of deposition rate in Equations 5-1 and 5-2., the calculated deposition rate is the same at different flow rates for Brownian particles. Therefore, if the permeability decline is plotted against real time, the permeability trends should be identical for different flow rates.

Figure 5-4 serves such a purpose, and the permeability damage curves are very similar at different flow rates. Figures 5-3 and 5-4 show that for Brownian particles, the resultant permeability is independent of injection rate. This, on the other hand proves the understanding is correct: diffusion is dominant for Brownian particles. Even though pore volume gives a very straight-forward indication of injected volume, it can also lead to misunderstanding for Brownian particles.

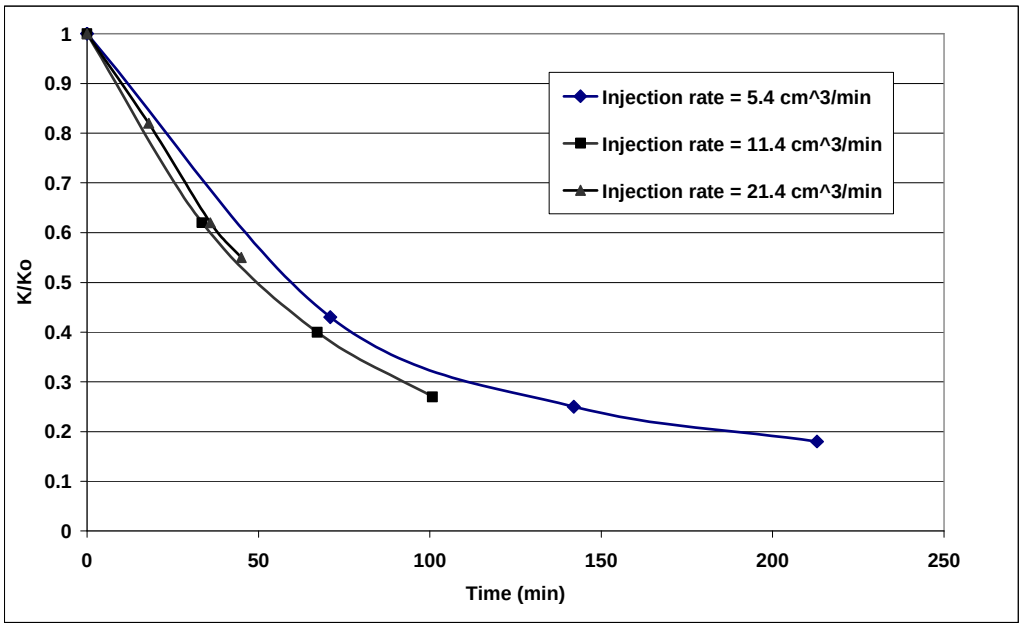

Figure 5-4: Test data plotted against real time

While for non-Brownian particles (see next chapter), injection velocity has significant effect on permeability damage. This is because particles travel further into the rock at higher injection velocity. The damage is averaged over the core, thus leading to less overall damage at higher flow rate.

The model prediction is shown in Figure 5-5. The model over predicts the damage in the end, but the overall agreement is reasonably good.

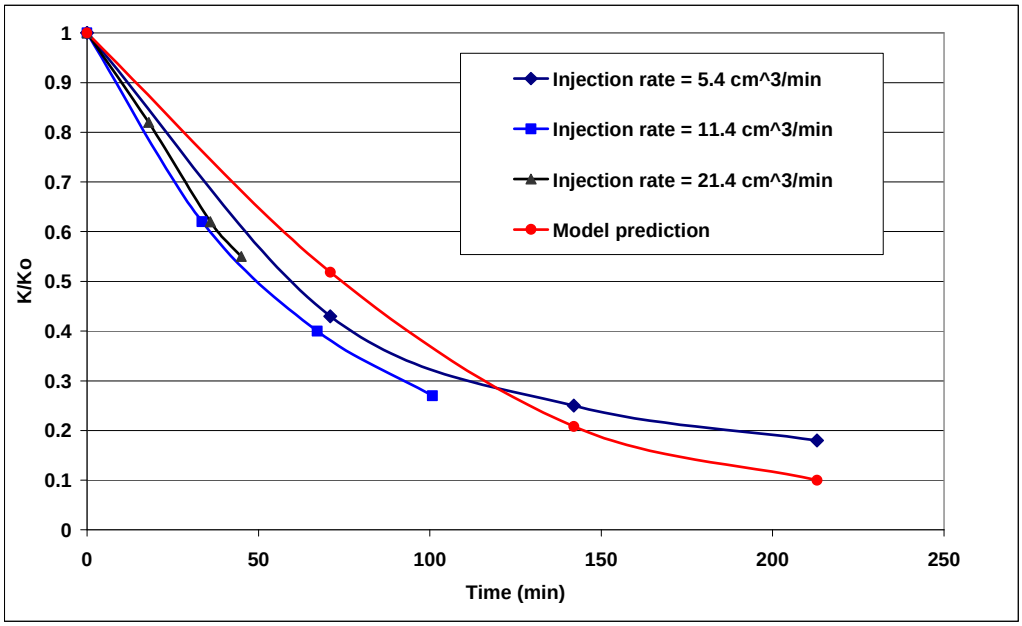

Figure 5-5: Test data under various velocities and model prediction

5.3.2 Effect of Particle Concentration

Kaolin clay suspensions with two concentrations were injected through the same sand pack. The majority of the particles in the suspensions were smaller than 1 μm in diameter. The test conditions are listed in Table 5-3.

Table 5-3: Test conditions with Kaolin clay suspension

Test parameter	Test value
Particle concentration (ppm)	1000, 2000
Flow rate (cm^3/min)	6.5
Particle size range (μm)	0.02 to 3
Mean particle size (μm)	about 1

Figures 5-6 and 5-7 illustrate the test results and comparisons with model predictions. The test data indicate that a higher solid concentration causes more damage. As we can see, the model can predict the trend well at lower concentration, but overestimates the permeability damage at higher concentration.

Because tested Kaolin clay has bigger particle size than Bentonite clay, the diffusion and deposition rates for Kaolin clay are lower. As such, Kaolin clay causes less damage.

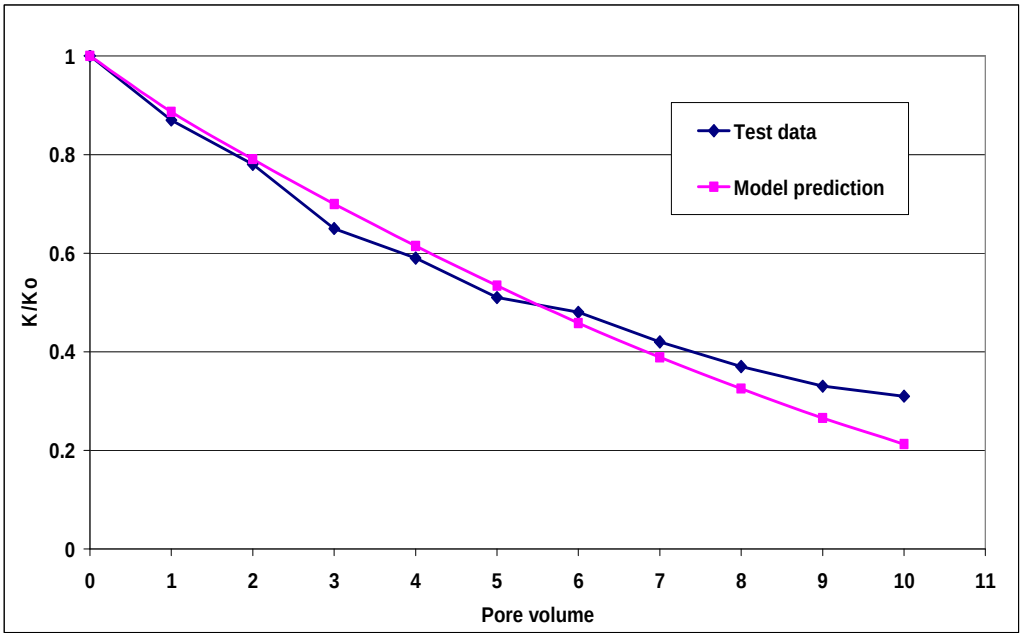

Figure 5-6: Test data and model prediction for concentration of 1000 ppm

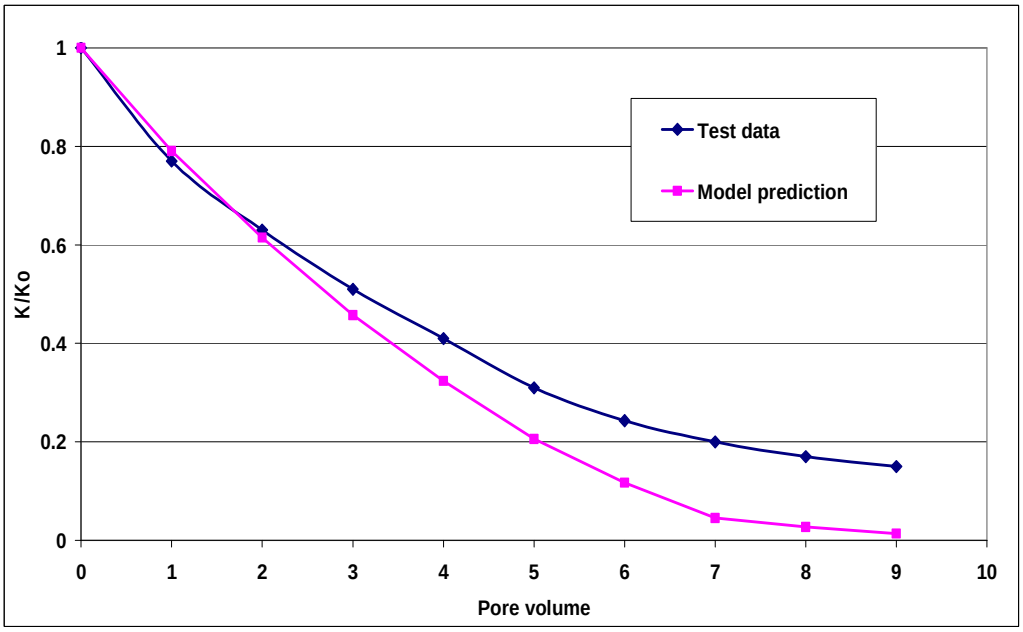

Figure 5-7: Test data and model prediction for concentration of 2000 ppm

5.4 Discussions

Particle deposition is a complex issue. The discrepancy in model simulation can be attributed to two aspects. On one hand, the understanding and the description of the porous media may contain certain errors. On the other hand, the pore size and particle size measurements may introduce some errors too.

First of all, the network model has limitations. The network cannot completely imitate the real porous media. Even though the pore size distribution, site diameters and bond lengths were assigned to the network in a meaningful way, it cannot be denied that the network model is indeed different from the real structure and parameters of the porous media.

Second, the pore size distribution is not exactly the real size distribution. The porosimetry measurement uses a capillary-tube model to derive the pore size distribution, which causes the measurement to have a lower mean and standard deviation than the real pore size distribution (Baghdlklan et al., 1989). While this distribution is applied to the network, some errors will be introduced.

Third, the particle size measurements may not be accurate, as mentioned in the original paper (Baghdlklan et al., 1989). It is difficult to obtain accurate size measurement for sub-micron particles. However, most the clay particles in the tests were in the sub-micron range, which undoubtedly introduced errors to the model. According to Equations 5-1 and 5-2, larger particles, within the submicron range, lead to less deposition and less permeability damage.

Fourth, when a particle arrives at pore surface, it will encounter a repulsive double layer force and an attractive London force. A simulation study revels that for Brownian particles, the effect of double layer force is negligible (Payatakes et al., 1974). Therefore, these minor forces are neglected.

It is worth mentioning that no empirical parameter is introduced into the model. The empirical models may be able to generate better match after applying several tuning parameters. However they have to be tuned almost in each run, while the proposed model generated reasonable results without applying any tuning parameter.

5.5 Model Application

Two parameters, damage radius and damage permeability, are required for up-scaling with reservoir flow equations. The proposed model is capable of predicting permeability decline. However, the model can not give direct prediction of damage radius. It is very difficult to obtain the concentration profiles in a structure such as a square network. However, it is relatively easy to obtain such profile in a tube. An approximate solution is to assume the reservoir rock as a bundle of tubes, and calculate the concentration profile inside these tubes.

Assume a circular reservoir is going through PWRI. The reservoir properties are identical to those of the sand pack tested by (Baghdlklan et al., 1989). The particle size and concentration are as in Table 5-2. And the well data are listed in Table 5-4.

Table 5-4: Well data for model up-scaling

Well parameter	Well data
Wellbore radius (mm)	63
Reservoir radius (m)	200
Height of the injection zone (m)	50
Water injection rate (bbl/day)	1220
Water injection rate (m^3/day)	194
Linear injection velocity (mm/s)	0.3

The steady-sate injection rate q can be expressed as (Ahmed, 2001):

$$q = \frac{2 \cdot \pi \cdot K_o \cdot h \cdot (P_r - P_{wf})}{\mu_L \cdot (\ln \frac{r_e}{r_w} + S)} \qquad \text{(Equation 5-3)}$$

where h is the height of the injection zone; P_r and P_{wf} are reservoir pressure and well flowing pressure, respectively; r_e and r_w are reservoir radius and wellbore radius respectively; and S is skin factor. In petroleum industry, skin factor is used to

quantify the damage in the near wellbore region. Skin factor S is expressed as (Ahmed, 2001):

$$S = (\frac{K_o}{K} - 1) \cdot \ln(\frac{r_d}{r_w}) \quad \text{(Equation 5-4)}$$

where K is the permeability of the damaged region at a certain time; r_d is the damage radius or invasion depth; and r_w is the wellbore radius. The damaged permeability K can be predicted by the proposed method in this chapter.

The damage radius (r_d) or invasion depth is the difficulty for up-scaling. The network can only simulate a very small fraction of the reservoir rock, commonly from less than 1 mm to several millimeters. The invasion depth is generally over 10 mm. A very large network is required to match the invasion depth. Therefore the invasion depth can not be directly obtained by network simulation. Previous research in network models (Rege and Fogler, 1988; Imdakm and Sahimi, 1991) did not provide the method for up-scaling, possibly because of this reason.

If the concentration profile inside the porous media is obtained, the invasion depth can be easily determined. However, it is not an easy task to do so. The compromise is to assume the rock as a bundle of tubes. The pores in porous media have a range of sizes. For the simulated bundle of tubes, the invasion depth is also different in each tube. Nevertheless, the average invasion depth can be regarded as the distance that the particles travel in a tube with average pore size.

Davies (1973) solved the diffusion equation (Fick's second law) and obtained an approximate solution to the Brownian particle concentration profile along a tube:

$$\frac{c}{c_o} = 0.819 \cdot \exp(-14.63 \cdot \Delta) + 0.0976 \cdot \exp(-89.22 \cdot \Delta) \quad \text{(Equation 5-5)}$$

Where c is the particle concentration at a certain distance inside the tube; c_o is the inlet particle concentration, and Δ, the diffusion parameter is calculated by:

$$\Delta = \frac{D \cdot L}{4 \cdot v_L \cdot R^2} \qquad \text{(Equation 5-6)}$$

Where D is the diffusion coefficient; L is the length of the tube; v_L is the average fluid velocity in the tube; and R is the tube radius.

It is obvious that the particle concentration decreases along the tube. The distance between particle inlet and the point where the concentration ratio (c/c_o) reduces to zero is the damage radius. The relationship between the concentration ratio (c/c_o) and diffusion parameter (Δ) is plotted in Figure 5-8. It can be seen that when the diffusion parameter is reduced to 0.4, the particle concentration approximates zero. Now assume reservoir as a bundle of tubes. Inside the tube with average pore size, the distance for particle concentration to drop to zero can be easily calculated with other known parameters.

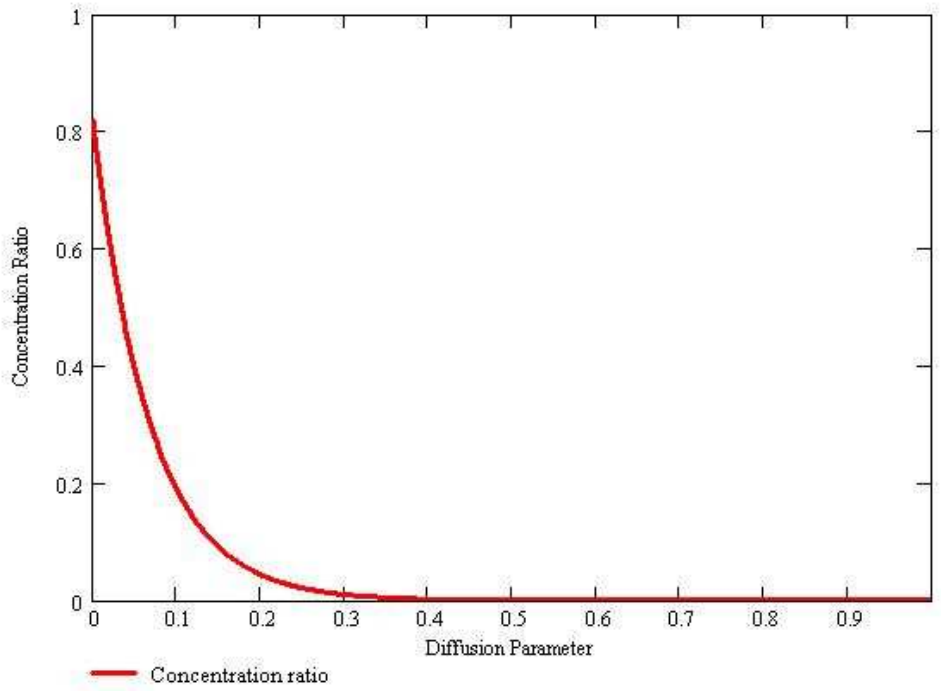

Figure 5-8: Relationship between diffusion parameter and particle concentration

With the fluid temperature and viscosity, the diffusion coefficient is obtained, as seen in Table 5-5. With the values injection velocity, diffusion coefficient, average pore radius (listed in Table 5-5), and a diffusion parameter of 0.4, the average damage radius is calculated to be 18.2 cm. Equation 5-4 is then used to obtain the

skin factor. Porous media are more capable of capturing particles than straight tubes, so the real damage radius is less.

Table 5-5: Assumed parameters for damage radius calculation

Parameter	Value
Temperature (ºC)	50
Suspension viscosity (kg/ms)	5.6×10^{-4}
Diffusion coefficient (mm^2/s)	8.62×10^{-7}
Average pore radius (μm)	18
Linear injection velocity (mm/s)	0.3

The ratio of damaged flow rate (I) and original flow rate (I_o) is thus expressed as:

$$\frac{I}{I_o} = \frac{\ln \frac{r_e}{r_w}}{\ln \frac{r_e}{r_w} + S} \qquad \text{(Equation 5-7)}$$

To sum up, the procedure is as follow. At a certain time, the damaged permeability K is calculated with the proposed model. Then the skin factor S is obtained by Equation 5-4. With the skin factor, the flow rate ratio can be calculated with Equation 5-7. A sample calculation is given in Table 5-6, for a particle concentration of 400 ppm.

Table 5-6: Simulation results for particle concentration of 400 ppm

Time (min)	Skin factor	Injectivity ratio
71	1.4	0.85
142	3.16	0.72
213	4.8	0.63

The simulation result with the above field conditions is shown in Figure 5-9. The y axis is the ratio of current injection rate (I) to original injection rate (Io). It can be seen that with the particle concentration of 400 ppm, the injector will lose almost

40% of its injectivity within 4 hours. If the injected water is filtered to a particle concentration of 40 ppm, the decline is much less severe. If the injected water is further filtered to a particle concentration of 4 ppm, the decline is slow and the well is likely to sustain its injection rate over a much longer period of time.

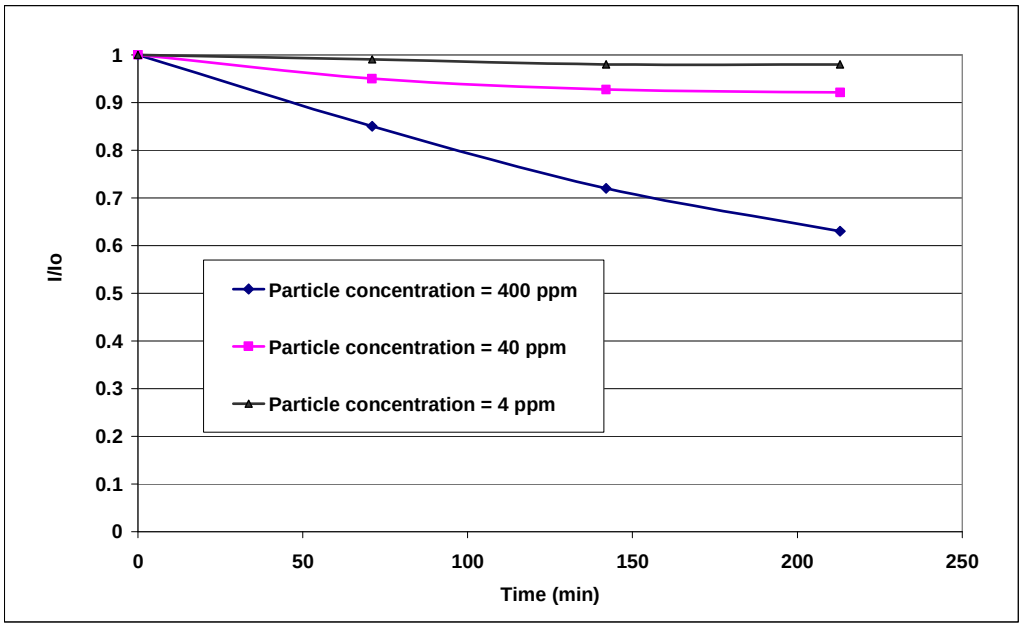

Figure 5-9: Prediction of well injectivity under invasion of Brownian particles

5.6 Concluding Remarks

- Diffusion is the dominant mechanism for deposition for Brownian particles in porous media. Analysis on previous test data reveals that for capture of Brownian particles in porous media, injection velocity does not have a significant effect on resultant permeability damage.

- Fick's diffusion law is applied to each bond in a network model to obtain the particle deposition rate. The model is validated with previous test data and reasonably good agreements are achieved, without introducing any empirical parameter. Discrepancies in simulation results can be attributed to the limitations of network model, and pore size and particle size measurements.

- Previous research in the same topic did not provide method for model up-scaling and field application. This is attributed to the limitation of network

model: network size is not large enough to predict the particle invasion depth. In this work, the reservoir is assumes as a bundle of tubes, and the damage radius is obtained with the concentration profile inside the tubes. Based on the invasion depth and permeability values, the model is able to predict a well's injectivity over time.

- The injectivity simulation with certain input data suggests that the injected water needs to contain less than 5 ppm of Brownian particles, in order to maintain the well's injection rate. However, this criterion may not be applicable to other cases. Reservoirs have largely different characteristics. Each field case must be analysed individually.

CHAPTER 6

CAPTURE OF NON-BROWNIAN PARTICLES IN POROUS MEDIA AND RESULTANT PERMEABILITY DAMAGE*

6.1 Introduction

As discussed in Chapter 4, established deep bed filtration models have some major disadvantages. Empirical models have to rely on core filtration data to determine the key parameters. Trajectory analysis model tracks each particle's movement inside pores, which makes the model very computationally demanding and difficult to be adopted by the industry. Above all, the available models do not give the prediction of damage radius (or invasion depth) which is required for model up-scaling with traditional reservoir engineering solutions. These shortages must be overcome to make a model useful.

6.2 Model Formulation

The experiments reported in Chapter 3 reveal that for core flooding tests with large (non-Brownian) particles, the several millimeters to several centimeters of the core from the particle entrance are generally severely damaged. The remaining rock is either slightly damaged or not damaged at all. It is therefore acceptable to assume the damaged rock to be composed of two sections: one section being damaged, while the other section being undamaged.

Previous experiments also show that the invasion depth is larger at higher flow rate or injection velocity. This indicates that the transport of large particles inside porous media is governed by the forces acting on them. As such, trajectory analysis is required to obtain the invasion depth. The invasion depth is also required for model up-scaling purpose.

After obtaining the invasion depth, the next step is to determine the capture of the particles in the network. The trajectory analysis on each particle should be avoided to simplify the computation. The pores in the network have a range of sizes. The

** Accepted for publication in APPEA Journal with slight modifications*

pore size has a certain relationship with the amount of particles it receives. In other words, a reasonable rule is required to distribute the particles inside the network.

As explained in Chapter 3, particles with various sizes may cause damage due to different mechanisms at the pore level. For a non-Brownian particle, its size may be comparable to the pore it enters or attempts to enter. As a result, pore throat bridging and plugging may become the dominant damage mechanism.

In brief, three questions must be answered before achieving simulation results. (1) How far do the particles travel into the reservoir rock? (2) How to determine a pore's chance in receiving particles? (3) How to incorporate the damage mechanisms into the model?

6.2.1 Particle Trajectory Analysis

The objective of the trajectory analysis is to determine the particle invasion depth. Particle invasion depth refers to the length of the most severely damage rock. It is an approximate value in nature. The ideal procedure is to program a network as large as the damaged rock, and track each particle's movement inside the network. However, this ideal is impossible for up-scaling purpose. The following simplifications have to be employed.

(1) The network size is not adequately large to obtain the invasion depth directly. The invasion depth can be several centimeters, while most network models can only simulate several millimeters of a rock. Moreover, computing particles' movements inside network geometry is very complex. A compromise is to assume the reservoir rock as a bundle of tubes with the mean pore size. The distance that a particle travels into a tube can be taken as the approximate invasion depth. This is also based on the fact that most porous media have rather narrow pore size distributions.

(2) the particles in injected suspension have a range of sizes. However, it is impossible to calculate an invasion depth for each particle. Particle size distributions are generally quite narrow (Shook and Roco, 1991). This means most of the particles in a suspension center around one size. Therefore, the mean particle size can be used to obtain the invasion depth for most particles in the suspension.

This assumption is also based on experimental observations. As explained in Chapter 3, the first several millimeters to several centimeters of a core invaded by particles are severely damaged. The rest of the core is often slightly damaged. However, the boundary between the severely damaged and slightly damaged sections is not clear. This indicates that the majority of the invading particles settle down within a certain distance. But many smaller particles do travel further into the core.

(3) For non-Brownian particles, their movements are governed by various forces, such as gravity, buoyancy and drag force. Minor forces such as London force and surface repulsive force are ignored, because they have minor effects on trajectories. Injected water normally contains very dilute particles (Newtonian fluid), so the influence of particle collision is not considered.

(4) The direction parallel to the fluid flow is referred to as x direction, and the y direction is perpendicular to the fluid direction, as shown in Figure 6-1. The network lies horizontally, perpendicular to the direction of a vertical well.

(5) Suspension velocity and particles velocities are all vectors with directions. It is assumed that inside pores, the suspended particles have same velocities as the suspension in x direction, and particles settle down in the y direction (Figure 6-1). Suspension's velocity in the y direction is zero. This assumption is based on the fact that a suspended particle has very similar velocity as the carrying fluid in the x direction, so the settling point of the particle is controlled by gravity and drag force in the y direction.

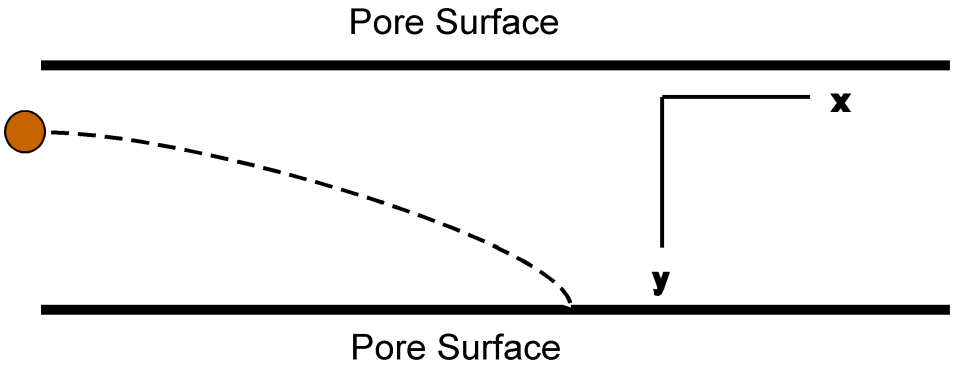

Figure 6-1: Trajectory of a particle

(6) Another difficulty lies in that a particle can enter the pore from any possible position at pore entrance, which makes it difficult to obtain the particle invasion depth. In previous work (Payatakes et al., 1974), a random number generator is used to generate a particle's entry point, and tracks each particle's movement inside the pores. This approach is sophisticated but does not give a valid invasion depth for up-scaling purpose. Moreover, this approach is extremely time-consuming.

A simplification is to assume the particles enter from the top of the pore. For a certain particle, it travels the furthest distance when entering from the top of the pore, as seen in Figure 6-1. This distance can be regarded as the maximum possible invasion depth. As such, the approximate invasion depth can be calculated with the mean particle size and mean pore size.

The gravity on a particle is:

$$F_g = (\rho_p - \rho_L) \cdot V_p \cdot g \qquad \text{(Equation 6-1)}$$

In equation 6-1, F_g is gravity; ρ_p and ρ_L are the densities of the particle and liquid respectively; and V_p is the volume of the particle.

Drag force can be calculated by (Shook and Roco, 1991):

$$F_d = Dc \cdot (v_L - v_p) \qquad \text{(Equation 6-2)}$$

The drag coefficient Dc in the above equation can be calculated by:

$$Dc = 6 \cdot \pi \cdot \mu_L \cdot r_p \qquad \text{(Equation 6-3)}$$

In equations 6-2 and 6-3, F_d is drag force; Dc is drag coefficient; r_p is the radius of the particle; v_L is the velocity of the suspension; and v_p is the velocity of the particle. The injected water is a Newtonian fluid, therefore Equations 6-2 and 6-3 are valid.

Many drag coefficient correlations have been developed for different situations, such as laminar flow and turbulent flow (Yue, 1999). For particulate flow inside porous media, the flow velocity is very low, resulting in low particle Reynolds number of less than 1. Equation 6-3 is valid for this Stokes region.

As explained earlier, a particle's invasion depth is determined by its velocity in the y direction. The forces and velocities in Equations 6-1 and 6-2 are vectors. Here, a force balance is established only in the y direction:

$$F_g + F_d = \rho_p \cdot V_p \cdot \frac{dv_p}{dt} \qquad \text{(Equation 6-4)}$$

Solving this ordinary differential equation with proper initial condition (v=0 at t=0), the velocity of the particle in y direction is found to be:

$$v_p(t) = \frac{F_g - \exp[\ln(F_g) - \frac{Dc}{\rho_p \cdot V_p} \cdot t]}{Dc} \qquad \text{(Equation 6-5)}$$

The time required for a particle to reach the pore surface can be evaluated by Equation 6-5. In fact, the solution of equation 6-5 reveals that a non-Brownian particle immediately reaches its terminal velocity. Terminal velocity (vt) is reached when the gravity force balances the drag force, which lead to:

$$vt = \frac{(\rho_p - \rho_L) \cdot V_p \cdot g}{Dc} \qquad \text{(Equation 6-6)}$$

The time for a particle to reach its terminal velocity is minimal (less than 0.1 second for a 2 micron particle with a density of 2 g/ml). Therefore, the retention time required for the particle to land on pore surface can be calculated by equation 6-6. The particle invasion depth then can be calculated by multiplying the retention time

with suspension velocity. It is assumed that no particles can travel further than the invasion depth.

6.2.2 Distribution of Particles in Network

The fluid flow rate in each bond is determined by the size of the bond. As a result, a large pore receives more fluid than a small pore. Since particles are uniformly suspended in the fluid, it is reasonable to assume that a large pore receives more particles. This assumption is referred to as flow biased probability theory (Rege and Fogler, 1988). To be specific, the number of particles that a pore captures is proportional to the pore's conductance, as calculated with Equation 4-13. Accordingly, a small pore has lower probability in capturing particles.

The capture of particles can be regarded as three phases. In the first stage, most particles are captured by large pores, resulting in moderate permeability drop. After the sizes of the large pores are reduced to a certain level, particles start to enter originally smaller pores. Some of the smaller pores have sizes comparable to the particle size, causing many small pores to be bridged or plugged. A quick drop in permeability can be observed in this stage. In the third stage, because the smaller pores have lost their flow capability, the particles in the suspension have to enter the unplugged pores. This again results in moderate permeability reduction.

This trend can be clearly seen in Figure 6-2, a test conducted by Roque et al. (1995). Till injection of 150 pore volumes of fluid, the permeability reduction is moderate. A quick drop in permeability reduction is observed between 150 to 300 pore volumes injected. And the permeability decrease slows down afterwards. Test data in another literature demonstrated similar behavior (Blauch et al., 1999).

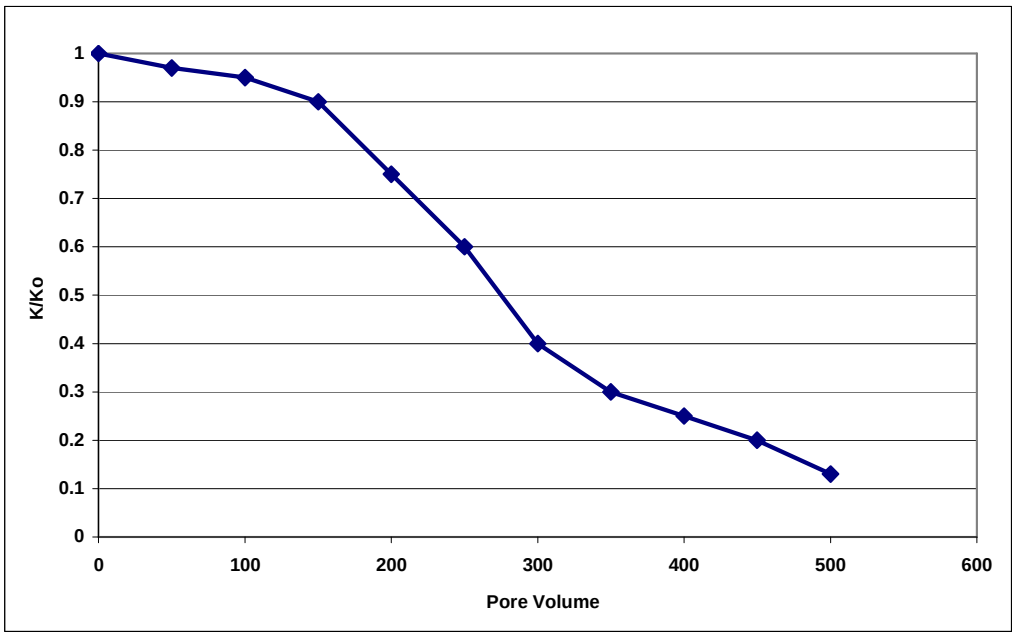

Figure 6-2: Three stages of permeability reduction

However, this trend is not clear in some other tests. Figure 6-3 gives such an example. In this test conducted by Roque et al. (1995), the permeability reduced almost linearly. Probably, the tested core in Figure 6-3 is more homogeneous than the one in Figure 6-2. The pores have very similar sizes, resulting in a uniform deposition of particles.

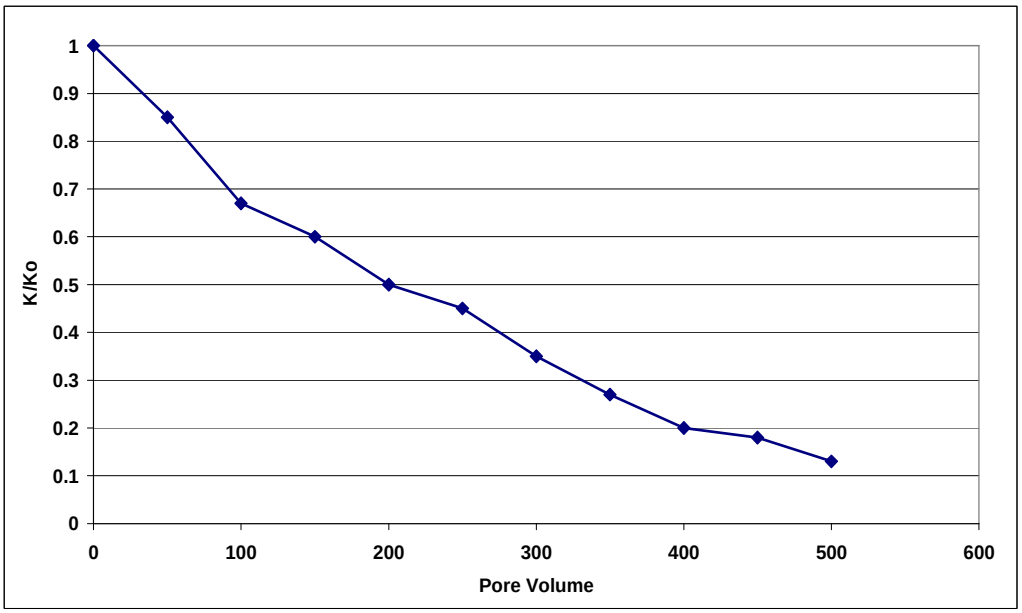

Figure 6-3: Linear permeability reduction phenomenon

6.2.3 Incorporating Damaging Mechanisms

Particles with different sizes may cause permeability reduction according to different mechanisms. For a particle much smaller than the pore where it is captured, the particle settles inside the pore and has a gradual effect on the resultant permeability decline. While for a particle bigger than the pore where it is captured, the particle plugs the pore and causes more severe permeability damage.

For the particle size in between, there is no clear guideline to determine the damaging mechanism at pore level. For a particle somewhat smaller than the pore where it is captured, the pore is left partially open but its flow capacity is badly reduced. Moreover, the captured particle greatly enhances the possibility of capturing incoming particles and bridging at the pore throat.

Todd et al. (1984) observed the damaged core with scanning electron micrographs. The observation reveals that the particles bridging at pore throats have a size between 1/7 and 1/3 the size of the pores, which supports the 1/7-1/3 rule. Accordingly, the following criteria are applied to the simulations:

(1) If the size of a pore is smaller than the particle diameter, the particle plugs the pore and the pore loses its flow capacity. The radius of such a pore is set to zero.

(2) If the size of a pore is larger than 3 times the particle diameter, the particle enters and deposits inside the pore. For example, if a number of particles (*n* particles) with volume of V_p deposit inside a bond with a volume of V_b, the new equivalent pore radius (R_b) is expressed as:

$$R_b = \left(\frac{V_b - n \cdot V_p}{\pi \cdot L_b}\right)^{0.5} \qquad \text{(Equation 6-7)}$$

(3) For a pore size in between, the particle bridges at the pore throat and the pore may lose most of its flow capacity. After particles form bridges at the throat, injected fluid can only flow through the gap between the particles. For example, if a number of particles (*n* particles) with a radius of r_p bridge at the throat of a bond with a radius of r_b, the new equivalent pore radius (R_b) is expressed as:

$$R_b = (r_b{}^2 - n \cdot r_p{}^2)^{0.5} \qquad \text{(Equation 6-8)}$$

The bond sizes in the network model need to be updated regularly to avoid errors in flow field calculation. The computation algorithm is illustrated in Figure 6-4. This procedure should be repeated until the desired duration is reached. A few realisations are generally required to achieve simulation results.

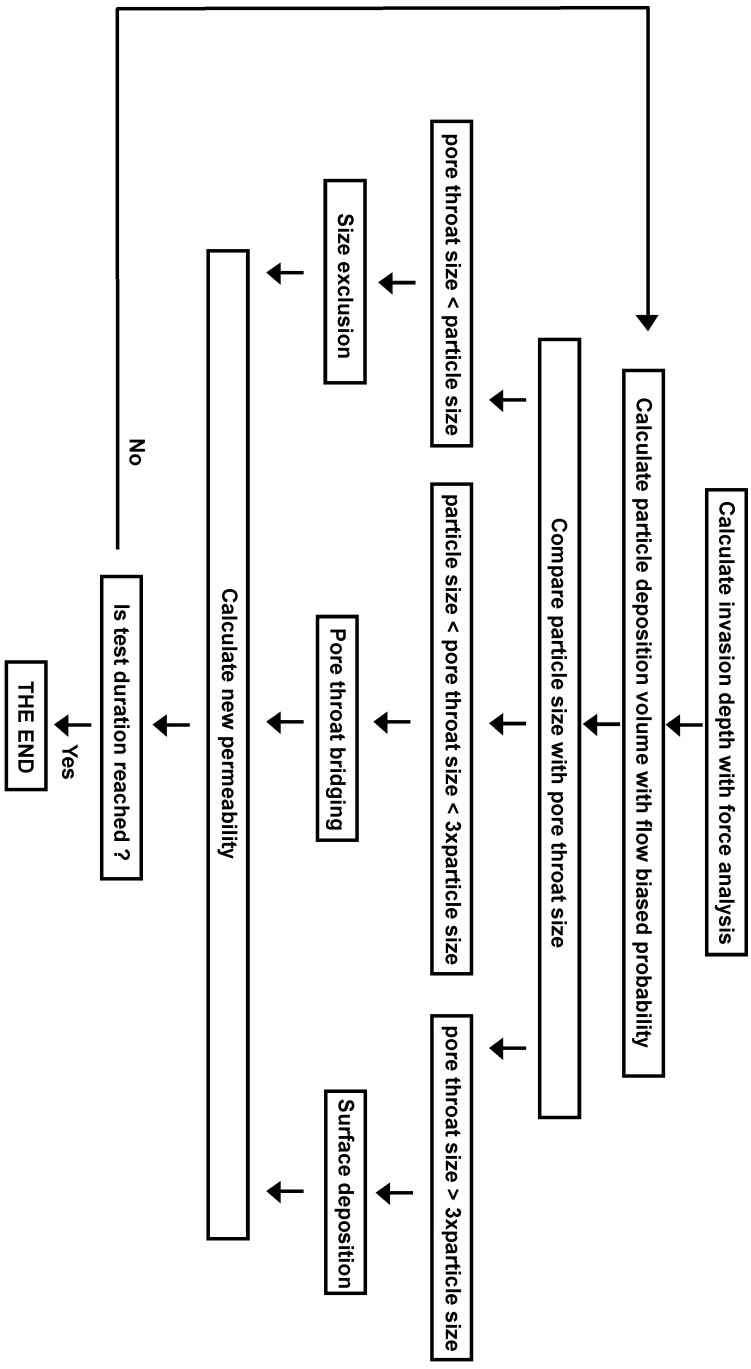

Figure 6-4: Computation algorithm for capture of large particles

6.3 Model Validation

Roque et al. (1995) documented their test data very well. Their tests on 2.35-micron particle at different flow rates are used to validate the proposed model. The three test cores had the same dimension: 50 mm in length and 100 mm in diameter. Their permeabilities ranged from low (224 mD) to high (3000 mD). The injection rates also ranged from low (3.4 ml/min) to high (50 ml/min). These test data with a wide range of parameters can serve as convincing approaches to validate the model.

6.3.1 Validation with Test 2

The test conditions of tests 2 are listed in Table 6-1. Experiment 2 was conducted with a low fluid velocity (1 cm/min).

Table 6-1: Test parameters of test 2 (Roque et al., 1995)

Test conditions	Value
Core porosity (%)	17.4
Core permeability (mD)	3000
Mean pore diameter (μm)	27.2
Average particle diameter (μm)	2.35
Particle concentration (mg/L)	20
Fluid flow rate (ml/min)	3.4
Injection velocity (cm/min)	1

A number generator is used to produce 100 numbers that follow a Normal distribution with a mean of 26.6 and a standard deviation of 2.6. These numbers are then assigned to the diameters of the bonds in the network. The simulated mean pore size (26.6 μm) is very close to that of the test core (27.2 μm). The simulated porosity and permeability have good agreements with those of the core, as seen in Table 6-2.

Trajectory analysis reveals an invasion depth of 7.5 mm, while the measurement showed the core was severely damaged in the first 7 mm section. The pore sizes are quite large compared with the particle size, so surface deposition are dominant. Figure 6-5 shows the comparison between test data and simulation results. The

simulated permeability damage is more sever at the early stage, and starts to gain better match with the test data after 300 pore volumes of fluid has been injected.

Table 6-2: Simulated parameters for test 2 (Roque et al., 1995)

Simulated parameters	Value
Actual vs. simulated porosity (%)	17.4 / 16.3
Actual vs. simulated permeability (mD)	3000 / 3192
Actual vs. simulated mean pore diameter (μm)	27.2 / 26.6
Simulated invasion depth (mm)	7.5

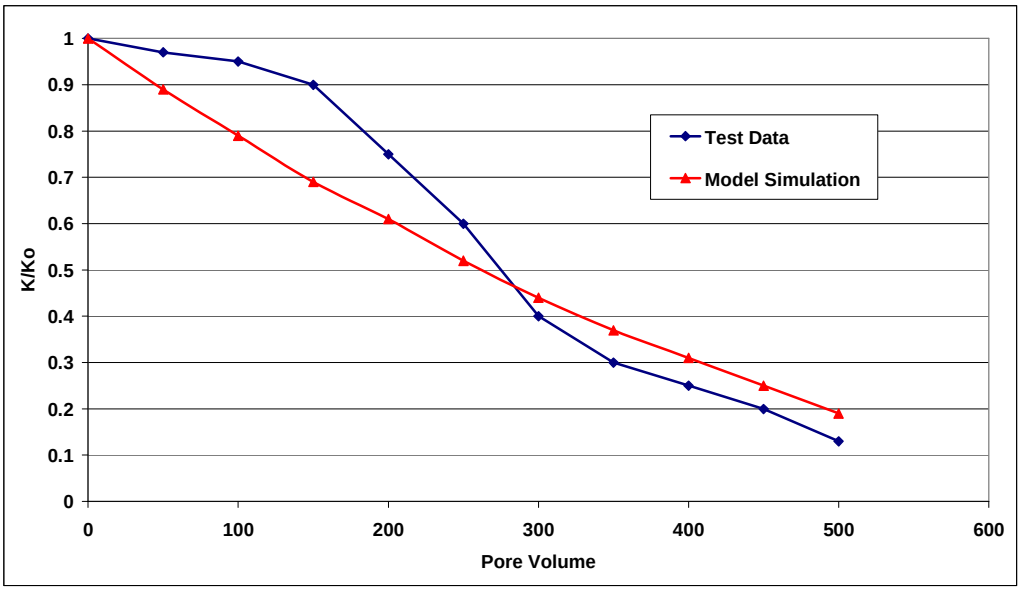

Figure 6-5: Test data and model simulation for experiment 2

Besides, the simulation can not reproduce the shape of the test curve, and the cause is not clear. One possibility is that the pore size distribution used for simulation is not adequate to represent the reality. On the other hand, the '1/3 rule' may be an oversimplified criterion. Pores with various sizes may have respective criterion for bridging.

6.3.2 Validation with Test 3

Test 3 was conducted with a medium injection velocity (4 cm/min). The test conditions are listed in Table 6-3. A Normal distribution with a mean of 16.6 and a

standard deviation of 5.7 is assigned to the bonds in the network. The simulated mean pore size (14 μm) is quite close to that of the test core (16.6 μm). The simulated porosity and permeability have good agreements with those of the cores, as seen in Table 6-4.

Table 6-3: Test conditions of test 3 (Roque et al., 1995)

Test conditions	**Value**
Core Porosity (%)	10.2
Core Permeability (mD)	224
Mean Pore Diameter (μm)	14.0
Average Particle Diameter (μm)	2.35
Particle Concentration (mg/L)	8
Fluid Flow Rate (ml/min)	7.9
Injection Velocity (cm/min)	4

Table 6-4: Simulated parameters for test 3 (Roque et al., 1995)

Simulated parameters	**Value**
Actual vs. simulated porosity (%)	10.2 / 10.9
Actual vs. simulated permeability (mD)	224 / 230
Actual vs. simulated mean pore diameter (μm)	14 / 16.6
Simulated invasion depth (mm)	15.5

The trajectory analysis reveals an average invasion depth of 15.5 mm, while no measurement was made. The mean pore size of the core used in experiment 3 (14 μm) is much smaller that that of the core used in experiment 2 (27.2 μm). Ten pores in the network are smaller than 3 times the particle diameter, and four bonds are even smaller than the particle diameter. In this case, pore throat bridging and plugging lead to significant permeability loss.

Figure 6-6 shows the simulation results versus experimental data. It can be seen that the simulation result appears very different from previous model output. The simulation is a “stairs”-style curve, rather than a smooth curve. After 100 pore volumes of suspension have been injected, some of the pores start to be bridged or

plugged, causing the permeability to drop sharply. After 150 pore volumes injected, more small bonds are bridged, causing permeability to drop again.

For a real rock, this change is not so dramatic because the flow is directed to other pores that are not plugged or bridged. While for the simulation, this effect is dramatic due to limited number of pores. Nevertheless, a curve formed by selected points can still represent the trend.

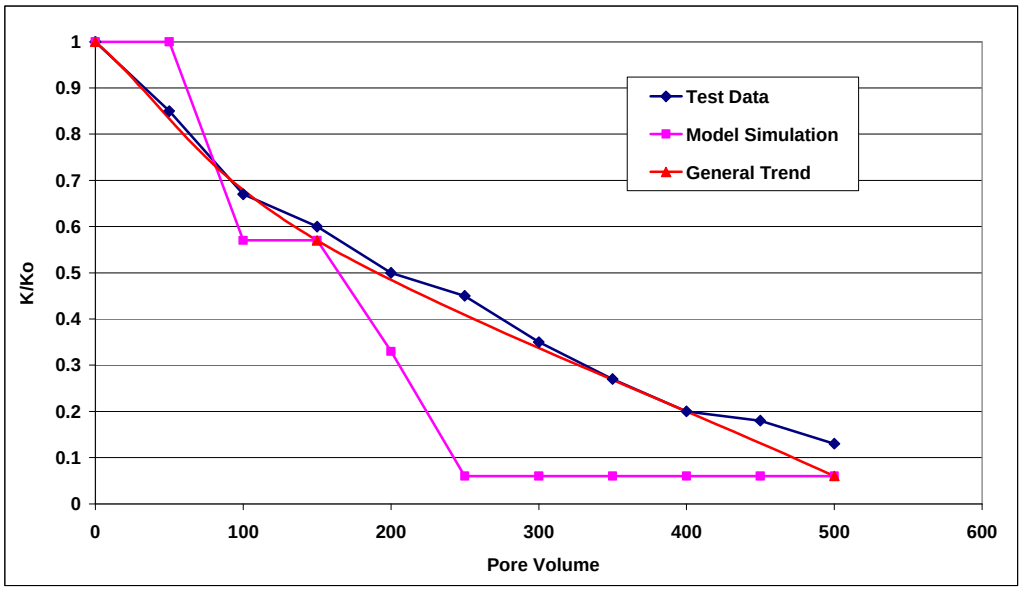

Figure 6-6: Test data and model simulation for experiment 3

6.3.3 Validation with Test 9

Test 9 was conducted with a high injection velocity (20 cm/min). The test conditions are listed in Table 6-5. A Normal distribution with a mean of 20.1 and a standard deviation of 2.65 is assigned to the bonds in the network. The simulated porosity and permeability have good agreements with those of the cores, as seen in Table 6-6. The trajectory analysis reveals an average invasion depth of 111.1 mm, which is greater than the length of the core (100 mm). This explains the very high particle concentration in the effluent that was measured during the experiment.

Figure 6-7 shows the comparison between test data and simulation results. The pores are big enough to allow particles to enter and deposit. As a result, the

simulation is similar to that for experiment 2. The high linear velocity also leads to less overall damage to the core, compared with test 2.

Table 6-5: Test parameters for test 9 (Roque et al., 1995)

Test conditions	Value
Core porosity (%)	14.2
Core permeability (mD)	1082
Mean pore diameter (μm)	20.0
Average particle diameter (μm)	2.35
Particle concentration (mg/L)	14
Fluid flow rate (ml/min)	50
Injection velocity (cm/min)	20

Table 6-6: Simulated parameters for test 9 (Roque et al., 1995)

Simulated parameters	Value
Actual vs. simulated porosity (%)	14.2 / 15.8
Actual vs. simulated permeability (mD)	1082 / 1128
Actual vs. simulated mean pore diameter (μm)	20 / 20.1
Simulated invasion depth (mm)	111.1

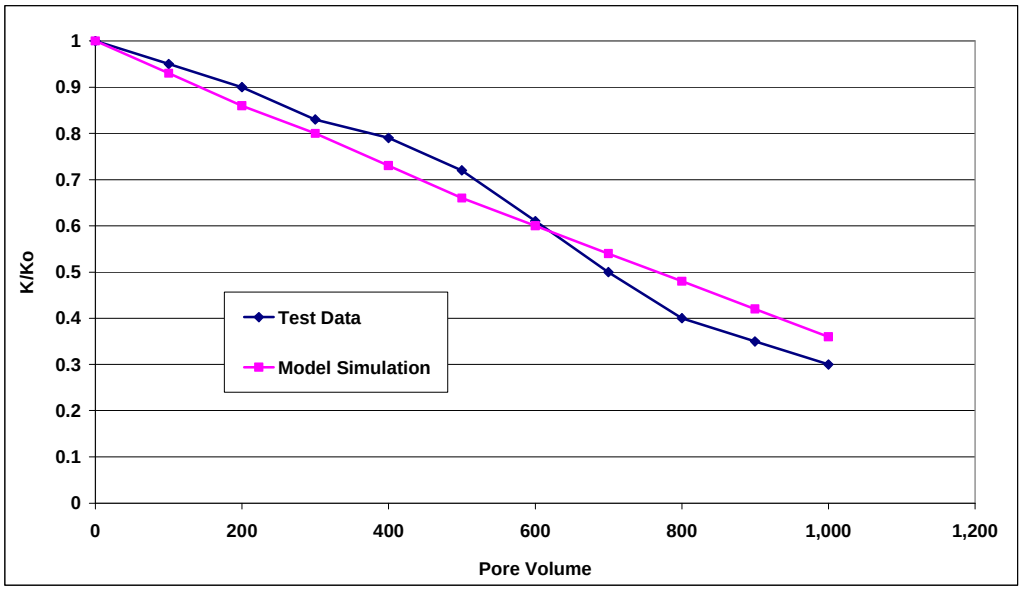

Figure 6-7: Test data and model simulation for experiment 9

6.3.4 Improvement on Simulation Results

Figure 6-8 compares the simulations of permeability decline with three network sizes. The simulations indicate that when the damage is cause by surface deposition of particles, the size of the network has no significant effects on simulation results. This is because surface deposition causes gradual permeability decline, similar to the phenomenon in real reservoir rocks. It can be seen that when surface deposition is dominant, network size has minor effect on simulation result.

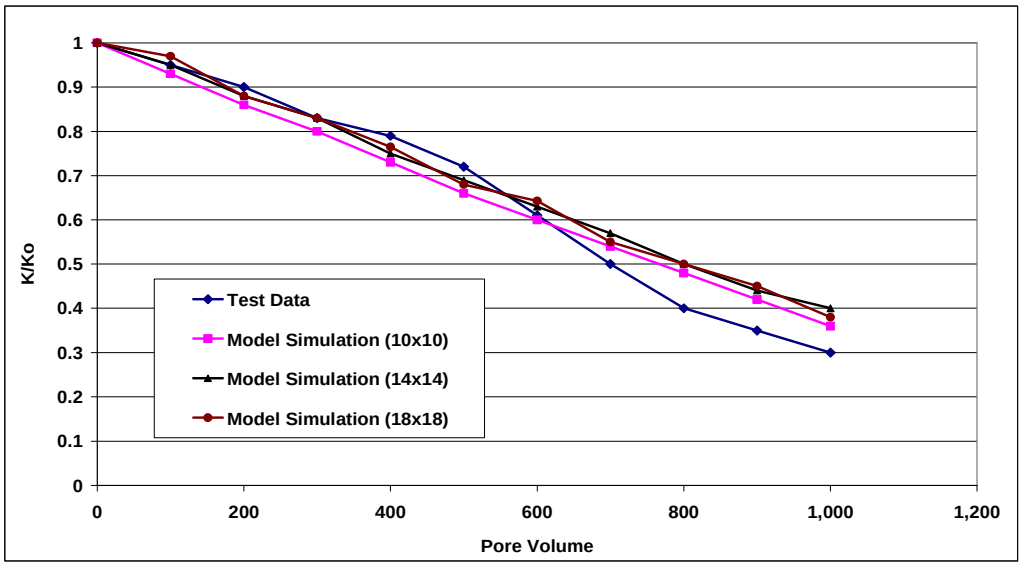

Figure 6-8: Effect of network size for deposition as dominant mechanism

However, when plugging or bridging is the main case of permeability decline, the network size may have a significant effect. For a real rock, if some of the pores are plugged, millions of unplugged pore will receive the biased flow. For a network with limited pores, when one or more bonds are plugged, the flow is biased to other unplugged pores in the network. However, if the network is not adequately large, the biased flow rate can cause very high pressure losses at receiving bonds. This will cause the calculated permeability to plunge, which does not represent the situation for a real rock.

Figure 6-9 compares the simulations of permeability decline with three sizes of network, when size exclusion is dominant. It can be seen that network size has

significant effect on simulation results. A larger network (18x18) performs better than a small network (10x10). However, for scenarios with different rock properties, particle concentrations and particle sizes, the proper network size may need to be determined individually.

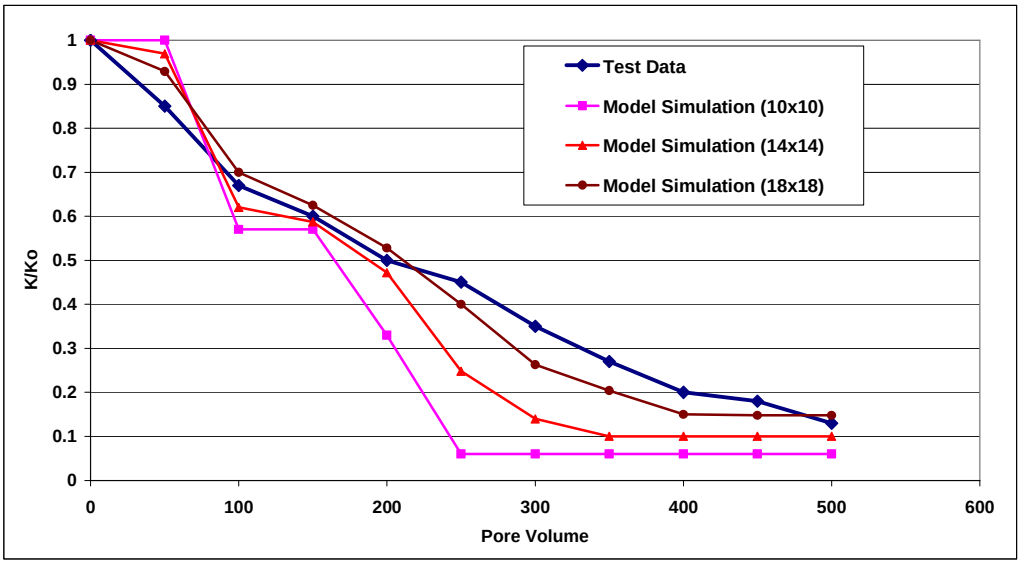

Figure 6-9: Effect of network size for plugging as dominant mechanism

Based on the simulation results in Figure 6-9, it can be seen that network size has certain effects on model output, especially when pore plugging and bridging are the dominant damage mechanisms. A network with 324 bonds performs better than a network with 100 bonds. Unfortunately, it is impossible to determine a proper size for all simulations. The model performance is controlled by many factors, such as pore size, particle sizes, particle concentration, and injection velocity. Each scenario has to be analysed individually to determine the proper network size for simulation. It is believed that a large network size is required for large particles and high particle concentrations, as these factors lead to a more severe permeability decline.

6.4 Discussions

Unlike previous work (Rege and Fogler, 1988), the proposed method in this chapter does not involve empirical parameters and achieved reasonably satisfactory results. However, the approach does require more computations than empirical models.

Besides, even though the approach employs many simplifications, a few parameters are involved in the proposed model, which may cause discrepancies in simulation.

First, pore network models (both 2D and 3D) involve many assumptions. Previous research has proved that pore network model is realistic to reproduce many reservoir characteristics. However, it can not be denied that the network model is indeed different from a real porous medium.

Second, many simplifications and assumptions are employed in simulation procedures:

(1) Force analysis is applied to obtain the distance particles travel inside porous media. Due to the complex nature of porous media and particle dynamics, the calculated invasion depth is only approximate.

(2) Flow biased probability was used to distribute the particles in the network model. Majority of the particles are believed to abide by this law, but it can not be denied that some particles do move in random pathways inside porous media.

(3) Previous tests revealed that the damage is not uniform along the core. The damage profile is determined by many factors such as particle size, particle concentration and fluid velocity. In this work, it is assumed that the damage profile is uniform within the invasion depth.

(4) Surface properties are either measured or predicted by empirical equations (Riley, 2005). The author attempts to avoid introducing empirical parameters into the model. Therefore, the surface properties of porous media and particles are ignored.

(5) The model assumes that particles will not reenter the flow once captured. This is based on the fact that the calculated fluid Reynolds number is a fraction of 1 inside the network. With this low Reynolds number, particles are not expected to re-suspend once captured (Yue, 1995).

(6) The criteria for determination of damage mechanisms are not yet clear. In the proposed model, the size of a particle is compared with the size of the pore where

the particle is captured to determine the damaging mechanism. However, this may be an oversimplified criterion.

6.5 Model Application

The proposed method is able to predict the necessary parameters for model up-scaling, such as the damage radius and the permeability change within the damage radius. Traditional radial flow equations can be applied to predict injectivity decline.

Assume that a circular reservoir is going through PWRI. The reservoir properties are identical to those of the core tested in experiment 9, so are the particle size and concentration. The wellbore radius is 63 mm. The reservoir radius is 200 m. The height of the injection zone is 25 m. The water injection rate is 2580 bbl/day (412 m^3/day), which translates into a linear flow velocity of 20 cm/min.

Skin factor S is expressed as (Ahmed, 2001):

$$S = (\frac{K_o}{K} - 1) \cdot \ln(\frac{r_d}{r_w}) \qquad \text{(Equation 6-7)}$$

where K is the permeability of the damaged region at a certain time; r_d is the damage radius or invasion depth. These two parameters can be predicted by the proposed method in this chapter. r_w is the wellbore radius. The ratio of damaged flow rate (I) and original flow rate (I_o) is expressed as:

$$\frac{I}{I_o} = \frac{\ln \frac{r_e}{r_w}}{\ln \frac{r_e}{r_w} + S} \qquad \text{(Equation 6-9)}$$

At a certain time, the damaged permeability K is calculated with the proposed model. Then the skin factor S is obtained by Equation 6-8. With the skin factor, the flow rate ratio can be calculated with Equation 6-9.

The simulation result with the above field conditions is shown in Figure 6-10. It can be seen that with the particle concentration of 14 ppm, the injector will lose almost half of its injection rate within one day. If the injected water is filtered to a particle concentration of 7 ppm, the decline is much less severe. Above that, the sudden drop in injection rate between 0.4 and 1 day is not observed. If the injected water is further filtered to a particle concentration of 3 ppm, the decline is slow and the well is likely to sustain its injection rate over a long period of time.

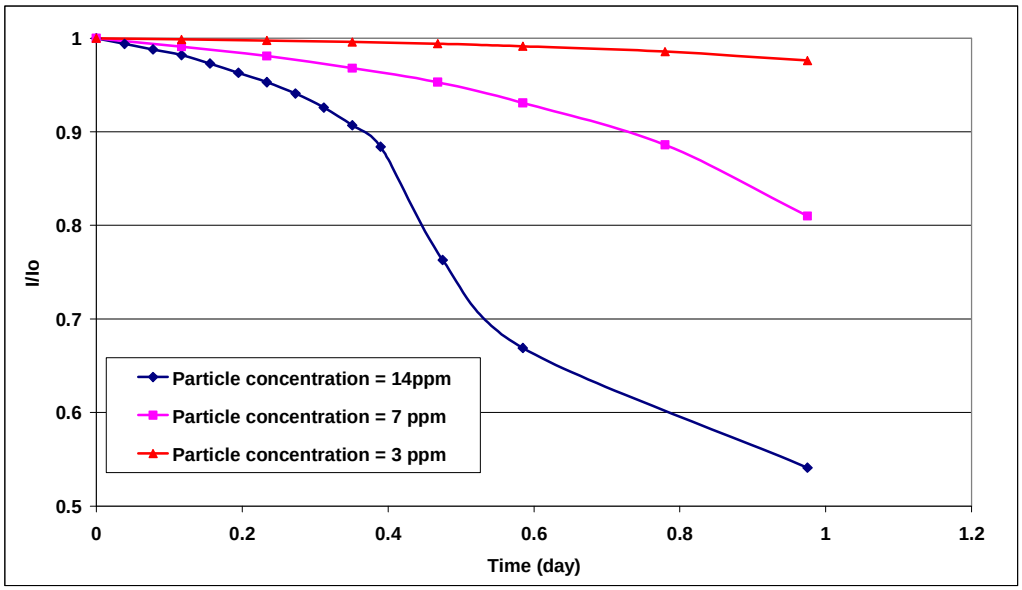

Figure 6-10: Prediction of well injectivity under invasion of non-Brownian particles

6.6 Concluding Remarks

- Particle deposition in porous media is a complex process due to the complex nature of porous media and the properties of injected particles and fluids. In this work, network model is employed to gain better understanding of the capture of non-Brownian particles in porous media.

- A novel procedure is proposed in the model. First, trajectory analysis is carried out to obtain particle invasion depth. Second, particles are distributed in the network model according to flow biased probability. Third, particle sizes are compared with pore sizes to determine damaging mechanism – surface deposition, size exclusion, or pore-throat bridging. The proposed procedure is based on reasonable theoretical and

experimental evidence. The model is able to produce simulation results without large-scale computation.

- The model is validated with test data and achieved reasonably good results, without introducing empirical parameters. The relatively good match between simulation and test data leads to the conclusion that for non-Brownian particles, the damage mechanisms are controlled by particle size to pore size ratio.

- When pore bridging and plugging is the dominant cause of permeability damage, the model performance may not be satisfactory if the network size is not large enough. The simulation can be improved by expanding the network size.

- Model up-scaling method is also provided. The case study based on certain parameters shows that injected water is to be filtered to contain less than 3ppm of non-Brownian particles, in order to maintain the well's injectivity.

CHAPTER 7

CAPTURE OF EMULSION DROPLETS

IN POROUS MEDIA AND RESULTANT PERMEABILITY REDUCTION *

7.1 Introduction

In petroleum industry, research in flow of oil droplets in porous media has been driven by two purposes. On one hand, produced water contains certain amounts of oil droplets. When the oily water is injected back into reservoir for pressure maintenance, the droplets can plug the injection zone and cause severe decline in well injectivity (Ali et al., 2007). On the other hand, injected water tends to enter the formations with higher permeability, leaving behind the reserves in zones with lower permeability. Some EOR (enhanced oil recovery) projects take advantage of this feature and employs emulsion to block the high permeability zone that absorbs large amounts of the injected water, so that injected water is able to sweep the reservoir with poor permeability (Thomas and Ali, 1989).

Emulsions are colloidal dispersions in which a liquid is dispersed in a continuous liquid phase of different composition (Schramm, 2005). The dispersed phase is sometimes referred to as the internal (disperse) phase and the continuous phase as the external phase. In most emulsions, one of the liquids is aqueous while the other is hydrocarbon and referred to as oil. Two types of emulsion are readily distinguished in principle, depending upon which kind of liquid forms the continuous phase:

- Oil-in-water (O/W) emulsion for oil droplets dispersed in water
- Water-in-oil (W/O) emulsion for water droplets dispersed in oil.

The type of emulsion and its stability is determined by many factors, such as the water to oil ratio, surfactant type and concentration, temperature of the system, and mixing conditions (Binks, 1998). For the injected water and injected emulsion for EOR purpose, the oil concentration is very low and the solution is oil-in-water

*Accepted for publication in APPEA Journal with slight modifications

emulsion. Therefore, previous research has been focusing on the flow of oil-in-water emulsion in porous media.

7.2 Previous Work

Experiments were carried out to study the capture of emulsion droplets in porous media. Some previous tests are summarised in Table 7-1.

Table 7-1: Some previous tests on flow of emulsions in porous media

Researcher	Cartmill and Dickey (1969)	McAuliffe (1973)	Soo and Radke (1984a)	Romero et al. (1996)
Tested Porous Media	Glass beads and sand pack	Sandstone cores	Sand packs	Sandstone cores and sand packs
Media Length (cm)	41	7.6	5	About 5
Media Diameter (cm)	2.48	3.8	2.5	About 2.5
Media Permeability (mD)	9500 and 53000	1600	570 and 1150	22 to 2615
Test Oil	Crude Oil	Crude Oil	Mineral Oil	Crude Oil
Oil Volume Concentration (%)	0.002 to 0.004	0.5	0.5	unknown
Mean Droplet Size (micron)	0.5 to 1.5	1 to 12	2 to 10	3 to 14

Cartmill and Dickey (1969) injected micro-emulsions into glass beads and sand packs. They analysed the porous media under a microscope and observed many oil droplets were captured on grain surfaces, while others formed clusters in big pores.

McAuliffe (1973) first proposed to inject emulsion for enhanced oil recovery. He reported that the emulsion with more than 60% of oil showed non-Newtonian flow behaviors. He found large droplets caused more severe permeability decline, and the reduction was irreversible even after subsequent injection of clean water.

Soo and Radke (1984a) injected emulsions made from mineral oil into two sand packs with different permeabilities. Their test results revealed that larger droplets generally led to more severe permeability reduction. They also observed the porous media through a micro-model while emulsion was being injected. At the end of the

test, the sand surfaces were coated by droplets, and some droplets formed clusters in bigger pores formed by sand grains.

In another work by Soo and Radke (1984b), emulsions were injected at very different superficial velocities and the permeability declines were about the same under different velocities. Previously, it was believed that the captured droplets could squeeze through pore throats when the injection velocity is higher. However, their work proved otherwise: higher velocity can not remove plugging.

Soo and Radke (1985) also compared the permeability damages caused by emulsion droplets versus suspended particles. Solutions containing droplets or particles with the same size of 2.2 microns and the same volume concentration of 0.5% were injected into sand packs with the same permeability of 1.15 Darcy. The emulsion caused the sand pack to lose 25% of its original permeability, while the particles cause 90% of permeability loss. Moreover, the permeability decline reached equilibrium (i.e., the decline ceased) at a certain stage of emulsion injection. While for the injections of particles, the decline did not reach equilibrium even at the end of injection.

Romero et al. (1996) injected dilute oil-in-water emulsion into sandstone cores and unconsolidated sand packs under reservoir conditions. They also injected clean water to displace the emulsion, but the damage to permeability was not affected.

The observations can be summarised as follows. Injection of emulsion can cause severe permeability losses to porous media. The tested porous media lost 50% to 99% of their original permeability to water. And the damage is not reversible by subsequent injection of clean water. Larger droplets lead to more severe damage, but severe permeability reduction can occur even when the sizes of emulsion droplets are much smaller than the mean size of the pore restrictions. Superficial velocity has minor effect on permeability decline.

The previous experimental observations (Soo and Radke, 1984a) also reveal that the droplets are captured in porous media by two mechanisms: straining and interception, as illustrated in Figure 7-1. Straining capture occurs when an emulsion droplet gets trapped in a pore constriction of size smaller than its own diameter. Emulsion droplets can also attach themselves onto the rock surfaces due to van der Waals, electrical, gravitational, and hydrodynamic forces. This mode of capture is

denoted as interception. Capture of emulsion droplets reduces the effective pore diameter, diverts flow to the larger pores, and thereby effectively reduces permeability.

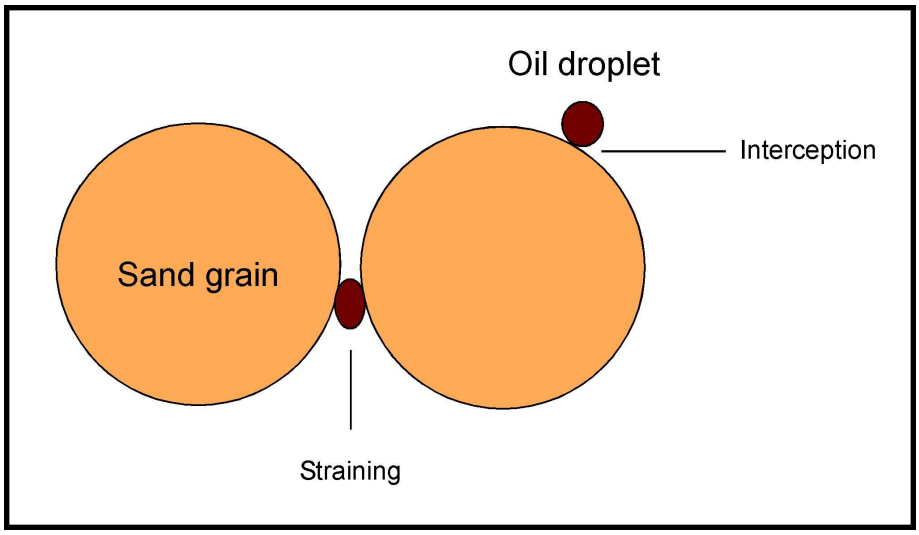

Figure 7-1: Two mechanisms for capture of oil droplets in porous media

Droplet retardation model and filtration model were proposed to simulate capture of emulsion droplets in porous media and predict resultant permeability decline.

The droplet retardation model (Devereux, 1974) is based on the concept that when an emulsion droplet enters a pore constriction having a pore throat smaller than its own diameter, it deforms and squeezes through. During this process it experiences a capillary resistance force and as a result moves at a slower speed than the continuous phase and thereby causes a reduction in permeability. Steady state is reached when the emulsion breaks through the porous medium. The model requires the knowledge of the relative permeabilities of the oil droplets in the emulsion and the continuous water phase, which must be determined before the model can be used.

The main drawback of the model is that the permeability reduction is maintained as long as the emulsion is flowing, and the initial permeability is restored once the emulsion injection is followed by water. In other words, the emulsion droplets all pass through the porous medium and none of them is captured inside. However, experimental evidence suggests that the permeability reduction cannot be restored after subsequent water injection. Apparently, the droplet retardation model is

inadequate at understanding the mechanisms of permeability reduction induced by oil droplets.

A more advanced model based on deep-bed filtration principles was proposed by Soo and Radke (1986). They suggested that the emulsion droplets are not only retarded, but they are also captured in the pore constrictions. In their filtration model, three empirical parameters were defined: the filter coefficient that controls the sharpness of the emulsion front, the flow redistribution parameter that describes the redistribution phenomenon as well as the steady-state retention of emulsion droplets, and the flow restriction parameter that addresses the effectiveness of the droplets in reducing permeability. The major drawback of this filtration model is that the three empirical parameters are obtained by fitting filtration data, which makes this model heavily dependent on test data.

7.3 Model Formulation

The aim of this work is to develop a model that relies less on core flooding data. In order to do so, pore network model is used to gain better understanding of the porous media. Moreover, the mechanism for droplet attachment on rock surfaces must be clarified.

7.3.1 Capture-Equilibrium Theory

As discussed earlier, the fluid flow rate in each bond is determined by the size of the bond: a large pore receives more fluid than a small pore. Because droplets are suspended in the injected emulsion, more droplets enter the larger pores, rather than the small ones. This theory is referred to as flow biased probability theory (Rege and Fogler, 1988). In the simulation, the number of droplets that a pore receives is directly proportional to its hydraulic conductance. It is worth mentioning that even though the chance for a small pore to receive droplets is low, once this happens, the permeability of the network is reduced more dramatically due to the big pressure build-up at the small pore.

Once a droplet is captured on sand surface, it occupies a certain area. Unlike solid, a droplet can not be captured on top of another droplet. So it is assumed that once the sand surface is coated with oil, the deposition process reaches equilibrium and

no more oil droplets will deposit on sand surface. Afterwards, oil droplets flow freely through the porous media without being captured. This assumption is illustrated in Figure 7-2 and named capture-equilibrium theory by the author.

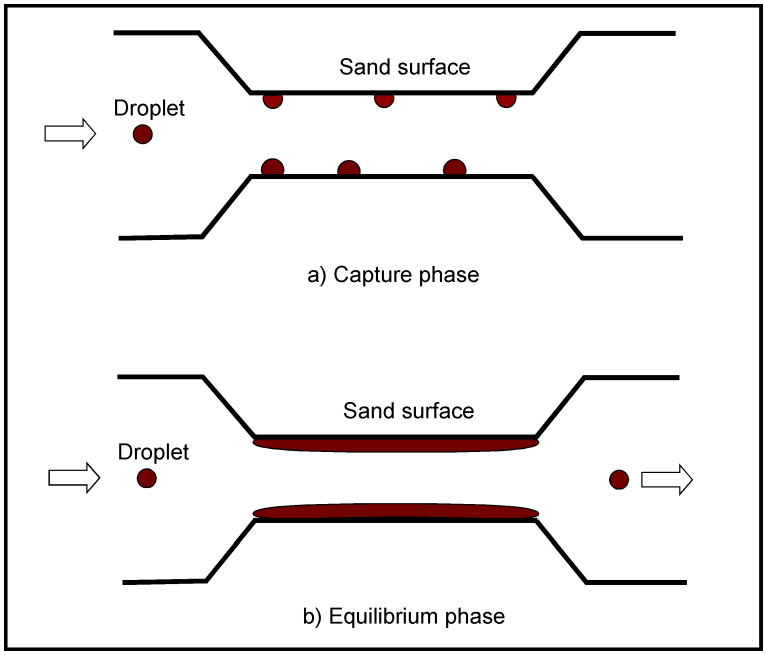

Figure 7-2: Two phases of droplet capture

7.3.2 Effect of Surface Wettability

The two damaging mechanisms, interception and straining should be incorporated into the model. If the size of a droplet is bigger than that of the pore that it attempts to pass through, the droplet blocks the pore and the pore loses its flow capacity. The flow is then biased to other open pores, increasing the pressure loss, which translates into permeability decline.

If the size of a droplet is smaller than that of the pore that it attempts to pass through, the droplet enters the pore and adheres to sand surface until equilibrium is reached. The effective diameters of the pores are reduced, which translates into permeability damage. The computation algorithm is summarised in Figure 7-3.

Oil droplets are captured on sand surfaces, and form an oil layer. In order to calculate the permeability reduction, the thickness of the oil layer formed by

droplets must be determined. The wettability of the reservoir rock directly determines the forms of the droplets on sand surfaces.

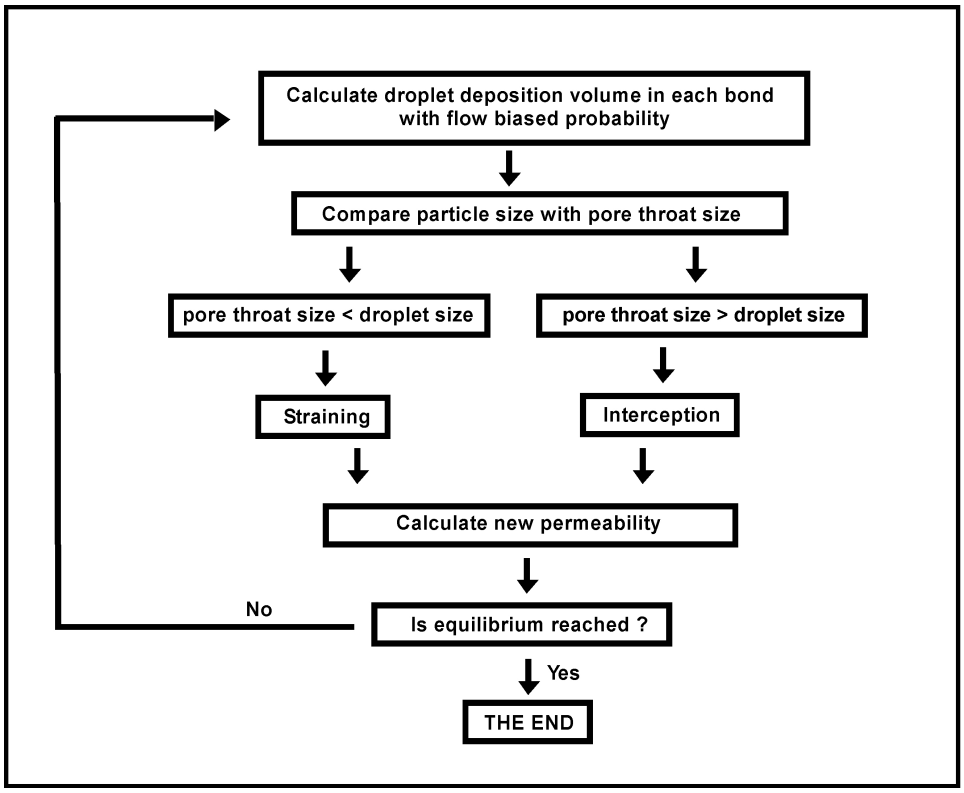

Figure 7-3: Computation algorithm for capture of droplets

Wettability is quantified by contact angle (Webb and Orr, 1997). If the rock surface is strongly oil-wet, oil droplets will have a high contact angle which leads to a thin oil layer. If the rock surface is strongly water-wet, oil droplets form small contact angle which leads to a thicker deposit, as shown in Figure 7-4. If the contact angle is smaller than 75 degrees, the rock is considered to be water-wet. If the contact angle is between 75 and 105 degrees, the rock is considered to be neutrally wet. If the contact angle is smaller than 75 degrees, the rock is considered to be oil-wet (Anderson, 1986).

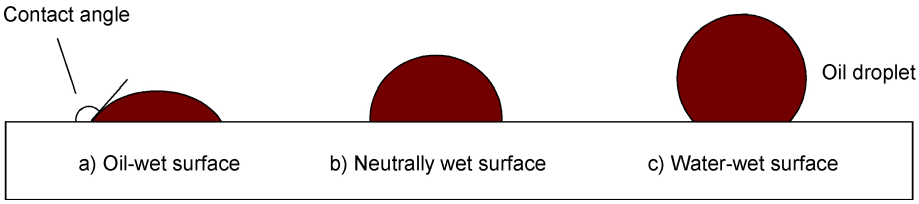

Figure 7-4: Higher contact angle leads to thin oil layer

After an oil droplet adheres to pore surface, it deforms according to the wettabilities in Figure 7-4. However, a droplet's volume does not change. If the contact angle is known, the thickness of the oil layer can be easily calculated by the following volume balance equation:

$$\frac{4}{3}\cdot\pi\cdot r_p^{\,3}=\frac{1}{3}\cdot\pi\cdot H^3\cdot\left(\frac{2-\cos\theta}{1+\cos\theta}\right) \qquad \text{(Equation 6-1)}$$

In Equation 6-1, r_p is droplet radius instead of particle radius; H is the oil layer thickness; and θ is the contact angle. The left hand side of Equation 6-1 is the original droplet volume, and the right hand side is the droplet volume after deform. Equation 6-1 is valid for contact angles higher than 90 degrees. For contact angles lower than 90 degrees, the following correlation should be used:

$$\frac{4}{3}\cdot\pi\cdot r_p^{\,3}=\frac{4}{3}\cdot\pi\cdot\frac{H^3}{(1+\cos\theta)^3}-\frac{1}{3}\cdot\pi\cdot H^3\cdot\left(\frac{2-\cos\theta}{1+\cos\theta}\right)$$

(Equation 6-2)

Unfortunately, there have been many controversies over rock wettability. Traditionally, reservoir rocks were believed to be strongly water-wet. However, most reservoirs were found to be oil-wet or neutrally wet in the literature. In one study (Treiber, 1972), out of the 30 sandstone reservoirs, 15 were found to be oil-wet, and 2 to be neutrally wet; for the 25 carbonate reservoirs, 21 were found to be oil-wet and 2 to be neutrally wet. In another study (Cuiec, 1984), out of the 12 carbonate reservoirs, 6 were found to be oil-wet; 5 were neutrally wet, and 1 were strongly water-wet. In fact, only a small fraction of the reservoirs demonstrate strong water wettability.

Rock wettability can be estimated from some laboratory techniques, such as USBM and Amott methods (Anderson, 1986). Both methods interpret drainage and imbibition test data to quantify the overall rock wettability. However, these methods only give a rough indication of wettability, rather than the accurate value of contact angel. In the model validation section, a trial-and-error process has to be employed to determine the most suitable contact angle.

7.4 Model Validation

Soo and Radke (1984a) documented their test procedures and test data very well. Their data are used to validate the proposed model.

Ottawa sand was packed into a steel cylinder to serve as the porous media. The sand used was thoroughly washed with dilute acid solution to establish a strongly water-wet and reproducible surface. By adjusting the sizes of the sand grains, the sand packs achieved permeabilities of 1.15 Darcy (referred to as sand pack 1) and 0.57 Darcy (referred to as sand pack 2). The porosities are 0.34 and 0.31 for sand packs 1 and 2 respectively.

The emulsion was made by diluting Chevron 410H mineral oil with caustic solution to achieve an oil volume concentration of 0.5%. The emulsion was stabilised by sodium oleate and oleic acid. A certain droplet size was achieved and maintained by controlling the blender speed. The injection flow rate was kept constant at 0.02 cm^3/s.

Table 7-2 lists the parameters of the tested sand packs and the simulated parameters with the proposed network model. The measured and simulated pore size distributions for sand packs 1 and 2 are compared in Figure 7-5 and 7-6 respectively. Although the simulated average pore-throat sizes are relatively higher than the measured values, the proposed network model can represent the permeabilities and porosities of the sand packs fairly well.

Table 7-2: Simulated parameters for tested sand packs

Sand pack	1	2
Measured mean pore-throat diameter vs. simulated value (μm)	29.5 vs. 35.5	17.3 vs. 24.0
Measured permeability vs. simulated permeability (Darcy)	1.15 vs. 1.10	0.570 vs. 0.597
Measured porosity vs. simulated porosity	0.34 vs. 0.33	0.31 vs. 0.30

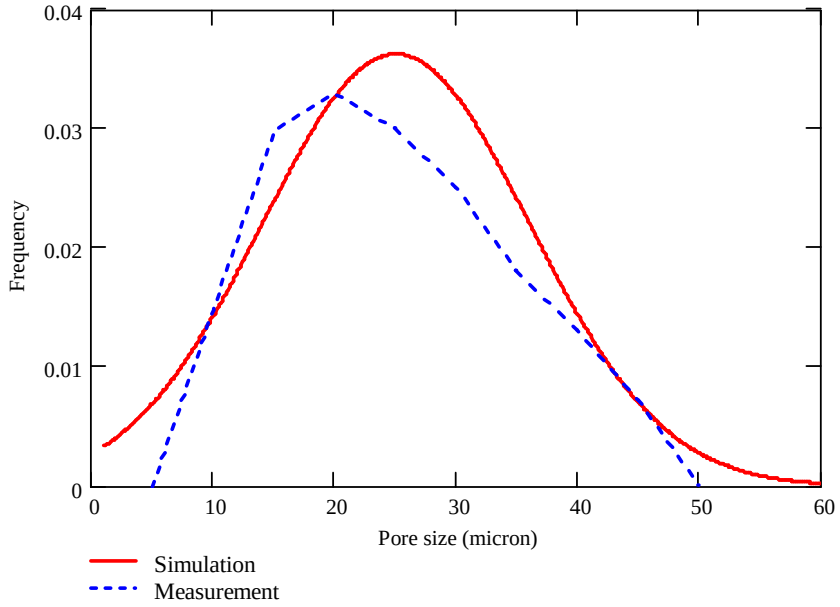

Figure 7-5: Measured and simulated pore size distributions for sand pack 1

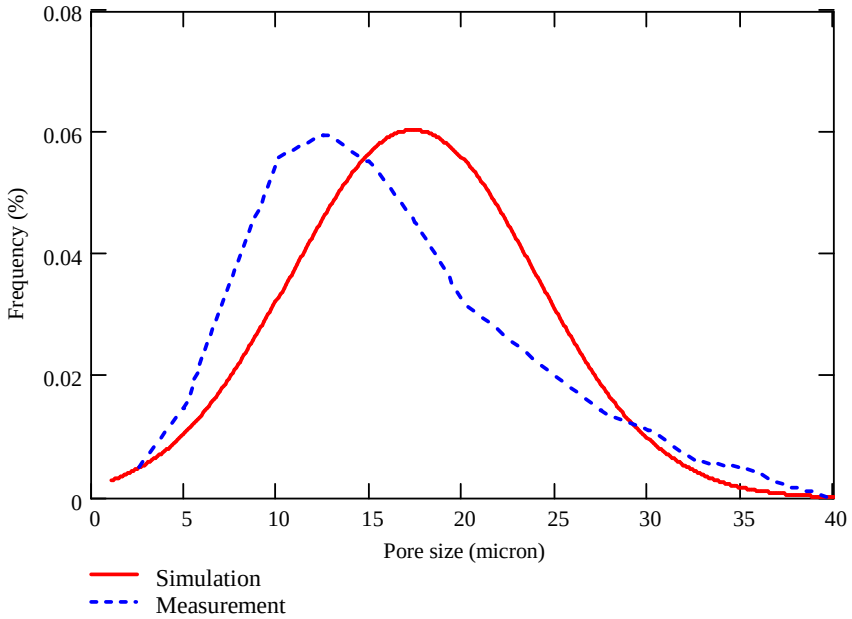

Figure 7-6: Measured and simulated pore size distributions for sand pack 2

Emulsions with droplet sizes of 2.1, 3.1 and 4.5 microns were injected into sand pack 1. Figures 7-7, 7-8 and 7-9 illustrate the test data versus model simulation. The y axis is permeability ratio of damaged permeability over original permeability. The x axis is pore volumes injected.

As explained earlier, it is assumed that once the surface of the pore throats are coated by oil droplets, equilibrium is reached and oil droplets pass through the porous media freely without being captured. This assumption is validated by the test data in Figure 7-7: permeability decline leveled off after injection of about 10 pore volumes of emulsion. For the test data in Figure 7-8, permeability decline was about to reach equilibrium after injection of 20 pore volumes of emulsion. In Figure 7-9, permeability did not reach equilibrium after injection of 20 pore volumes of emulsion.

The simulation results in Figures 7-7, 7-8 and 7-9 with similar contact angles follow a very similar trend: permeability declines linearly and levels off after equilibrium. It is also clear that larger droplets lead to more severe permeability loss, simply because larger droplets form a thicker deposit on sand surfaces. The simulation result in Figure 7-7 matches the test data quite well. In Figures 7-8 and 7-9, some discrepancies exist and the possible reasons will be analysed later.

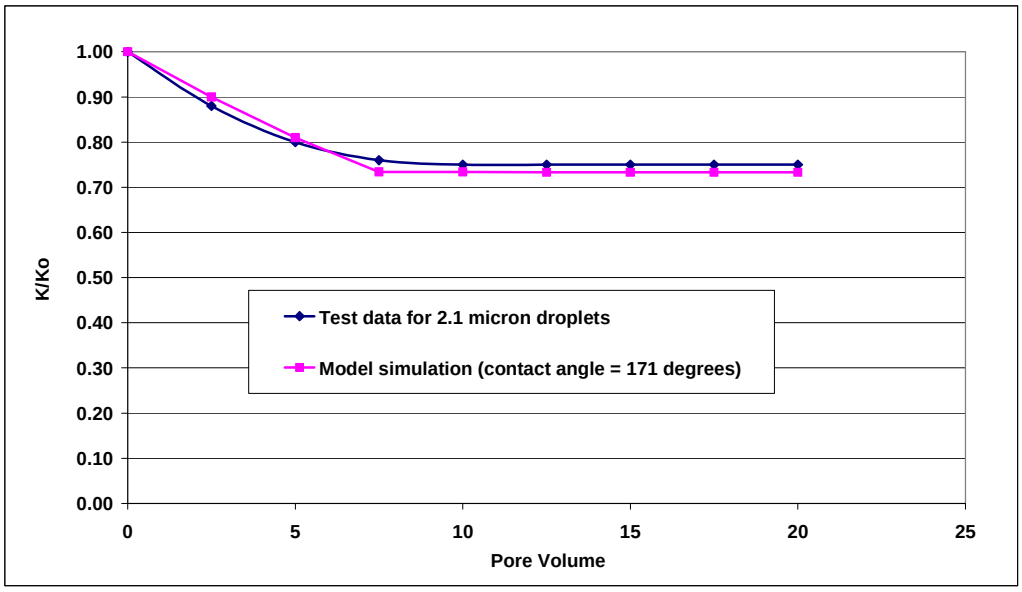

Figure 7-7: Test data and model simulation for injection of 2.1-micron droplets

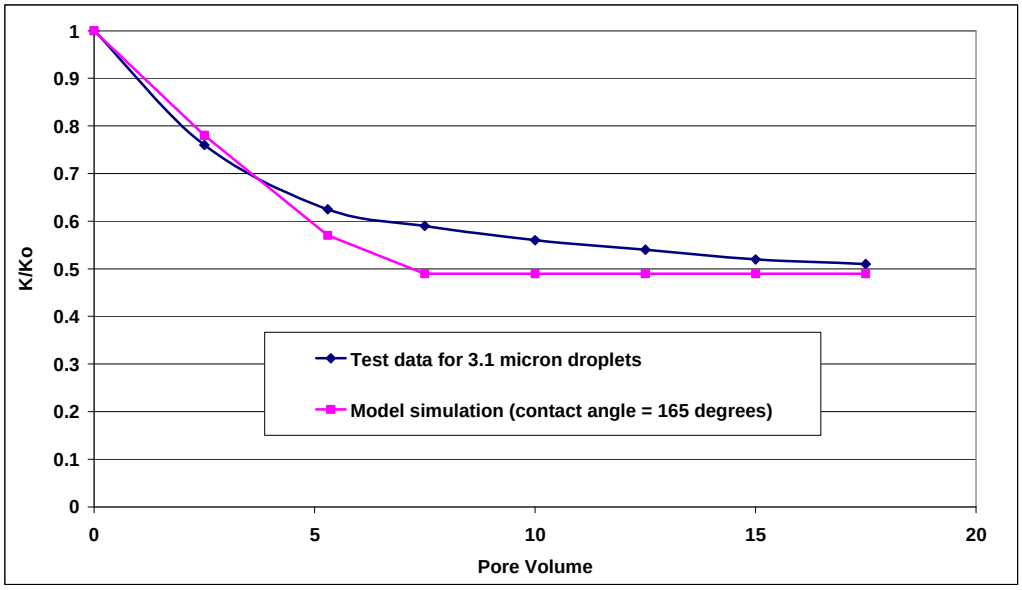

Figure 7-8: Test data and model simulation for injection of 3.1-micron droplets

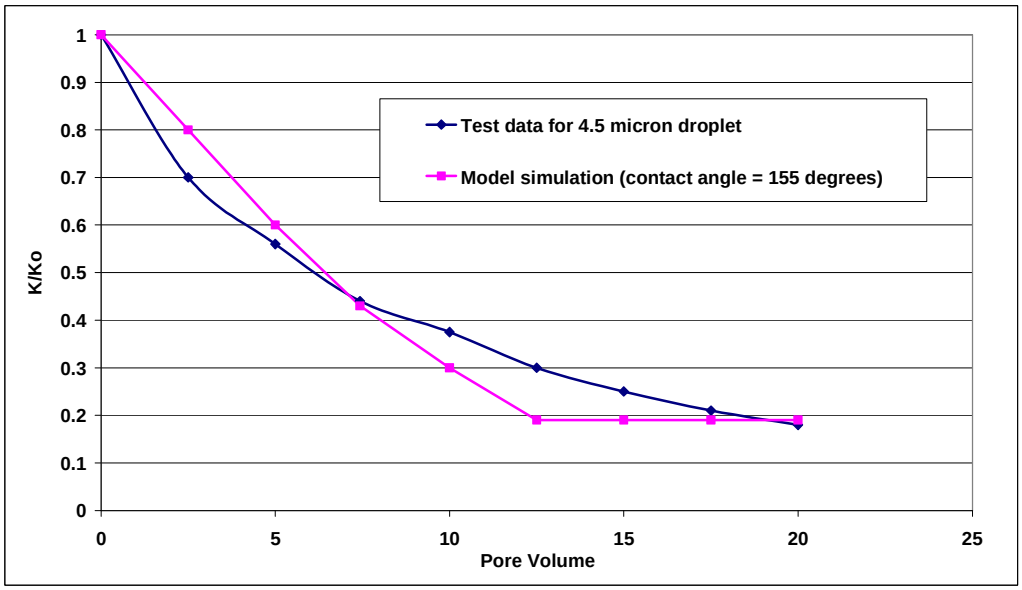

Figure 7-9: Test data and model simulation for injection of 4.5-micron droplets

Emulsions with droplet sizes of 3.3 and 5.3 microns were injected into sand pack 2. Figures 7-10 and 7-11 illustrate the test data versus model simulation. Sand pack 2 has much smaller pores than sand pack 1, as shown in Table 2. Therefore more severe permeability reductions were observed. It is worth mentioning that some of the pore throats in the network model for sand pack 2 have sizes smaller than the injected droplets. As such, straining mechanism also contributes to the permeability reduction in Figure 7-11.

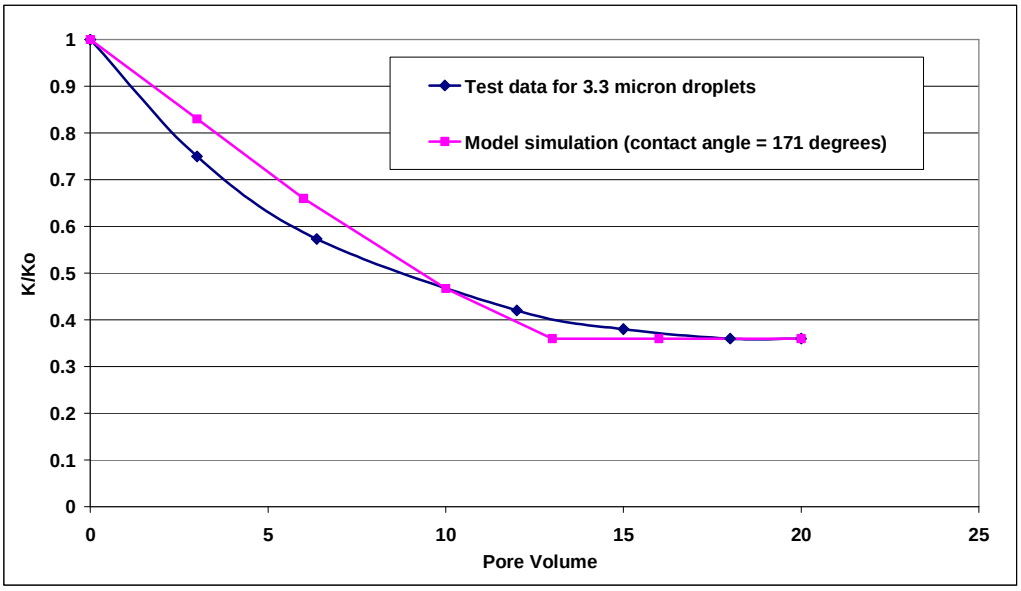

Figure 7-10: Test data and model simulation for injection of 3.3-micron droplets

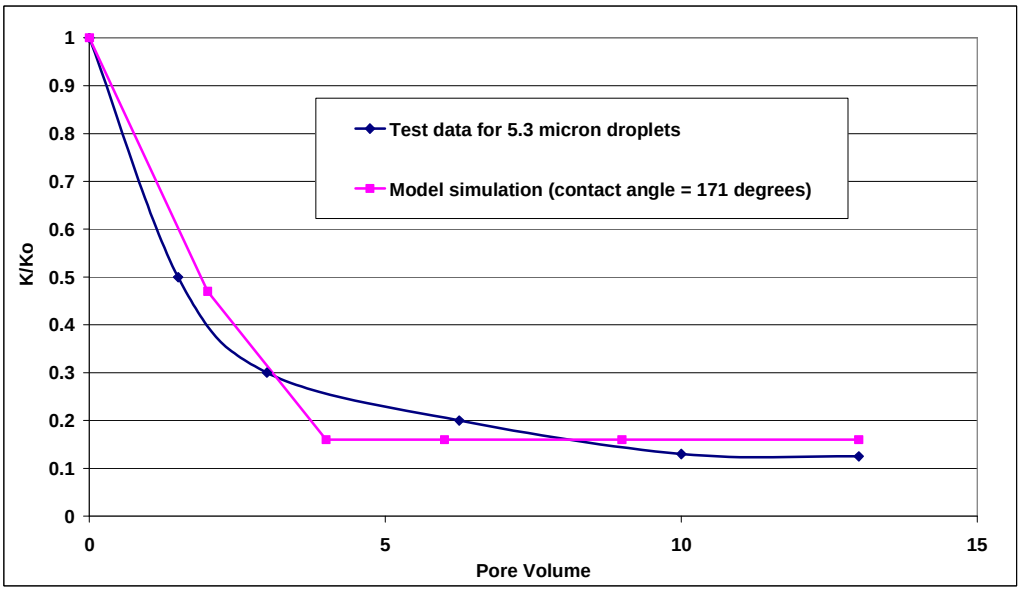

Figure 7-11: Test data and model simulation for injection of 5.3-micron droplets

Good simulation results are obtained in Figures 7-7 to 7-11 with contact angles from 155º to 171º. In fact, various contact angles were assumed and the best matches are shown. The high contact angles indicate strongly oil-wet sand surface. However, the sand packs were originally prepared to be strongly water-wet. This on the other hand reveals that injection of emulsion can significantly alter the

wettability of the sand surface, which will be discussed in more details in the next section.

7.5 Discussions

The proposed model is able to predict the trends of permeability decline under invasion of emulsion droplets. The discrepancies in simulation may be attributed to following factors.

First, the network model itself employs many assumptions. Previous research has proved that network models are realistic for simulating many reservoir characteristics such as relative permeability and two phase flow behavior. However, it can not be denied that the assumed parameters are indeed different from those of the real porous media. As seen in table 7-2, the average pore-throat size in simulation is higher than that of the sand pack. This may be the cause of the simulated contact angles being lower in Figures 7-8 and 7-9 than in other simulation runs. In other words, the discrepancy may be attributed to the network model, rather than the assumed contact angle.

Second, significant uncertainty exists while determining rock wettability. Reservoir rocks can have very different wettability, from strong water-wettability to strong oil-wettability, even though strong water-wettability is rare. Moreover, rock wettability can be altered by many factors, such as the chemistry of crude oil and injected fluids. Therefore, it is very difficult to determine the contact angle which is required as model input. In this work, simulations with contact angles between 155º and 171º generated good agreements with the test data. This indicates that the sand surfaces are strongly oil-wet. However, the tested sand packs were prepared to be water-wet originally. Some procedure caused the tested sand packs to alter their wettabilities.

The mechanisms of wettability alteration are not yet clear. It is suspected that the crude oil can deposit a layer of asphaltene or other polar compounds on sand surfaces, thus causing wettability to become more oil-wet (Morrow et al., 1986). Tweheyo et al. (1999) discovered that addition of small amount of organic acid to the oil could change the water wettability to neutral or even oil wettability. In another study, six crude oils were injected into Berea sandstone cores (Crocker and

Marchin, 1988). It was observed that the crude with the highest polar fraction being nitrogen/sulfur compounds caused the rock to turn most oil-wet.

Wettability alteration can also be triggered by certain chemicals, especially surfactants. The tested emulsions were stabilised with sodium oleate, a surfactant commonly used to waterproof materials. Some research shows that sodium oleate can significantly increase contact angle (Sis and Chander, 2003; Gence, 2006). In the tests of Soo and Radke (1984), the oil phase of the emulsion was mineral oil. Mineral oil lacks polar components and can not alter wettability. The wettability alteration is believed to be triggered by sodium oleate.

Figure 7-12 compares the simulation output with three contact angles for injection of 2.1-micron droplets into sand pack 1. It can be seen that contact angle has a significant effect on simulation results. The contact angles in the simulation runs are very high, however it can not be concluded that contact angles within this range can be used in other situations. In fact, most natural reservoirs demonstrate neutral wettability to oil-wettability, thus contact angles between 75 and 105 degrees are more realistic in future simulation runs.

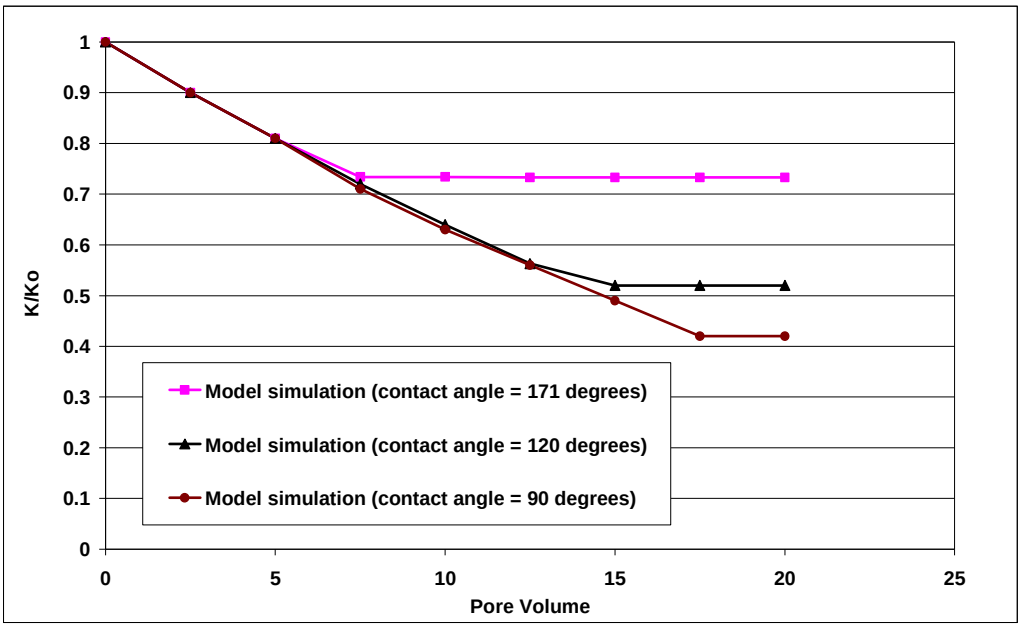

Figure 7-12: Effect of contact angle on model prediction

Third, the distribution of droplets in the network is assumed to abide by flow biased probability theory. However, flow of droplets in porous media is relatively random in nature. Flow biased probability theory may be an oversimplified assumption.

7.6 Model Application

Assume a circular reservoir is going through PWRI. The reservoir properties are identical to those of sand pack 1. The injected water contains 0.5% volume concentration of oil droplets, and the droplet size is 2.1 micron. The reservoir surface is oil-wet projecting a contact angle of 120 degrees. The wellbore radius is 63mm, and the reservoir radius is 200 m. The height of the injection zone is 80 m. The water injection rate is 1000 bbl/day (159 m^3/day), which equals a linear flow velocity of 1 cm/min.

Skin factor S is expressed as (Ahmed, 2001):

$$S = (\frac{K_o}{K} - 1) \cdot \ln(\frac{r_d}{r_w}) \qquad \text{(Equation 7-1)}$$

According to the capture-equilibrium theory explained earlier, once the rock within a certain radius reaches equilibrium, oil droplets will travel further into the reservoir. In other words, the invasion depth extends with time. The ratio of damaged flow rate (I) and original flow rate (I_o) is thus expressed as:

$$\frac{I}{I_o} = \frac{\ln \frac{r_e}{r_w}}{\ln \frac{r_e}{r_w} + S} \qquad \text{(Equation 7-2)}$$

At a certain time, the damaged permeability K is calculated with the proposed model, while the invasion depth r_d can be obtained by a mass balance calculation. The procedure is to first assume an invasions depth, and the total pore volume within the invasion depth PV_s can be easily calculated:

$$PV_s = \pi \cdot (r_s^{\,2} - r_w^{\,2}) \cdot h \cdot \phi \qquad \text{(Equation 7-3)}$$

The model prediction in Figure 7-12 shows that the number of pore volumes of injection required (N_{PV}) to reduce the permeability ratio (K/K_o) to 52% is 15. The equivalent time required to arrive at such damage is:

$$T_S = \frac{PV_S \cdot N_{PV}}{q_s} \qquad \text{(Equation 7-4)}$$

Then, the skin factor S can be obtained by Equation 7-1. The calculation results are shown in Table 7-3. With the skin factor, the flow rate ratio can be calculated with Equation 7-2.The result with the field conditions is shown in Figure 7-13. It can be seen that the injectivity declines fast in the first 100 days, but the decline slows down after one year. With the oil concentration of 4000 ppm, the injector will lose about 40% of its injection rate within 3.5 years. If the injected water is filtered to 40ppm of oil, the permeability damage is mild.

Table 7-3: Model prediction of skin factor

Invasion depth (m)	Time (day)	Skin factor
1	7.5	2.76
2	30	3.45
3	67.6	3.86
4	120.2	4.14
5	187	4.37
6	270	4.55
8	481	4.84
10	751	5.06
15	1691	5.47
20	3006	5.75

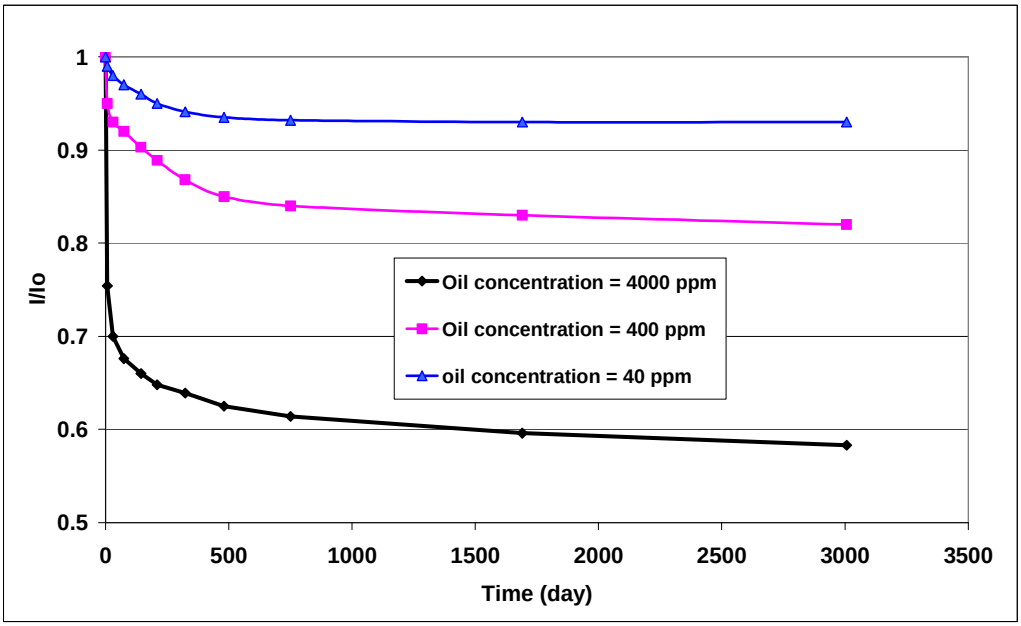

Figure 7-13: Prediction of well injectivity under invasion of droplets

7.7 Concluding Remarks

- A network model incorporating the proposed capture-equilibrium theory is applied to the simulation of capture of emulsion droplets in porous media. The approach is validated with test data and reasonably good agreements are achieved. The field application of the model is also provided.

- The errors in simulations can be attributed to the following three aspects. The network model may not completely represent the porous media. Second, the wettability of the rock surface presents significant uncertainty. It can vary anywhere from strong water-wettability to strong oil-wettability, and can even alter when contacting with crude oil or certain surfactants. Third, the flow of droplets in porous media is a random process in nature. Flow biased probability theory can reduce but can not completely eliminate this uncertainty.

- The simulation reveals that the tested porous media turned oil-wet after injection of emulsion. This may be attributed to the adsorption of surfactants onto the sand surfaces. It is recommended to assume oil-wettability to neutral-wettability when doing such simulations.

CHAPTER 8

FINAL DISCUSSIONS, CONCLUSIONS AND FUTURE WORK

8.1 Final Discussions on Well Injectivity

As discussed in Chapter 3, many injection wells suffered from severe injectivity decline, even at relatively good water quality. The injectivity has often been a concern for produced water re-injection (PWRI) projects. However, Beryl and Statfjord fields in North Sea do not fine-filter seawater prior to injection and no severe injectivity decline was observed. Based on such experiences, the fine filters in the Ula, Gyda and Magnus fields were removed (Paige and Murray, 1994).

It is known that when fractures are created near wellbore, the productivity and injectivity of a well can be greatly improved. The sustained injectivity in some fields indicates that the injection zones have been fractured under the water injection conditions, intentionally or not (Bansal and Caudle, 1992).

If the injection pressure is not high enough to fracture the injection zone, the injected water must be filtered to a certain purity, which can be determined by the numerical model presented in this thesis. In other words, the proposed model in this thesis is for matrix injection. On the other hand, if the injection pressure is high enough to fracture the injection zone, the well is unlikely to have injectivity issues.

It is thus crucial to determine if the injection pressure is high enough to fracture the injection zone while designing a downhole separation project. Fracturing is closely rated to rock mechanics, which is beyond the scope of this thesis. Only a brief discussion about the fracture closure pressure is given in this section. More details can be found elsewhere (Gidley et al., 1989).

Underground formations are confined and under stress. Local stress fields dominate fracture orientation and fracture growth. The most important factor affecting fracturing is the in-situ stress, which is the local stress state in a given rock mass at depth. The magnitude and direction of the principal stresses are important because they control the pressure required to create and propagate a fracture, and

the shape and direction of the fracture. Fractures usually propagate perpendicularly to the direction of the minimum in-situ stress. It is generally believed that at depths below 1000 ft (305 m), fractures are usually oriented vertically.

At present, the only reliable approach to determine the in-situ stress or minimum horizontal stress at depth is analysis of hydraulic fracturing data. Two variations of this technique are currently in use: injection/fall-off test and step-rate/flow-back test.

The procedure for the injection/fall-off test is to isolate the interval of interest with packers, to pump a small volume of low-viscosity fluid into the formation to break it down, and to shut in and determine the fracture-closure pressure based on the recorded pressure data. For a vertical fracture, it is generally accepted that fracture-closure pressure is synonymous with minimum in-situ stress and minimum horizontal stress.

The step-rate/flow-back method is more applicable for determining stress over a larger permeable interval. An upper bound for the minimum stress can be found by a step-rate test. Fluid is injected into a previously initiated fracture at various flow rates, and a stabilised pressure for each rate is recorded. The pressure is plotted against flow rate. The break point of the step-rate test is the fracture extension pressure. The fracture closure pressure can be determined by flow-back test. The procedure is to follow the step-rate test with immediate flow-back at a constant flow rate controlled by a valve or chock and recorded by an accurate low-rate flow meter.

Due to the high costs, in-situ stress tests are not run on every well. However, it is common to run such tests in new fields or new reservoirs to develop correlations to optimise hydraulic fracturing. Even though such tests are normally run on production wells, the test data are also valuable for design of PWRI, because an injection zone is expected to have similar properties as the connected production zone.

Before implementing a downhole separator or designing a PWRI project, it is necessary to analyse the available fracturing data and determine if the injection zone can be fractured under the injection pressure. It is obviously preferable to be able to fracture the injection zone for a downhole separation system. For normal onshore or subsea PWRI projects, the injection pumps are not limited by space. They may be able to generate adequately high pressure to fracture the formation.

However, the downhole injection pumps work in a confined space. Therefore, it is doubtful that the small downhole injection pumps are able to offer pressures high enough to fracture the formation.

8.2 Conclusions

Mature oil and gas fields produce large quantities of waste water. Produced water presents economical and environmental challenges to oil producers. The ingenious concept of downhole separation technology is to separate oil, gas and water inside the wellbore. Oil and gas are produced to the surface, and waste water is injected into a disposal zone. This technology not only greatly reduces waste water production, but also saves energy from lifting large amounts of produced water. Moreover, this technology may have great potential in offshore gas field developments.

Downhole separation technology received lots of attention during 1990s. However, about 40% of the previous installations failed. The most common issue is that the coarsely separated water contains high concentrations of particles and droplets, which can severely damage the permeability of the injection zone. Field installations are rare in recent years.

Particle-induced formation damage has been a research topic for many years. Abundant laboratory testing was devoted to the study of the permeability decline under invasion of particles. Previous research reveals that high particle concentration, low fluid velocity, and large particle size lead to more severe damage. Several models are available to predict particle-induced permeability decline. Empirical correlations have to rely on filtration date to determine the key parameters. Trajectory analysis model tracks each particle's movement in unrealistically defined pore structures. Besides, previous models did not provide up-scaling methods. Therefore, their industrial adoptions are limited. An efficient and reliable model is required to predict the reservoir permeability decline under the invasion of particles and droplets.

In this work, a pore network model is employed to simulate the capture of Brownian particles, non-Brownian particles and oil droplets in porous media and resultant permeability damage, incorporating respective damage mechanisms. The required model inputs include reservoir porosity, reservoir absolute permeability, mean pore

size and pore size distribution, particle/droplet concentration, and mean particle/droplet size. These parameters can be readily measured with current laboratory technology.

Particles and droplets cause permeability damage according to different mechanisms. For Brownian particles, diffusion is the dominant mechanism for deposition. For non-Brownian particles, a trajectory analysis is required to obtain particle invasion depth and particle size is compared with pore size to determine the respective damage mechanisms: plugging, pore throat bridging, or surface deposition. Droplets are captured on sand surfaces until equilibrium is reached. The model is validated with published test data and reasonably good agreements are achieved.

Model up-scaling methods with traditional steady-sate radial flow solution are also provided. Case studies show that injected water containing Brownian and non-Brownian particles should be filtered to less than 5 ppm of solids in order to maintain well injectivity. Injected water containing oil droplets should be filtered to less than 40 ppm of oil in order to maintain well injectivity. However, these conclusions are only applicable to the conditions in the case studies (i.e., the rock and particle properties). Each case must be analysed individually.

It is not yet completely clear why some wells do not demonstrate injectivity damage without finely filtering injected water. It is suspected that in these cases, the injection pressures are high enough to fracture the injection zones, enhancing the wells' tolerance to impurities. It is necessary to analyse the available fracturing data before implementing a downhole separator or PWRI project. If the formation can not be fractured under injection pressure, injected water must be filtered to a certain quality in order to maintain well injectivity. The required water quality can be predicted by the model presented in this thesis. If the formation can be fractured under injection pressure, the well is unlikely to have injectivity issues.

8.3 Future Work

Even though the proposed model involves many parameters, it is still a very much simplified approach. The following aspects may be improved in future work.

With the aim to reduce dependence on empirical correlations, the proposed model neglects the surface properties of particles and porous media, such as the particle shapes and surface charges. The model prediction may be improved by including such factors. However, these properties are very difficult to quantify. For example, it is a common belief that particle surface and rock surface carry an electronic double layer, which leads to the repulsive force when the particle is close to the sand surface. Electronic double layer is very difficult to model theoretically. It requires solution to Poisson-Boltzmann equation and is a function of ionic strength, temperature, and the surface potential of the two interacting particles (Stephan and Chase, 2001). The surface potential is experimentally immeasurable, therefore can only be quantitatively represented by the zeta potential. Unfortunately, zeta potential measurements are often inaccurate, depending on the method used. Besides, some factors are not fully understood, such as the particle shape factor. Such calculations have to rely on empirical correlations (Riley, 2005). A model that takes account of such surface properties definitely seems more sophisticated. And good agreement with test data can be achieved by tuning the many empirical parameters involved. However, the model may turn into another version of empirical model in the end.

The model relies on measured pore size distribution to achieve realistic representation of a porous medium. This approach has scientific foundation and pore network models have achieved great success in the study of macroscopic flow. In recent years, more advanced methods such as CT scanning and reconstruction gained more applications in characterisation of porous media. In one study, cores damaged by particles are scanned to measure particle invasion depth (Bailey, 2000). In another study, CT was applied to image the saturation distribution of wetting and non-wetting phases inside a sand pack and a Berea sandstone core (Turner et al., 2004). Because the flow field can not be directly solved inside the scanned images, the common purpose of CT scanning is to construct more accurate or 3-dimensioanl pore network models (Hou et al, 2007).

CT scanning is a powerful tool to study the fluid saturation at lore level. In the past, the multiphase fluid distribution inside porous media can only be assumed according to certain theories. But now the 3-dimensioanl fluid distribution can be vividly viewed with the help of CT scan. Currently, the distribution of particles inside the porous media and the damage mechanisms are also assumed based on scientific reasoning. CT scan may be applied to image the cores damaged by

particles and droplets. This technology may lead to new insights and better understanding in the damage mechanisms of particles and droplets.

The network size used in this work is relatively small. The calculations of the transport of particles and droplets limit the network size. As discussed in Chapter 3, the particle and droplet induced damage is commonly restricted to the near wellbore region. However, it may not be possible to program a network as large as the damage radius and calculate the movements of particles and droplets in such a huge network. If this large network can be achieved one day, network model can be coupled with reservoir simulators and give a much better description of the near-wellbore region.

REFERENCES

Abrams, A., 1977. Mud design to minimize rock impairment due to particle invasion. Journal of Petroleum Technology, 29 (5): 586-592.

Ahmed, T., 2001. Reservoir Engineering Handbook. Gulf Professional Publishing. Houston Texas USA. pp. 423-424.

Al-Abduwani, F.A.H., A. Shirzadi, W.M.G.T. van den Broek, and P.K. Currie, 2003. Formation damage vs. solid particles deposition profile during laboratory simulated PWRI, SPE Journal, 10 (2): 138-151.

Ali, M.A.J., P.K. Currie, and M.J. Salman, 2007. Permeability damage due to water injection containing oil droplets and solid particles at residual oil saturation, SPE 104608 presented at the 15th SPE Middle East oil and gas show and conference, Bahrain, 11-14 March.

Allen, T., 1997. Particle size measurement (fifth edition) volume 2. Cahpman & Hall, pp. 149-187.

Anderson, W.G., 1986. Wettability literature survey part 2: wettability measurement. Journal of Petroleum Technology, 38 (11), 1246-1268.

API, 2000. Overview of exploration and production waste volumes and waste management practices in the United States. prepared by ICF Consulting for the American Petroleum Institute, Washington DC, May.

Baghdlklan, S.Y., M.M. Sharma and L.L. Handy, 1989. Flow of clay suspensions through porous media. SPE Reservoir Engineering Journal, 4 (2): 213-220.

Bansal, K.M., and D.D. Caudle, 1992. A new approach for injection water quality. SPE 24803 presented at 67th annual technical conference and exhibition, Washington D.C., 4-7 October.

** Abide by Journal of Petroleum Science and Engineering referencing style*

Bailey, L., E.S. Boek, S.D.M. Jacques, T. Boassen, O.M. Selle, J.F. Argillier, and D.G. Longeron, 2000. Particulate invasion from drilling fluids. SPE Journal, 5 (4): 412-417.

Binks, B.P., 1998. Modern Aspects of Emulsion Science. The Royal Society of Chemistry. Cambridge UK. p. 179

Bird R.B., W.E. Stewart, E.N. Lightfoot, 2002. Transport phenomena second edition. John Wiley & Sons Inc, p. 529.

Blauch, M., J. Weaver, M. Parker, B. Todd, and M. Glover, 1999. New insights into proppant-pack damage due to infiltration of formation fines. SPE 56833 presented at annual technical conference and exhibition, Houston Texas, 3-6 October.

Blunt, M.J., 2001. Flow in porous media – pore-network models and multiphase flow. Current Opinion in Colloid and Interface Science, 6 (3): 197-207.

Blunt, M.J., M.D. Jackson, M. Piri, and P.H. Valvatne, 2002. Detailed physics, predictive capabilities and macroscopic consequences for pore-network models of multiphase flow. Advances in Water Resources, 25 (8-12): 1069-1089.

Bowers, B.E., R.F. Brownlee, and P.J. Schrenkel, 2000. Development of a downhole oil/water separation and reinjection system for offshore application. SPE Production and Facilities Journal, 15 (2), 119.

Carman, P.C., 1938. The determination of the specific surfaces of powders. Jour. Soc. Chem. Ind., 57: 225-234.

Cartmill, J.C., and P.A. Dickey, 1969. Flow of a disperse emulsion of crude oil in water in porous media. SPE 2481 presented at the 44th annual fall meeting, Denver Colorado, 28 September - 1 October.

Chang, Y.I, S.C. Chen, H.C. Chan, and E. Lee. 2004. Network simulation for deep bed filtration of Brownian particles. Chemical Engineering Science, 59 (21): 4467-4479 .

Chang, J.S., and S. Vigneswaran, 1990. Ionic strength in deep bed filtration. Water Research, 24 (11): 1425-1430.

Chen, R.Y., 1977. Diffusive deposition of particles in a short channel. Powder Technology, 16 (1): 131-135.

Chen, R.Y., H.C. Chiou, and D. Sun, 1996. Deposition of particles in a convergent channel. Powder Technology, 87 (1): 83-86.

Civan F., 2000. Reservoir formation damage. Gulf Publishing Company, Houston Texas USA, pp. 140-144.

Cline, J.T., 1998. Treatment and discharge of produced water for deep offshore disposal, presented at the API Produced Water Management Technical Forum and Exhibition, Lafayette Louisiana, 17-18 November.

Cobby, G.L., 2004. Produced water regulatory requirements offshore Australia. SPE 86711 presented at the 7th SPE international conference on HSE in oil and gas exploration and production, Calgary Alberta Canada, 29-31 March.

Compere, F., G. Porel, and F. Delay, 2000. Transport and retention of clay particles in saturated porous media: influence of ionic strength and pore velocity. Journal of Contaminant Hydrology, 49 (1-2): 1-21.

Constantinides, G.N., and A.C. Payatakes. 1996. Network simulation of steady-state two-phase flow in consolidated porous media. AIChE Journal, 42 (2): 369-382.

Crocker, M.E., and L.M. Marchin, 1988. Wettability and adsorption characteristics of crude oil asphaltene and polar fractions. Journal of Petroleum Technology, 40 (4): 470-474.

Cuiec, L., 1984. Rock/crude-oil interactions and wettability: an attempt to understand their interaction. SPE 13211 presented at the 59th annual technical conference and exhibition, Houston Texas, 16-19 September.

Cussler, E.L., 1976. Multicomponent diffusion. Elsevier Scientific Publishing Company. pp. 5-27.

Darby, R., 1996. Chemical Engineering Fluid Mechanics. Marcel Dekker, Inc. New York, USA. pp. 143 and 366.

Davies, C.N., 1973. Diffusion and sedimentation of aerosol particles from Poiseuille flow in pipes. Aerosol Science, 4 (4): 317-328.

Devereux, O.F., 1974. Emulsion flow in porous solids. Chemical Engineering Journal, 7: 121-128.

DoIR (Department of Industry and Resources), 2006. Overview of Development and Production Activities in 2005. Petroleum in Western Australia Magazine, April, 32.

Eastman, J., Colloid science principles, methods and applications (Terence Cosgrove as editor). Blackwell Publishing, Oxford UK. pp. 42-43.

EPA, 1993. Development document for effluent limitations guidelines and new source performance standards for the offshore subcategory of the oil and gas extraction point source category. EPA 821-R-93-003, U.S. Environmental Protection Agency.

Gence, N., 2006. Wetting behavior of magnesite and dolomite surfaces. Applied Surface Science, 252 (10): 3744-3750.

Gidley, J.L., S.A. Holditch, D.E. Nierode, and R.W. Veatch, 1989. Recent Advances in Hydraulic Fracturing. SPE Monograph Volume 12, Richardson Texas, pp. 57-74.

Gomez, C., J. Caldentey, S. Wang, L. Gomez, R. Mohan, and O. Shoham, 2001. Oil-water separation in liquid-liquid hydrocyclones – experimental and modeling. SPE 71538 presented at SPE annual technical conference and exhibition, New Orleans Louisiana, 30 September - 3 October.

Hampton, J.H.D., S.B. Savage, and R.A.L. Drew. 1993. Computer modeling of filter pressing and clogging in a random tube model. Chemical Engineering Science, 48 (9): 1601-1611.

Hou, J., S.K. Zhang, R.Y. Sun, Z.Q. Li, and Y.B. Liu, 2007. Reconstruction of 3D network model through CT scanning. SPE 106603 presented at Europec/EAGE annual conference and exhibition, London UK, 11-14 June.

Imdakm, A.O., and M. Sahimi. 1991. Computer simulation of particle transport processes through porous media. Chemical Engineering Science, 46 (8): 1977-1993.

Ioannidis, M.A., and I. Chatzis. 1993. Network modeling of pore structure and transport properties of porous media. Chemical Engineering Science, 48 (5): 951-972.

Ison, C.R., and K.J. Ives, 1969. Removal mechanisms in deep-bed filtration. Chemical Engineering Science, 24 (4): 717.

Iwasaki, T., 1937. Some notes on sand filtration. Journal of American Water Works Association, 29: 1591.

Jacobs, R.P.W.M., R.O.H. Grant, J. Kwant, J.M. Marqueine, and E. Mentzer, 1992. The composition of produced water from Shell operated oil and gas production in the North Sea, Produced Water (J.P. Ray and F.R. Englehart as editors), Plenum Press, New York.

Jegatheesan, V., and S. Vigneswaran, 1997. Interaction between organic substances and submicron particles in deep bed filtration, Separation and Purification Technology, 12 (1): 61-66.

Khatib, Z., and P. Verbeek, 2002. Water to value – produced water management for sustainable field development of mature and green fields, SPE 73853 present at SPE international conference on health, safety and environment in oil and gas exploration and production, Kuala Lumpur Malaysia, 20-22 March.

Matthews, C.M., R. Chachula, B.R. Peachey, and S.C. Solanki, 1996. Application of downhole oil/water separation systems in the Alliance field. SPE 35817 presented at SPE health, safety and environment in oil and gas exploration and production conference, New Orleans Louisiana, 9-12 June.

Maximenko, A., and V.V. Kadet. 2000. Determination of relative permeabilities using the network models of porous media. Journal of Petroleum Science and Engineering, 28 (3): 145-152.

McAuliffe, C.D., 1973. Oil-in-water emulsions and their flow properties in porous media. Journal of Petroleum Technology, 25 (6): 727-733.

Moghadasi, J., H. Muller, M. Jamialahmadi, and A. Sharif, 2004. Theoretical and experimental study of particle movement and deposition in porous media during water injection. Journal of Petroleum Science and Engineering. 43 (3-4): 164.

Morrow, N.R., H.T. Lim, and J.S. Ward, 1986. Effect of crude oil induced wettability changes on oil recovery. SPE Formation Evaluation Journal, 1 (1): 89-103.

Myers, M., 2001. Calculation of Brownian particle transmission in long, wide channels. AIChE Journal, 47 (2): 250-255.

Nichol, J.R., and J. Marsh, 1997. Downhole gas/water separation: engineering assessment and field experience. SPE 38828 presented at SPE annual technical conference and exhibition, San Antonio Texas, 5-8 October.

Ogunsina, O.O., and M.L. Wiggins, 2005. A review of downhole separation technology. SPE 94276 presented in SPE production operations symposium, Oklahoma City Oklahoma, 16-19 April.

Oren, P.E., S. Bakke, and O.J. Arntzen. 1998. Extending predictive capabilities to network models. SPE Journal, 3 (4): 324-336.

Paige, R.W., and L.R. Murray, 1994. Re-injection of produced water- field experience and current understanding. SPE 28121 presented at the 1994 Eurock SPE/ISRM rock mechanics in petroleum engineering conference, Delft Netherlands, 29-31 August.

Pang, S., and M.M. Sharma, 1997. A model for predicting injectivity decline in water injection wells. SPE Formation Evaluation Journal, 12 (3): 194-201.

Patzek, T.W., 2001. Verification of a complete pore network simulation of drainage and imbibition. SPE Journal, 6 (2): 144-156.

Payatakes A.C., C. Tien, and R.M. Turian, 1973. A new model for granular porous media. AIChE Journal, 19 (1): 58-66.

Payatakes A.C., C. Tien, and R.M. Turian, 1974. Trajectory calculation of particle deposition in deep bed filtration: part 1 and part 2. AIChE Journal, 20 (5): 889-905.

Peachey, P.R., and C.M. Mathews, 1994. Downhole oil-water separator development. Journal of Canadian Petroleum Technology, September, 17-21.

Peats, A., and P. Schrenkel, 1997. Application of ESP oil water separation system in the Swan Hills Unit One field - a case study. SPE 39079 presented at the SPE electric submersible pump workshop, Houston Texas, 30 April.

Petty, C.A., and S.M. Parks, 2004. Flow structures within miniature hydrocyclones. Minerals Engineering, 17 (5): 615.

Philip, J.R., 1995. Deposition in narrow channels. Chemical Engineering Science, 50 (5): 793-802.

Prieve, D.C., and E. Ruckenstein, 1974. Effect of London force upon the rate of deposition of Brownian particles. AIChE Journal, 20 (6): 1178-1186.

Rabalais, N.N., B.A. McKee, D.J. Reed, and J.C. Means, 1992. Fate and effects of produced water discharged in coastal Louisiana, Gulf of Mexico, USA. Produced Water (J.P. Ray and F.R. Englehart as editors), Plenum Press, New York.

Rege, S.D., and H.S. Fogler, 1988. A network model for deep bed filtration of solid particles and emulsion drops. AIChE Journal, 34 (11): 1761-1772.

Renn, J., 2005. Einstein's invention of Brownian motion. Annalen der Physik, 14 (Supplement 1): 25.

Reynolds, R., B. Kiker, and L. Cole, 2002. Produced water, and the issues associated with it, PTTC Network News, 8 (3).

Rickford, .L., and T.P. Finney, 1991. Formation damage from fine particulate invasion: an example from the Lost Soldier Tensleep formation. SPE Production Engineering Journal, 6 (3): 247-251.

Riley, J., 2005. Colloid science principles, methods and applications (Terence Cosgrove as editor). Blackwell Publishing, Oxford UK. pp. 14-35

Romero, L., J.L. Ziritt, A. Marin, F. Rojas, J.L. Mogollon, E. Manrique, and F. Paz, 1996. Plugging of high permeability fractured zones using emulsions. SPE/DOE 35461 presented at the tenth symposium on improved oil recovery, Tulsa Oklahoma, 21-24 April.

Roque, C., G. Chauveteau, M. Renard, G. Thibault, and M. Bouteca, 1995. Mechanism of formation damage by retention of particles suspended in water. SPE 30110 presented at the European formation damage conference, Hague Netherlands, 15-16 May.

Rushton, A., A.S. Ward, and R.G. Holdich, 1996. Solid-liquid filtration and separation technology. VCH, Weinheim Germany, p. 185.

Salles J., J.F. Thovert, P.M. Adler, 1993. Deposition in porous media and clogging. Chemical Engineering Science, 48 (16): 2844.

Santiwong, S.R., J. Guan, T.D. Waite, 2008. Effect of ionic strength and pH on hydraulic properties and structure of accumulating solid assemblages during microfiltration of montmorillonite suspensions. Journal of Colloid and Interface Science. 317 (1), 214-227.

Santoro, T., and G. Stotzky, 1967. Effect of electrolyte composition and pH on the particle size distribution of microorganisms and clay minerals as determined by the electrical sensing zone method. Archives of Biochemistry and Biophysics, 122 (3), 664-669.

Schramm, L.L., 2005. Emulsions, Foams, and Suspensions: Fundamentals and Applications. Wiley-VCH Weinheim. p. 4.

Seright, R.S., R.H. Lane, and R.D. Sydansk, 2001. A strategy for attacking excess water production, SPE 70067 presented at the SPE Permian Basin oil and gas recovery conference, Midland Texas, 15-16 May.

Sharma, M.M., S. Pang, K.E. Wennberg, and L.N. Morgenthaler, 2000. Injectivity decline in water injection wells: an offshore Gulf of Mexico case study. SPE Production and Facilities Journal, 15 (1): 6-13.

Shook, C.A., and M.C. Roco, 1991. Slurry Flow: Principles and Practices. Butterworth-Heinemann, Stoneham USA, p. 9.

Sis, H. and S. Chander, 2003. Adsorption and contact angle of single and binary mixtures of surfactants on apatite. Minerals Engineering. 16 (9): 839-848.

Smith, W.O., 1932. Physics. p. 139.

Soo, H., and C.J. Radke, 1984a. The flow mechanism of dilute, stable emulsions in porous media. Industrial and Engineering Chemistry Fundamentals. 23: 342-347.

Soo, H., and C.J. Radke, 1984b. Velocity effects in emulsion flow through porous media. Journal of Colloid and Surface Science, 102 (2), 462-476.

Soo, H., and C.J. Radke, 1985. Flow of dilute stable liquid and solid dispersions in underground porous media. American Institute of Chemical Engineers Journal, 31 (11), 1926-1928.

Soo, H., and C.J. Radke, 1986. A filtration model for the flow of dilute stable emulsions in porous media. Chemical Engineering Science, 41 (2), 263-272.

Stephan, E.A., and G.G. Chase, 2001. A preliminary examination of zeta potential and deep bed filtration activity. Separation and Purification Technology, 21 (3): 220.

Stephan, E.A., and G.G. Chase, 2003. Use of generic algorithms as an aid in modeling deep bed filtration. Computers and Chemical Engineering, 27 (2): 281-292.

Stevenson, K., M. Ferer, G.S. Bromhal, J. Gump, J. Wilder, and D.H. Smith, 2006. 2-D network model simulations of miscible two-phase flow displacements in porous media: effects of heterogeneity and viscosity. Physica A, 367: 7-24.

Stuebinger, L., K. Bowlin, J. Wright, M. Poythress, and B. Watson, 1997. Dual injection and lifting systems: rod pumps. SPE 38790 presented at SPE annual technical conference and exhibition, San Antonio Texas, 5-8 October.

Swisher, M., 2000. Summary of DWS application in northern Louisiana, presented at downhole water separation technology workshop, Baton Rouge.

Thomas, S., and S.M.F. Ali, 1989. Flow of emulsions in porous media and potential for enhanced oil recovery. Journal of Petroleum Science and Engineering, 3 (1-2): 121-136

Tibbetts, P.J.C., I.T. Buchanan, L.J. Gawel, and R. Large, 1992. A comprehensive determination of produced water composition, Produced Water (J.P. Ray and F.R. Englehart as editors), Plenum Press, New York.

Todd, A.C., T. Kumar, and S. Mohammadi, 1990. The value and analysis of core based water quality experiments as related to water injection schemes. SPE Formation Evaluation Journal, 5 (2): 185-191.

Todd, A.C., J.E. Somerville, and G. Scott, 1984. The application of depth of formation damage measurements in predicting water injectivity decline. SPE 12498 Presented in SPE formation damage control symposium, Bakersfield California, 13-14 February.

Treiber, L.E., and W.W. Owens, 1972. A laboratory evaluation of the wettability of fifty oil-producing reservoirs. SPE Journal, 12 (6): 531.

Tsakiroglou A.D., and A.C. Payatakes, 2000. Characterization of the pore structure of reservoir rocks with the aid of serial sectioning analysis, mercury porosimetry and network simulation. Advances in Water Resources, 23 (7): 773-789.

Turner, M.L., L. Knufing, C.H. Arns, A. Sakellarious, T.J. Senden, A.P. Sheppard, R.M. Sok, A. Limaye, W.V. Pinczewski, and M.A. Knackstedt, 2004. Three-dimensional imaging of multiphase flow in porous media. Physica A, 339 (1-2): 166-172.

Tweheyo, M.T., T. Holt, and O. Torsater, 1999. An experimental study of the relationship between wettability and oil production characteristics. Journal of Petroleum Science and Engineering, 24 (2-4): 179-188.

van den Broek, W.M.G.T., J.N. Bruin, T.K. Tran, M.J. van der Zande, and H. van der Meulen, 1999. Core-flow experiments with oil and solids containing water, SPE 54769 presented at the 1999 SPE European formation damage conference, Hague Netherlands, 31 May - 1 June.

van Oort, E., J.F.G. van Velzen, and K. Leerlooijer, 1993. Impairment by suspended solids invasion: testing and prediction, SPE Production and Facilities Journal, 8 (3): 178-184.

Veil, J.A., B.G. Longhus, and S. Belieu, 1999. Feasibility evaluation of downhole oil/water separator technology. Report prepared for US Department of Energy under contract W-31-109-Eng-38.

Veil, J.A., M.G. Puder, D. Elcock, and R.J. Redwick, 2004. A white paper describing produced water from production of crude oil, natural gas and coal bed methane. Report prepared for US Department of Energy under contract W-31-109-Eng-38.

Veil, J.A., and J.J. Quinn, 2004. Downhole separation technology performance: relationship to geologic conditions. Report prepared for US Department of Energy under contract W-31-109-Eng-38.

Veil, J.A., and J.J. Quinn, 2005. Performance of downhole separation technology and its relationship to geologic conditions. SPE 93920 presented at SPE/EPA/DOE exploration and production environmental conference, Galveston Texas, 7-9 March.

Vetter, O.J., V. Kandarpa, M. Stratton, and E. Veith, 1987. Particle invasion into porous medium and related injectivity problems. SPE 16255 presented in SPE international symposium on oil field chemistry, San Antonio Texas, 4-6 February.

Vincent, B., 2005. Colloid science principles, methods and applications (Terence Cosgrove as editor). Blackwell Publishing, Oxford UK. pp. 9-10

Webb, P.A., and C. Orr, 1997. Analytical Methods in Fine Particle Technology. Micromeritics Instrument Coporatio, Norcross GA USA. p. 280.

Wolff, E.A., 2000. Reduction of emissions to sea by improved produced water treatment and subsea separation systems, SPE 61182 presented at the SPE international conference on health, safety, and environment, Stavanger Norway, 26-28 June.

Yue, X., 1995. Sold-Liquid Two Phase Flow (in Chinese), Petroleum Industry Publishing, Beijing China, pp. 69-73

Zhang, N.S., J.M. Somerville, and A.C. Todd, 1993. An experimental investigation of the formation damage caused by produced oily water injection, SPE 26702 presented at the offshore Europe conference, Aberdeen UK, 7-10 September.